NUCLEAR LOCALIZATION OF DENGUE VIRUS NONSTRUCTURAL PROTEIN 5: THE INDUCTION OF RANTES PRODUCTION BY ACTIVATION OF NF-κB

SASIPRAPA KHUNCHAI

A THESIS SUBMITTED IN PARTIAL FULFILLMENT
OF THE REQUIREMENTS FOR
THE DEGREE OF DOCTOR OF PHILOSOPHY
(IMMUNOLOGY)
FACULTY OF GRADUATE STUDIES
MAHIDOL UNIVERSITY
2013

Thesis
entitled

NUCLEAR LOCALIZATION OF DENGUE VIRUS NONSTRUCTURAL PROTEIN 5: THE INDUCTION OF RANTES PRODUCTION BY ACTIVATION OF NF-κB

……..
Miss Sasiprapa Khunchai
Candidate

……..
Prof. Pa-thai Yenchitsomanus,
Ph.D.
Major advisor

……
Miss Sansanee Noisakran,
Ph.D.
Co-advisor

……..
Assoc. Prof. Thawornchai Limjindaporn,
M.D., Ph.D.
Co-advisor

……
Prof. Banchong Mahaisavariya,
M.D., Dip Thai Board of Orthopedics
Dean
Faculty of Graduate Studies
Mahidol University

……..
Prof. Kovit Pattanapanyasat, Ph.D.
Program Director
Doctor of Philosophy Programme in Immunology
Faculty of Medicine Siriraj Hospital
Mahidol University

Thesis
entitled

NUCLEAR LOCALIZATION OF DENGUE VIRUS NONSTRUCTURAL PROTEIN 5: THE INDUCTION OF RANTES PRODUCTION BY ACTIVATION OF NF-κB

was submitted to the Faculty of Graduate Studies, Mahidol University
for the degree of Doctor of Philosophy (Immunology)
on
October 1, 2013

……..
Miss Sasiprapa Khunchai
Candidate

……..
Assoc. Prof. Nattiya Hirankarn,
M.D., Ph.D.
Chair

……
Asst. Prof. Potjanee Srimanote,
Ph.D.
Member

……..
Prof. Pa-thai Yenchitsomanus,
Ph.D.
Member

……
Miss Sansanee Noisakran,
Ph.D.
Member

……..
Assoc. Prof. Thawornchai Limjindaporn,
M.D., Ph.D.
Member

……
Prof. Banchong Mahaisavariya,
M.D., Dip Thai Board of Orthopedics
Dean
Faculty of Graduate Studies
Mahidol University

……..
Clin. Prof. Udom Kachintorn,
M.D., Dip Thai Board of Medicine,
Dip Thai Board of Family Medicine
Dean
Faculty of Medicine Siriraj Hospital
Mahidol University

ACKNOWLEDGEMENTS

I would like to express my sincere appreciation to my major advisors, Prof. Dr. Pa-thai Yenchitsomanus and Assoc. Prof. Dr. Thawornchai Limjindaporn. My doctoral training would not be possible if I did not obtain their kind guidance, teaching, assistances, and moral support. Besides the research training, they also gave me the advices in every aspect of life in order to be "a good Ph.D.".

I also would like to present my sincere gratitude to my co-advisor, Dr. Sansanee Noisakarn, who always gave me useful suggestions and technical training.

The most important sincere appreciation I also give to my lovely family, especially for my father, mother, sister, and nephews. They always support me with everything in my life, give me the best living environments and education and always accompany me at the time when I needed someone along side with love and spirit.

I would like to thank all of my best friends, who gave me the warmest love and spirit during the whole time of my studies.

My appreciations also regards to all the members of Division of Molecular Medicine and Dengue Hemorrhangic Fever Unit for their helpfulness, technical assistances and warm companionship. The special thanks for Dr. Mutita Junking and Mrs. Aroonroong Suttitheptumrong for their great help in the research works, Ms. Pucharee Songprakron, Ms. Thanyaporn Dechtawewat, and Dr. Ornnutchar Poungpair for their kind helpfulness in research techniques.

I am thankful to all of lecturers and staffs of the Department of Immunology and my all best friends in the International Immunology programme 2008.

This thesis would not be able to accomplish without the financial support from Strategic Scholarships for Frontier Research Network for the Ph.D. Program, Commission on Higher Education that was granted to me during the whole time of my Ph.D. study and also a great life in Ghent University, Belgium. TRF-Senior Research Scholar, TRF-CHE Research Grant and Siriraj Chalearmprakiat Fund supported the finance to my major advisors.

I would like to thank Prof. Guy Haegeman for his helpfulness during the time in Ghent University, Belgium.

Finally, I would like to thank all the people who gave me love and helpfulness of whom I could not mention the name in this page, but they are a part of my successful study here, at Mahidol University.

Sasiprapa Khunchai

NUCLEAR LOCALIZATION OF DENGUE VIRUS NONSTRUCTURAL PROTEIN 5: THE INDUCTION OF RANTES PRODUCTION BY ACTIVATION OF NF-κB

SASIPRAPA KHUNCHAI 5136951 SIIM/D

Ph.D. (IMMUNOLOGY)

THESIS ADVISORY COMMITTEE: PA-THAI YENCHITSOMANUS, Ph.D., THAWORNCHAI LIMJINDAPORN, M.D., Ph.D., SANSANEE NOISAKRAN, Ph.D.

ABSTRACT

Dengue virus (DENV) infection can cause a severe and potentially life-threatening disease – dengue hemorrhangic fever (DHF) or dengue shock syndrome (DSS). Currently, no licensed vaccine or specific drug is available and the pathogenic mechanism of DENV infection is still unclear. Excessive cytokine secretion – the so called 'cytokine storm', positively correlating with increased vascular permeability, leading to plasma leakage – a hallmark of DHF/DSS. Among ten DENV proteins, non-structural protein 5 (NS5) shows a predominant role in several types of cytokine production including IL-6, IL-8, IP-10, and IFN-γ. DENV NS5 also activates the NF-κB function involved in cytokine production. Even though some cytokine genes have been found to be induced by DENV NS5, other DHF/DSS-immunopathogenic mediators have remained mysterious. Therefore, this work aims to investigate the induction of other cytokines by DENV NS5 and study the molecular mechanism how DENV NS5 mediates the cytokine production. Inflammatory cytokine gene expression profiles in HEK 293 cells infected with DENV 2 were screened by RT^2 Profiler PCR Array. The cytokines that were up-regulated were studied in HEK 293 cells transfected with plasmid constructs expressing wild-type NS5 (WT-NS5) or mutated NS5 (MT-NS5). MT-NS5 was mutated at its nuclear localization sequences (NLS) to inhibit the protein entering into the nucleus. Then, DENV NS5-induced cytokines were selected and tested for differential expression when DENV NS5 is located both within and outside or only outside the nucleus. The luciferase reporter gene assay was performed to determine the influence of DENV NS5 on the cytokine gene promoter and NF-κB involvement. In addition, chromatin immunoprecipitation (ChIP) assay was employed to examine the DNA-binding ability of NF-κB on such a gene promoter. The results demonstrated that RANTES, which can increase vascular permeability, was predominantly induced by DENV WT-NS5, but not by MT-NS5, at both mRNA and protein levels. Nuclear DENV WT-NS5 activated the RANTES promoter as detected by luciferase reporter assay. Increased DNA-binding activity of NF-κB on the RANTES promoter was also demonstrated by ChIP assay. Furthermore, nuclear DENV WT-NS5 interacted with an NF-κB inhibitor, Daxx, suggesting that this interaction may liberate NF-κB to activate the RANTES promoter. Taken together, DENV NS5 can activate RANTES production via its interaction with Daxx which may then liberate NF-κB to bind and activate the RANTES promoter.

KEY WORDS: DENGUE VIRUS / NONSTRUCTURAL PROTEIN 5 / NS5 / Daxx / RANTES

195 pages

การแสดงออกของโปรตีนเอ็นเอส 5 ของไวรัสเด็งกี่ในนิวเคลียส: การเหนี่ยวนำการสร้างสารซัยโตไคน์ RANTES โดยการกระตุ้นการทำงานของ NF-κB

NUCLEAR LOCALIZATION OF DENGUE VIRUS NONSTRUCTURAL PROTEIN 5: THE INDUCTION OF RANTES PRODUCTION BY ACTIVATION OF NF-κB

ศศิประภา ขุนชัย 5136951 SIIM/D

ปร.ด. (วิทยาภูมิคุ้มกัน)

คณะกรรมการที่ปรึกษาวิทยานิพนธ์: เพทาย เย็นจิตโสมนัส, ปร.ด., ถาวรชัย ลิ้มจินดาพร, พ.บ., ปร.ด., ศันสนีย น้อยสคราญ, ปร.ด.

บทคัดย่อ

การติดเชื้อไวรัสเด็งกี่อาจจะทำให้เกิดโรคที่รุนแรงและเป็นอันตรายถึงแก่ชีวิต คือ โรคไข้เลือดออก (DHF) และโรคไข้เลือดออกที่มีภาวะช็อกร่วมด้วย (DSS) ในปัจจุบัน ยังไม่มีวัคซีนที่ได้รับการขึ้นทะเบียน หรือยาที่จำเพาะในการรักษา และกลไกพยาธิกำเนิดของโรคยังไม่เป็นที่ทราบแน่ชัด การหลั่งซัยโตไคน์ที่มากผิดปกติ ซึ่งเรียกว่า 'พายุซัยโตไคน์' มีความสัมพันธ์กับการผ่านของสารน้ำออกนอกหลอดเลือด นำไปสู่ภาวะรั่วของพลาสมา ซึ่งเป็นอาการสำคัญที่พบในผู้ป่วยโรคไข้เลือดออก และโรคไข้เลือดออกที่มีภาวะช็อกร่วมด้วย เมื่อมีการศึกษาว่าโปรตีนชนิดใดของไวรัสเด็งกีมีบทบาทในการกระตุ้นการสร้างซัยโตไคน์ พบว่าจากโปรตีนทั้งหมด 10 ชนิดของไวรัสเด็งกี โปรตีนที่ไม่ได้เป็นส่วนประกอบของไวรัส ชนิดที่ 5 หรือโปรตีนเอ็นเอส 5 (NS5) มีความสามารถที่เด่นชัดที่สุดในการกระตุ้นการสร้างซัยโตไคน์หลายชนิด อาทิเช่น IL-6 IL-8 IP-10 และ IFN-γ นอกจากนี้ โปรตีนเอ็นเอส 5 ยังสามารถกระตุ้นการทำงานของโปรตีน NF-κB ซึ่งมีบทบาทควบคุมการสร้างซัยโตไคน์ แม้ว่าซัยโตไคน์ดังกล่าว จะถูกกระตุ้นให้มีการสร้างโดยโปรตีนเอ็นเอส 5 แต่ยังมีซัยโตไคน์ซึ่งมีบทบาทสำคัญต่อพยาธิกำเนิดของโรคอีกหลายชนิด ที่ยังไม่ทราบว่าโปรตีนชนิดใดของไวรัสเป็นตัวกระตุ้น ดังนั้น การศึกษานี้จึงมีวัตถุประสงค์ที่จะทดสอบว่าโปรตีนเอ็นเอส 5 สามารถเหนี่ยวนำการสร้างซัยโตไคน์ชนิดอื่นด้วยหรือไม่ และกลไกระดับอณูในการเหนี่ยวนำการสร้างซัยโตไคน์ของโปรตีนเอ็นเอส 5 เกิดขึ้นได้อย่างไร การตรวจกรองการสร้างซัยโตไคน์ของเซลล์ HEK 293 ที่ติดเชื้อไวรัสเด็งกี กระทำโดยใช้วิธี RT^2 Profiler PCR Array ซัยโตไคน์ชนิดที่พบว่ามีการกระตุ้นให้สร้างมากขึ้น จะนำมาศึกษาอีกครั้งหนึ่งในเซลล์ HEK 293 ทำให้มีการสร้างโปรตีนเอ็นเอส 5 ที่แตกต่างกัน 2 แบบ คือ โปรตีนเอ็นเอส 5 แบบปกติ ซึ่งมีการแสดงออกทั้งในไซโตพลาสมและนิวเคลียส และโปรตีนเอ็นเอส 5 แบบที่ไม่สามารถเข้าสู่นิวเคลียสได้ ซัยโตไคน์ที่ถูกกระตุ้นโดยโปรตีนเอ็นเอส 5 จะถูกเลือกเพื่อศึกษาต่อถึงกลไกกระตุ้นด้วยโปรตีนเอ็นเอส 5 การแสดงออกของโปรตีนเอ็นเอส 5 ที่มีต่อ promoter ของซัยโตไคน์ ทำการศึกษาโดย Luciferase reporter gene system บทบาทของโปรตีน NF-κB ในการจับบน promoter ทำการศึกษาโดยวิธี chromatin immunoprecipitation (ChIP) assay ผลการศึกษาพบว่าซัยโตไคน์ RANTES ซึ่งเกี่ยวข้องกับการกระตุ้นการผ่านของสารน้ำออกนอกหลอดเลือด ถูกกระตุ้นโดยโปรตีนเอ็นเอส 5 ในนิวเคลียส ให้มีการสร้างเพิ่มขึ้นทั้งในระดับอาร์เอ็นเอและโปรตีนอย่างโดดเด่นกว่าซัยโตไคน์ชนิดอื่น และพบว่าโปรตีนเอ็นเอส 5 กระตุ้นการทำงานของ RANTES promoter เมื่อศึกษาด้วยวิธี luciferase reporter assay และพบว่าโปรตีน NF-κB มีการจับบน promoter มากขึ้นในเซลล์ที่มีโปรตีนเอ็นเอส 5 โดยการตรวจด้วยวิธี ChIP assay นอกจากนี้ยังพบว่าโปรตีนเอ็นเอส 5 ที่อยู่ในนิวเคลียส มีจับกับโปรตีน Daxx ซึ่งทำหน้าที่ยับยั้งการทำงานของโปรตีน NF-κB ซึ่งอาจจะทำให้โปรตีน NF-κB หลุดออกมาเป็นอิสระจากโปรตีน Daxx ดังนั้นจึงสรุปจากผลการทดลองทั้งหมดได้ว่า โปรตีนเอ็นเอส 5 สามารถกระตุ้นการสร้างซัยโตไคน์ RANTES-ผ่านทางการจับกับโปรตีน Daxx ซึ่งทำให้โปรตีน NF-κB หลุดออกเป็นอิสระจากโปรตีน Daxx และเมื่อโปรตีน NF-κB เป็นอิสระจึงจับและกระตุ้นการทำงานของ RANTES promoter ในการสร้างซัยโตไคน์ RANTES

195 หน้า

CONTENTS

CONTENTS (cont.)

Page

CONTENTS (cont.)

Page

CONTENTS (cont.)

Page

CONTENTS (cont.)

Page

CONTENTS (cont.)

Page

CONTENTS (cont.)

Page

CONTENTS (cont.)

Page

LIST OF TABLES

.

LIST OF FIGURES

LIST OF FIGURES (cont.)

LIST OF FIGURES (cont.)

LIST OF FIGURES (cont.)

LIST OF ABBREVIATIONS

Abbreviation	Term
A	Alanine, Adenosine
A549	Lung adenocarcinoma epithelial cell line
Ab	Antibody
ADE	Antibody-dependent enhancement
Ag	Antigen
AP-1	Activating protein1
Bp	Basepair
BSA	Bovine serum albumin
C	Capsid or core protein
CCL-2	Chemokine (C-C motif) ligand 2
CCL-3	Chemokine (C-C motif) ligand 3
CCL-4	Chemokine (C-C motif) ligand 4
CCL-5	Chemokine (C-C motif) ligand 5
CCR-1	Chemokine (C-C motif) receptor 1
CCR-3	Chemokine (C-C motif) receptor 3
CCR-5	Chemokine (C-C motif) receptor 5
cDNA	Complementary DNA
ChIP	Chromatin immunoprecipitation
CK-II	Casein kinase II
Co-IP	Co-immunoprecipitation
CPE	Cytopathic effect
CRE	Cyclic AMP-responsive element
CRM-1	Chromosomal regional maintenance 1
CXCL-8	Chemokine (C-C motif) ligand 8
CXCL-10	Chemokine (C-X-C motif) ligand 10
DAB	Diaminobenzidine

LIST OF ABBREVIATIONS (cont.)

Abbreviation	Term
Daxx	Death domain-associated protein
DC	Dendritic cells
DENV	Dengue virus
DF	Dengue fever
DHF	Dengue hemorrhagic fever
DMEM	Dulbecco's Modified Eagle Medium
DNA	Deoxyribonucleic acid
dsDNA	Double-stranded DNA
DSS	Dengue shock syndrome
DTT	Dithiothreitol
E	Envelope protein
EDTA	Ethylenediaminetetraacetic acid
eIF4E	Eukaryotic translation initiation factor 4E
ELISA	Enzyme-linked immunosorbent assay
EMSA	Electrophoretic mobility shift assay
ER	Endoplasmic reticurum
FBS	Fetal bovine serum
FFU	Focus forming unit
g	Gram
G	Guanosine
gDNA	Genomic DNA
GOI	Gene of interest
H	Hour
HBx	Hepatitis B virus x protein
HCV	Hepatitis C virus
HEK	Human embryonic kidney cell line
HepG2	Human hepatoma epithelial cell line
HKG	Housekeeping gene

LIST OF ABBREVIATIONS (cont.)

Abbreviation	Term
h p.i.	Hour post infection
h p.t.	Hour post transfection
HUVEC	Human umbilical vein endothelial cells
HRP	Horseradish peroxidase
IFN	Interferon
IFN-α	Interferon alpha
IFN	Interferon beta
IFN-γ	Interferon gramma
Ig	Immunoglobulin
IgG	Immunoglobulin G
IKK	IκB kinase
IL-1β	Interleukin 1 beta
IL-2	Interleukin 2
IL-6	Interleukin 6
IL-8	Interleukin 8
IL-10	Interleukin 10
Imp β	Importin β
IP	Immunoprecipitation
IP-10	Interferon gamma-induced protein 10
IRFs	Interferon regulatory factors
ISRE	Interferon-stimulated responsive element
K	Lysine
kb	Kilobase
kDa	Kilodalton
KLF13	Kruepple-like factor 13
LB	Luria-Bertani
LMB	Leptomycin B
M	Membrane protein

LIST OF ABBREVIATIONS (cont.)

Abbreviation	Term
MCP-1	Monocyte chemotactic protein-1
MDA5	Melanoma differentiation-associated gene 5
MEM	Minimum Essential Medium
MHC	Major histocompatibilty complex
$MgSo_4$	Magnesium sulfate
MIF	Macrophage migration inhibitory factor
MIP-1α	Macrophage inflammatory protein-1 alpha
MIP-1β	Macrophage inflammatory protein-1 beta
ml	Millilitre
MOI	Multiplicity of infection
mRNA	Mesenger RNA
MT	Mutantion
MTase	Methyltransferase
NaCl	Sodium choride
NES	Nuclear exporting sequence
NFAT1	nuclear factor of activated T cells 1
Ng	Nanogram
NF-IL6	Nuclear factor of interleukin 6
NF-κB	Nuclear factor kappa-light-chain-enhancer of activated B cells
NK	Natural killer
NLK	Nemo-like kinase
NLS	Nuclear localization sequence
NS	Nonstructural protein
OAS	2', 5'-oligoadenylate synthetase
PAGE	Polyacrylamide gel electrophoresis
PBS	Phosphate buffer saline
PCAF	p300/CBP-associated factor kinase

LIST OF ABBREVIATIONS (cont.)

Abbreviation	Term
PCR	Polymerase chain reaction
PIC	Protease inhibitor cocktail
PKR	Double-stranded RNA-dependent protein kinase
PLB	Passive Lysis Buffer
PMSF	Phenylmethylsulfonylfluoride
prM	pre-membrane protein
qRT-PCR	Real-time reverse transcription polymerase chain reaction
RANTES	Regulated upon activation, normal T-cell expressed and secreted
RC	Replication complex
RdRp	RNA-dependent RNA-polymerase
RFLAT-1	RANTES factor of late activated T lymphocytes 1
RIG-I	Retinoic acid inducible gene I
RLU	Relative light unit
RNA	Ribonucleic acid
RSV	Respiratory syncytial virus
RT-PCR	Reverse transcription polymerase chain reaction
SDS	Sodium dodecyl sulfate
shRNA	Short hairpin RNA
sNS1	Endogenous NS1 signal peptide sequence
STAT	Signal transducer and activator of transcription
TBS	Tris buffered saline
TBST	Tris buffered saline with Tween

LIST OF ABBREVIATIONS (cont.)

Abbreviation	Term
TGN	Trans-Golgi network
Th	T helper cells
TLRs	Toll-like receptors
TNF-α	Tumor necrosis factor alpha
TPB	Tryptose phosphate broth
U	Unit
USA	United States of America
UTR	Un-translated region
VBP1	VHL binding protein 1
VEGF	Vascular endothelial growth factor
vRNA	viral RNA
WHO	World health organization
WT	Wild-type
ZO-1	Zonula occludens-1

CHAPTER I
INTRODUCTION

Dengue virus (DENV) is an important mosquito-borne virus that causes a global public health disease, dengue fever (DF) and its potentially life-threatening severity forms – dengue hemorrhagic fever (DHF) and dengue shock syndrome (DSS) (1). The clinical signs and symptomatic manifestations after DENV infection vary depending on several factors of individuals. The typical symptoms of DF include sudden onset of high fever, which could be biphasic lasting 3 to 7 days, severe headache, retro-orbital pain, muscle and joint, flushed skin (on face and neck), a macular papular rash, or a fine skin rash on the arms and legs (2), (3), (4) , whilst a few cases of DENV infection (1-2% of DENV-infected cases) can develop into the more severe form, DHF, which is characterized by presenting high fever and other symptoms as DF: hemorrhangic manifestations, thrombocytopenia, and increase of vascular permeability or plasma leakage phenomenon (3). Furthermore, other serious complications can also be observed in DHF cases, such as hepatomegaly, pleural effusions, pericardial effusion, ascites, and shock (5). DHF with shock complication known as DSS, is the most critical and severe form and causes mortality (9.3-47%) (6). Almost all DHF/DSS cases are observed in secondary infection with a different serotype from the previous infection.

Nowadays, the complete understanding of the pathologic mechanisms is still unclear, but several theories have been proposed to explain the mechanisms of dengue to cause the severity, especially in secondary infection with a different serotype from the previous. Antibody-dependent enhancement or the ‘ADE theory’ postulates that the raised antibodies from the previous infection with one serotype could not neutralize the current infection with a different serotype. Furthermore, these non-neutralizing antibodies are cross-active to the current infecting serotype and enhance a viral internalization of Fcγ receptor-bearing cells, resulting in an increase of viral upload/replication accompanied by massive soluble mediators, increased vascular

permeability of endothelial cells, and hemostatic disorder found in severe disease (7), (8). In addition, the excessive immune responses found in DHF/DSS cases are proposed to be the result of cross-active memory T and B cells of the original antigenic sin theory. These memory B and T cells are specific for the previous rather than the current DENV infection, which result in the abolished or delayed viral clearance and/or increased cytokine secretion along with an increase of apoptosis of both infected cells and uninfected bystander cells (9). The complement activation has been reported to be a cause of endothelial cell death, resulting in the vascular leakage, a hall mark of DHF/DSS. Recently, the overproduction of immunue mediators such as cytokines and chemokines has been demonstrated to be involved in the immunopathogenic mechanism of vascular leakage and organ injuries in DHF/DSS.

A massive cytokine/chemokine production or "cytokine storm" has become an intensive study during this decade. Several reports have demonstrated cytokine expression profiling of DENV-induced cytokines in both patient samples and *in vitro* cell lines. They found that the higher level production of several cytokines has been linked or related to the severity of the disease, including hypotension, thrombocytopenia, hepatic dysfunction, and hemorrhagic shock. The examples of those cytokines are TNF-α, IL-6, IL-8, IL-10, MCP-1, MIP-1α, CXCL-8, CXCL-10, IFN-γ, and RANTES (9), (10). However, these data are observed in a DENV infection in which all DENV proteins are expressed in the system. There are several research groups who have studied to identify which proteins of DENV control this induction. Among ten of the DENV proteins, nonstructural protein 5 or NS5 showed the most predominant role in cytokine induction, even though NS1 and NS4B have also been reported to play a role in cytokine induction. Medin et al reported that NS5 has a more predominant role than other DENV proteins in IL-8 induction (11). The THP-1 monocytic cell line, transfected with plasmid expressing all of the NS proteins (NS1 to NS5), individually showed that THP-1 cells expressing NS5, as well as NS4B, secrete higher levels of IL-6, IL-8, and IP-10 than other NSs, whilst only NS5 showed the significantly induced IFN-γ production (12). Furthermore, NS5 has been reported to activate NF-κB activity in TNF-α-treated HEK 293 cells and to activate the IL-8 promoter via c/EBP, AP-1 and NF-κB transcription factors (11). NS5 was found to interact with the NF-κB inhibitor protein, human death domain-associated protein or

Daxx, by our yeast two-hybrid screening. The interaction between NS5 and Daxx has been confirmed in HEK 293 cells by Co-IP, and the co-localization assay and has also been published (13). As already known, NF-κB is a major regulator of cytokine and chemokine gene expression; hence, this evidence might suggest the involvement of NS5 in cytokine regulation.

NS5 is the largest and most conserved *Flavivirus* protein (14), (15). It contains multiple enzymatic functions including N-7, 2'-*O*- methyltransferase or 2'-*O*-MTase (16), (17) and guanylyltransferase (18) which are required for RNA capping formation and RNA-dependent RNA-polymerase (RdRp) which is required for DENV RNA replication (19). In addition, NS5 contains two nuclear localization sequences (NLSs) including bNLS and a/bNLS (20) and nuclear exporting sequence (NES) (21) enabling NS5 to shuttle between cytoplasm and nucleus of infected or transfected cells. The a/bNLS is a critical domain for NS5 nuclear translocation and mutation in this site abrogates nuclear translocation of NS5, whereas bNLS contributes to maximal accumulation (22). NS5 has been reported to interact with NS3 in the cytoplasm of DENV-infected cells and this interaction is required for DENV RNA replication (23). Surprisingly, several studies demonstrated a large proportion of NS5 expressed in the nucleus of the cells, whereas a little amount was present in the cytoplasm suggesting that DENV NS5 might have additional roles or auxiliary functions, besides its RdRp activity, to support DENV replication or pathogenesis. In brief, the roles of nuclear NS5 are still a mystery. There is plenty of evidence demonstratingthat some viruses, predominantly replicating in the cytoplasm, often utilize the nucleus for functions, such as modulation of host cell defenses, manipulation of host gene expression and regulation of the cell cycle (24), (25). Alvisi et al. has suggested that nuclear NS5 might be involved in regulation of host cellular gene expression and apoptosis (26). Besides the role in RNA replication, NS5 has been reported to be important for cytokine induction, as described previously. Taken together, the study of the role of NS5, especially in the nucleus, in regulation of cytokine expression is very interesting. Thereby, this study aims to investigate whether, besides the known NS5-induced cytokine genes already reported, NS5 still induces other cytokine production, and how NS5 mediates cytokine production. In addition, the involvement of NF-κB activity in NS5-regulated cytokine gene expression is identified as well.

This work was designed by screening cytokine expression profiling in a DENV infection system in HEK 293 cells by RT^2 PCR Array to obtain the overall outcome of cytokine gene expression profiling, especially DENV-induced cytokine genes. Then, only DENV-induced cytokine genes were chosen for further studies as a result of NS5 to these cytokine expressions. DENV-induced cytokine genes were examined for their expression in HEK 293 cells, expressing either WT-NS5 or MT-NS5, by qRT-PCR using specific primers for each gene. MT-NS5 was mutated in a/bNLS to inhibit its nuclear translocation. Only one of the NS5-induced cytokine genes was chosen for further studies. A luciferase reporter plasmid, containing the promoter of the selected NS5-induced cytokine gene, was constructed and used to investigate the influence of NS5 on the selected NS5-induced cytokine promoter. To clarify whether expression of the selected cytokine promoter was mediated through NF-κB binding at the NF-kB site, it was mutated and analyzed by luciferase reporter gene assay. Chromatin immunoprecipitation assay was performed to examine the binding ability of NF-κB selected cytokine promoter in NS5-transfected HEK 293 cells. Finally, the proposed model of cytokine regulation by DENV NS5 was generated and the interaction between NS5 and Daxx was drawn in this proposed mechanism. All of the results from this study provide a better understanding of the pathogenic mechanism of DHF/DSS development, even though it is only part of the whole complicated mechanisms, but it might already be useful for future drug designs and vaccine developments.

CHAPTER II
OBJECTIVE

2.1 Main objectives

1. To identify whether DENV NS5 regulates the production of other host inflammatory cytokines besides IL-6, IL-8, IP-10 and IFN-γ
2. To identify the mechanism how DENV NS5 regulates the cytokine production

2.2 Specific objectives

1. To identify that DENV NS5 influences in the activation of such cytokine gene promoter
2. To identify whether the influence of DENV NS5 in cytokine promoter activation is mediated through NF-κB activation
3. To identify whether DENV NS5 influences in the DNA-binding activity of NF-κB

CHAPTER III
LITERATURE REVIEW

3.1 Epidemiology of dengue virus (DENV) infection

Dengue virus (DENV) is a serious mosquito-borne human disease worldwide, especially in Southeast Asia, Pacific, and America (27). About 50 to 100 million of infections lead to 500,000 hospitalizations, and 20,000 deaths, estimated by the World Health Organization (WHO) each year (28). In recent decades, the prevalence of dengue is endemic in more than 100 countries (1). DENV composes of 4 serotypes including serotype 1 to 4. They are related, but distinct in antigenic properties (29), (30). DENV is transmitted to human by biting of infective female mosquitoes of the *Aedes* genus, *Aedes aegypti* and *Aedes albopictus* (31), (16). DENV can affect all ages of people, including infants, children, youngsters, adults and elderly. However, it predominantly affects the morbidity and mortality in children. The epidemics caused by multiple serotypes of DENV have become increasingly frequent. The striking changes in the pattern of disease occurrence lead dengue to become one of the most important mosquito-borne viral diseases in the world (32).

3.2 Clinical signs and symptoms of DENV infection

DENV infection can be divided into two types, which are primary infection and secondary infection. Dengue infection causes a spectrum of illnesses ranging from acute febrile illness, known as dengue fever (DF), to the most severe life-threatening forms known as dengue hemorrhagic fever (DHF) and dengue shock syndrome (DSS) (1). DF is commonly found in dengue-infected patients both in primary and secondary infections. The typical symptoms include sudden onset of high fever, which can be biphasic, which lasts 3 to 7 days (2), (3), severe headache, retro-orbital pain, muscle and joint, flushed skin on face and neck, a macular papular rash,

or a fine skin rash on the arms and legs (33). Like DF, DHF can occur in both primary and secondary infection, but is usually found in secondary infection, especially in secondary infection with difference serotypes from the primary infection. In 1997, WHO defines the criteria for DHF/DSS diagnosis as shown in figure 3.1 (34). Recently, DHF/DSS cases have increased and the criteria for DHF/DSS diagnosis have become separately tailored to regional or national, resulting in the diversities of dengue diagnosis and treatments. To make a standardized guideline, WHO has defined a new guideline based on three different levels of clinical responses to dengue infection, including dengue, dengue with warning signs, and severe dengue for benefiting in diagnosis and therapeutic treatments as show in figure 3.2 (35). Furthermore, DHF/DSS also has severe complications, such as liver failure, disseminated intravascular coagulation, encephalopathy, myocarditis, acute renal failure, and hemolytic ureamic syndrome.

3.3 Diagnosis and treatments

As described previously, DF causes fever for 3-5 days with other symptoms, whilst DHF/DSS have the same symptoms as DF, but combined with the hallmark of symptoms including increase of vascular permeability and hemorrhage; thereby diagnosis of dengue infection is firstly done via clinical symptoms. However, laboratory tests are needed for the accuracy of diagnosis. There are many methods for dengue detection, including virus isolation, serology techniques (hemagglutination inhibition tests, enzyme-linked immunosorbent assay **(**ELISA), and neutralization tests), and molecular techniques for viral RNA/protein detection (reverse transcription polymerase chain reaction or RT-PCR and immunofluorescence staining) (5). Virus isolation, viral RNA/protein detection, and captured ELISA are the commonly used methods.

Currently, there is no effective vaccine for prevention of and antiviral drugs for treatment of dengue infection. Several research efforts have the goal to develop “an ideal vaccine” that can induce a long-life immune response against all four serotypes of dengue virus simultaneously, while avoiding the possible risk of developing the severe forms of disease through incomplete or modified responses.

Nowadays, various types of dengue vaccine have been developed both live (attenuated and chimeric) and living (inactivated, recombinant subunit, and naked DNA) dengue vaccines. All of them have undergone phase I and phase II clinical trials in populations in the United States (36), (37) and in Thailand (38), (39).

3.4 Molecular biology of DENV and DENV proteins

DENV is a member of the *Flavivirus* genus in the *Flaviviridae* family. As described previously, DENV is composed of 4 serotypes in which they are related but distinct in antigenic properties. The genome of DENV is a positive stranded RNA with 11 kb in length, including the sequences encoding ten proteins and two untranslated regions (5'- and 3'-UTR) (40). The DENV RNA genome is encapsulated within the nucleocapsid and the lipid bilayers of the envelope protein. The mature virion of DENV is about 60 nm in size and has a hexagonal shape. After getting into the host cells, the RNA genome is translated into a polyprotein precursor of about 3,000 amino acids, which is cleaved by viral and host proteases to generate three structural proteins, including capsid or core (C), membrane protein (M), and envelope (E), and seven nonstructural proteins (NS) including NS1, NS2A, NS2B, NS3, NS4A, NS4B, and NS5, respectively, as shown in figure 3.3 (41). DENV is believed to entry into the target cells via either non-classical or classical endocytosis, depending on the DENV strains or host cell types (42). In classical receptor-mediated endocytosis, the types of receptor depend on the serotype of DENV. The steps of DENV life cycle is shown in figure 3.4. As described above, the DENV genome generates 10 proteins; those are important for its replication and pathogenesis. Several proteins have been characterized for their roles in DENV infection, such as the structural proteins. Capsid protein plays a role in the nucleocapsid assembly through interaction with RNA (43) and involvement in apoptosis (44), the membrane protein works as a part of nucleocapsid (45), and the envelope protein plays a role in the step of viral attachment to the host cell surface (46) whilst all of dengue non-structural proteins are mainly involved in RNA

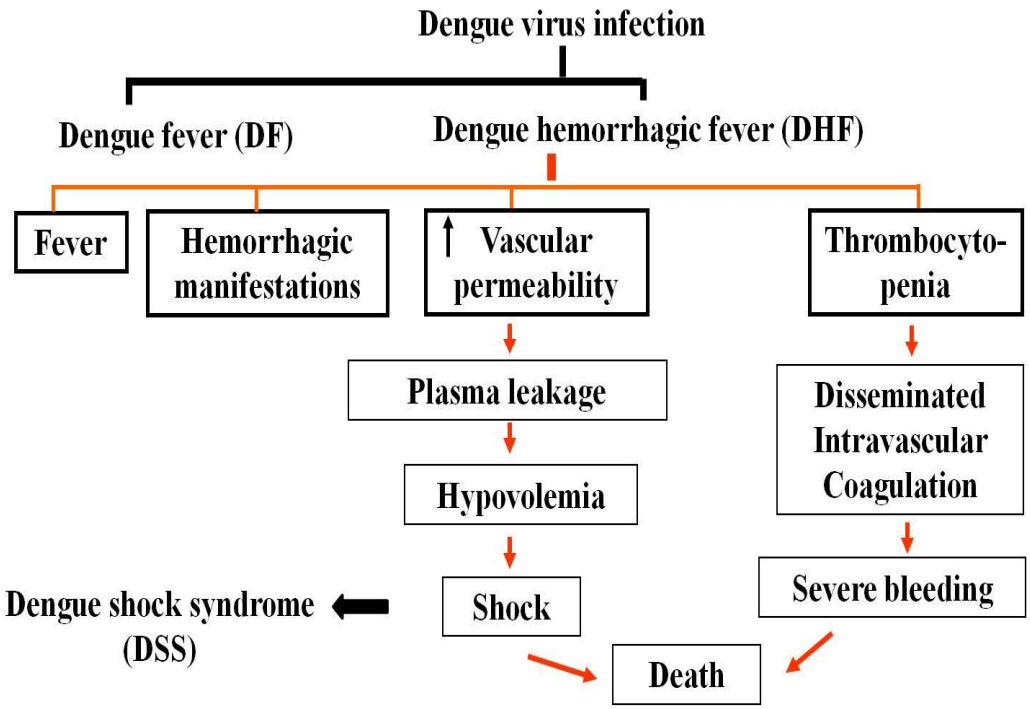

Figure 3.1 1997 WHO case definition for DHF and DSS (34).

Figure 3.2 2009 WHO dengue case definition (35).

replication by forming a replication complex. NS1, besides its role in the RNA replication complex, can be used as a marker for dengue diagnosis in early stage and can be a predictor of DHF progression, because it is secreted into the plasma of dengue patients (47). Furthermore, NS1 is involved in vascular leakage in DHF/DSS patients by activating the complement system leading to the forming of SC5b-9 (48). DENV contains two enzymatic proteins. The first is NS3 protein, which has a serine protease and helicase functions in its N-and C-terminus, respectively (49). The second is NS5, which has a methyltransferase (MTase) domain at N-terminus and a polymerase domain at C-terminus (50). Both of them are important for DENV replication. For other NSs, NS2B is a co-factor of NS3 protease, whilst NS2A and NS4B are identified to be interferon (IFN) inhibitor proteins. The summary of the characterized role of ten proteins of DENV involving in DENV replication is shown in figure 3.5.

3.5 Innate and adaptive immune responses in DENV infection

3.5.1 Innate immune response

Langerhans cells, interstitial dendritic cells, and dermal cells have been proposed as the first target cells for DENV infection after biting of dengue-infected mosquitoes (51), (52). Furthermore, dengue viral antigens have also been detected in lymphocytes, monocytes, alveolar macrophages, endothelial cells, and Kupffer cells of DENV-infected human (53). After entering into these cells, DENV RNA is recognized by endosomal Toll-like receptors (TLRs), including TLR-3 and TLR-7/8 (54) and cytoplasmic receptors, retinoic acid inducible gene I or RIG-I and melanoma differentiation-associated gene 5 or MDA5 (55). Then, the host innate immune response is rapidly initiated to defend against and limit dengue infection. The recognition of DENV RNA by host cell receptors lead to the activation of 2 major groups of transcription factors, which are nuclear factor kappa-light-chain-enhancer of activated B cells (NF-κB) and interferon regulatory factors (IRFs) and result in the production of type I.

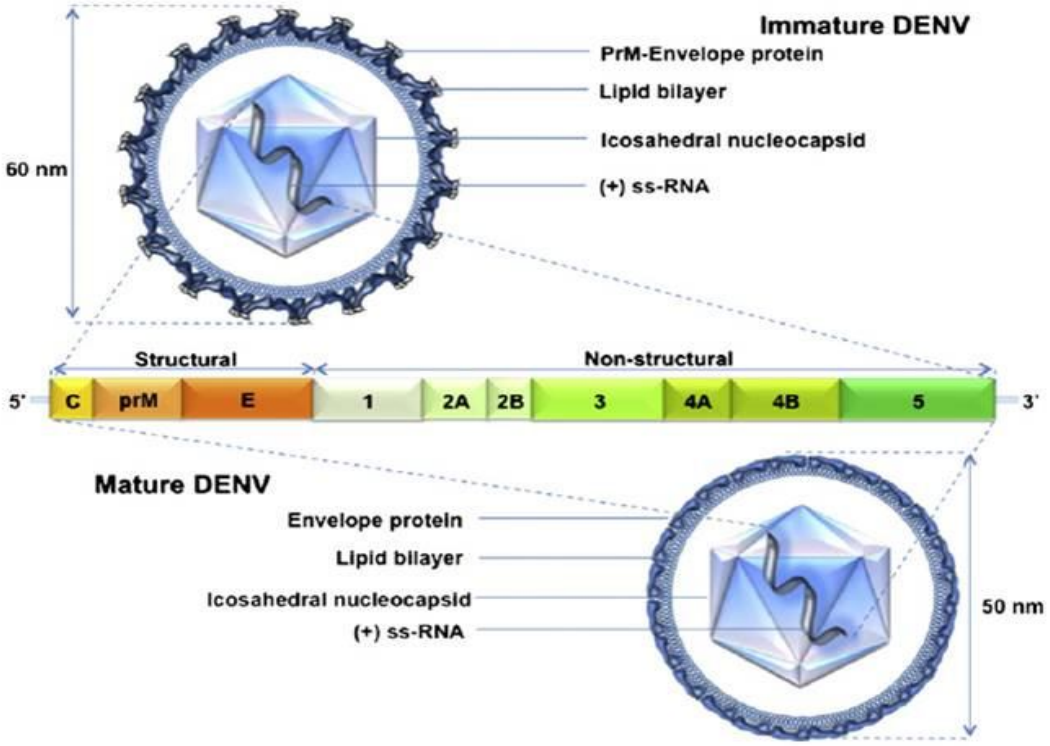

Figure 3.3 The structural and genomic structure of DENV (56).

A positive-strand genomic RNA of DENV is encapsulated with nucleocapsid and envelope protein. DENV genomic RNA contains 10 genes coding for three structural proteins (C, prM, and E) and seven non-structural proteins (NS1 to NS5), as displayed in figure1. An immature virion (upper most panel) of DENV has a spike glycoprotein shell, which is subsequently cleaved by the furin host enzyme to generate mature virion (lower most panel). ss RNA = single-stranded ribonucleic acid.

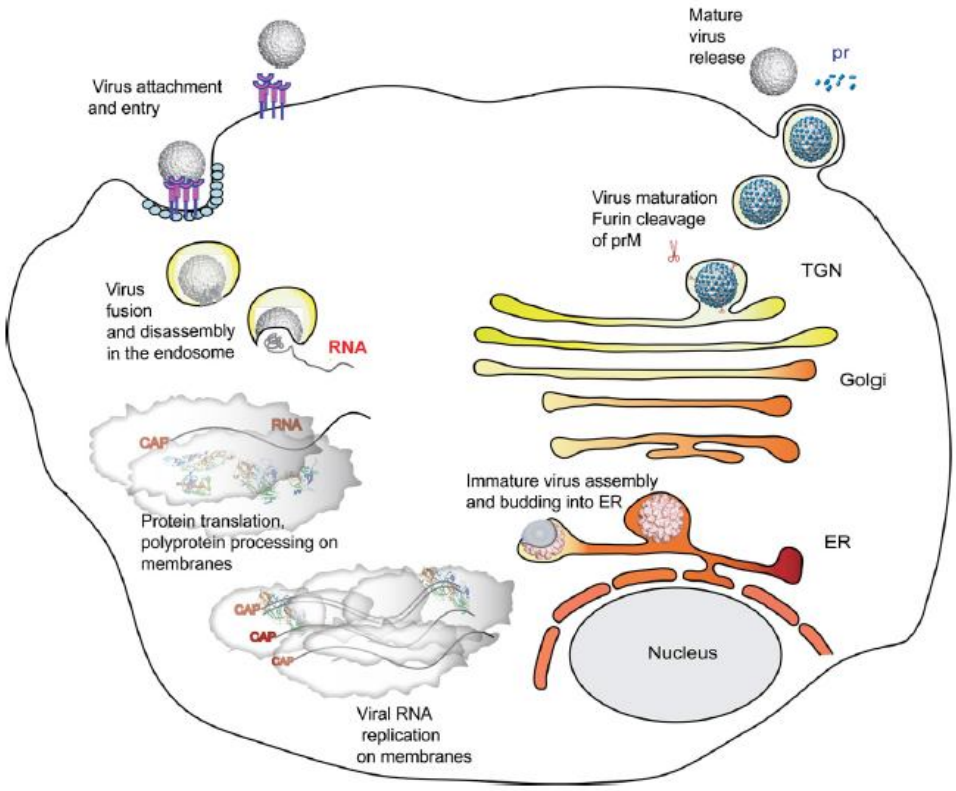

Figure 3.4 Intracellular life cycle of Flavivirus including DENV (57).

Dengue virus binds and enters into the cells. Endosomal acidification results in an irreversible trimerization of the viral E protein, exposing the fusion domain and release of genomic RNA into cytoplasm. After uncoating, vRNA is translated at ER-derived membranes, where it is processed into three structural and seven non-structural proteins. Then, RNA replication is initiated. Subsequently, the assembly of newly synthesized immature virions has occurred in the ER. Host cellular enzyme, furin, cleaves prM into M protein to generate mature virions at the Golgi compartment and exits via the host secretory pathway. vRNA = viral RNA, TGN = Trans-Golgi network.

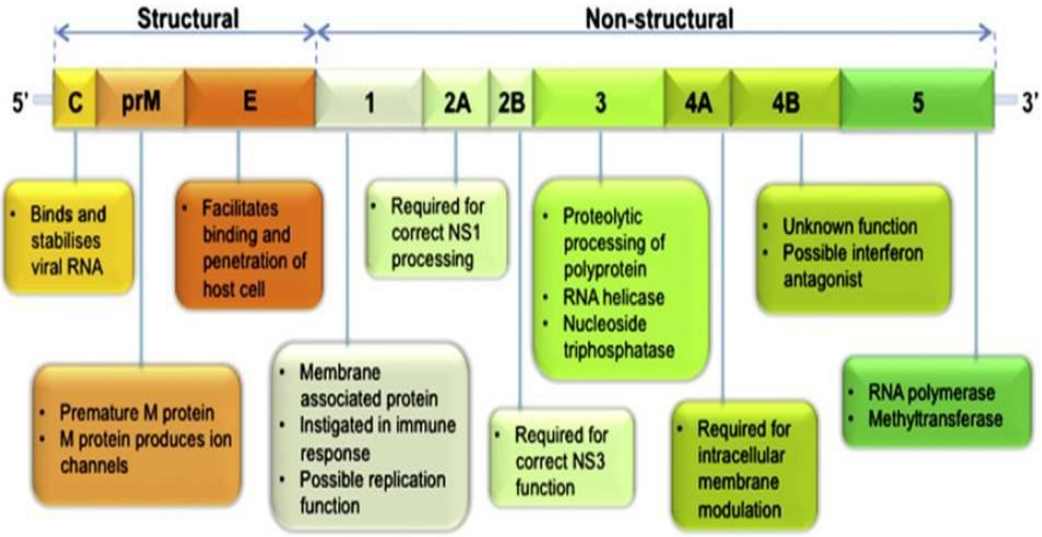

Figure 3.5 Functions of each DENV protein (56).

interferon (type I IFN), including IFN-α or IFN-β, and inflammatory cytokines/chemokines, such as TNF-α, IL-6, IL-8, CCL-2 or MCP-1, CCL-3 or MIP-1α, CXCL-10 or IP-10, and IFN-γ (58), (9), (11), (51). The sources of IFNs and various cytokines/chemokines include the immune cells, such as dendritic cells (DCs), neutrophils, monocytes, macrophages, and natural killer (NK) cells and other permissive cells, such as endothelial cells and fibroblasts (51). The IFN-α/β and cytokines/chemokines secreted from these infected cells induce the activation of other immune cells, such as DC (51), NK cells (59), monocytes/macrophages (60), and neutrophils (51). In addition for a role in the innate immune response, DC links an innate to adaptive immune response (61). The antiviral actions of these activated cells can occur via direct cytolysis or secreting some cytokines/chemokines to enhance the efficient viral clearance. Besides, the role of immune cells in cytolysis, humoral immune responses, including IFN and complement, also play important roles. IFN is a major defense mechanism of the innate immunity to counteract viral infection. The secreted IFN-α, IFN-β and IFN-γ exert their actions via binding to their IFN receptors on itself or the neighboring cells, resulting in the activation of signal transducers and activators of transcription (STAT2) or (STAT1) and the production of many antiviral genes, such as double-stranded RNA-dependent protein kinase (PKR) and 2', 5'-oligoadenylate synthetase (OAS) to limit the replication or enhance viral clearance (62), (63). The complement system is also a key modulator in the innate immune response. The complement system is composed of a number of small proteins, which normally circulate in the blood as an inactive precursor. When they are activated by some triggers, including cytokines, the proteases in the system cleave the precursor into an active form and amplify the cascade of further cleavages. The final end product of complement, called 'membrane attack complex', consists of C5b, C6, C7, C8, and C9. This complex forms a transmembrane channel or pore on infected cells, which cause the osmotic lysis of infected cells (64). The role of complement in dengue infection is almost activated by DENV antibody complex and seems to be involved in severity of secondary dengue infection (65).

3.5.2 Adaptive immune response

Both humoral and cellular immunity of the adaptive immune response are activated to resolve DENV infection by providing DENV-specific antibody from B lymphocytes for DENV neutralization and protection from re-infection, as well as activating T lymphocytes for viral clearance, respectively (7). As described previously, DC links an innate to adaptive immune response. The role of DC is to capture DENV antigens, process into the immunogenic peptides, to emigrate from infected area to paracortex of lymph nodes, and present the peptides to naïve B and T cells (66).

For humoral antibody responses, the robust neutralizing antibody responses are developed after DENV antigens are presented to B cells with an early IgM response, followed later by an IgG response (1). The raised antibody provides lifelong protection against the current infecting serotype, but has a short protection against the other serotypes. The predominant DENV antigen of B cells in antibody response is E glycoprotein and serves as a principle target for neutralizing antibody. Furthermore, prM, NS1, NS3, and NS5 also have been targets for DENV-activated antibody responses (67), (68). The neutralization of DENV infection by specific antibodies is achieved when there are enough molecules of antibody binding to an accessible epitope on the antigens, especially on E protein, thereby preventing binding of dengue to cell surface receptors or preventing the release of dengue RNA genome into the cytoplasm of infected cells (69), (70). Furthermore, other DENV-specific antibodies such as NS1-specific antibodies can activate the complement proteins, resulting in complement-mediated lysis of dengue-infected cells (71). Note that antibodies to all DENV antigens, especially against E protein, are highly serotype cross-reactive (72) whereby the antibody responses can cause the severity of dengue infection, especially in the secondary infection with different serotypes. The details for this phenomenon will be demonstrated later.

For cellular T cell responses, dengue infection causes the activation and proliferation of dengue-specific $CD4^+$ and $CD8^+$ T cells. The activation of T cells requires presentation of viral peptides on the surface of infected cells in the cortex of the major histocompatibilty complex (MHC) (66). MHC class II molecules present dengue antigen peptides to $CD4^+$ T cells, which predominantly produce cytokines,

molecules present dengue antigen peptides to $CD8^+$ T cells, which are predominant in lysis of dengue-infected cells (9). For most T cell studies, the pattern of cytokine production is T helper 1 (T_H1) or (T_01)-like profile such as IFN-γ, TNF-α, IL-2, and CCL-4 or MIP-1β whilst (T_H2)-type cytokines, IL-4, is less (73). The of T cell responses in dengue infection is summarized into 2 major aspects. In primary infection, T cells have the strong effects on the infecting serotype. In contrast to secondary infection, the T cells are highly serotype cross-reactive (74).

3.6 Immune responses associated with immunopathogenesis of DENV infection

Most dengue-infected cases show an asymptomatic disease, while less than 10% develops a severe disease, DHF or DSS (75). As described previously DHF/DSS can be found both in primary and secondary infections, but several incidences demonstrate that DHF/DSS cases occur predominantly either in individual persons with heterotypic DENV secondary infection or in infants with primary infection, but who were born from dengue immune mothers (7), (9). While the severe disease found in primary infection is favored by the combination of viral load, strain virulence, and individual host immune responses (76), the pathogenic mechanisms of dengue-induced severe disease involve a complex interplay between host and viral factors. The risk factors include age, virus, serotype/strain, and genetic background of the patients (27), (77). Several theories have been raised to explain the observation that most of severe cases occurred in the secondary infection. Most theories are agreeable that individual immune status or immune responses determine the outcome of dengue infection.

3.6.1 Antibody-dependent enhancement (ADE)

ADE postulated that the raised antibodies from the previous infection with one serotype could not neutralize the current infection with a different serotype. Furthermore, these non-neutralizing antibodies are cross-active to the current infecting serotype and enhance a viral internalization of Fcγ receptor-bearing cells resulting in increasing of viral upload/replication accompanied by massive soluble mediators, the

increased vascular permeability of endothelial cells, and hemostatic disorder found in severe disease (7), (8).

3.6.2 Cross-reactive B and T cells (original antigenic sin)

Another theory, which is distinct from ADE, but makes the complementary of immunopathological involvement in severe dengue disease, is the re-activation of cross-reactive memory B and T cells. These memory B and T cells are specific for the previous rather than current DENV infection, which results in the abolished viral clearance and/or increased cytokine secretion along with increase of apoptosis of both infected cells and non-infected bystander cells (9). This phenomenon is defined as original 'antigenic sin', which can be divided into 2 aspects. For the aspect of B cells in secondary infection, the titer of antibodies specific for the previous serotype infection increases substantially and remains higher than antibodies specific for the current infecting serotype, resulting in ineffective neutralization and other immune-mediated pathogenesis (78), (79). For the aspect of T cells, they have higher responses and expansion of memory T cell populations to the previous encountered DENV serotype than the current infecting serotype, and thereby an amplification of cytokine secretion (80).

3.6.3 Cytokine storm

The 'cytokine storm' was named for the phenomenon in which there is a massive inflammatory cytokine secretion in response to DENV infection. It seems to be a consensus of all theories and can occur in both primary (secreted directly from dengue-infected cells) and secondary infection (cross-reactive B, T and other immune cells). It is believed to contribute to the hallmarks of pathogenesis of severe dengue disease, including increase of vascular permeability, occurrence of hemorrhagic manifestations, hemoconcentration, development of intractable shock, leading to death in some cases, and organ injuries, such as liver (9), (76), (81), (82). Although the elevated level of inflammatory cytokines and chemokines can be found in DF patients, the higher level is always found in DHF/DSS patients (83), (84), (51). Several studies have demonstrated that the higher levels of TNF-α, IL-6, IL-8, IL-10, MCP-1, MIP-1α, CXCL-8 or IL-8, IP-10, and IFN-γ have been linked or are related to the severity

of disease, including hypotension, thrombocytopenia, hepatic dysfunction, and hemorrhagic shock (9). Avirutnan et al. also suggested that the selective production of IL-8 and CCL-5 or 'regulated upon activation, normal T-cell expressed and secreted' (RANTES) in dengue-infected endothelial cells was responsible for vascular leakage found in DSS patients (10). Furthermore, the higher level of other cytokines/chemokines has been reported to be involved in an increase of vascular permeability of endothelial cells such as TNF-α (77), MCP-1 (83), and macrophage migration inhibitory factor (MIF) (85). These cytokines/chemokines interfere with the arrangement of tight junction protein, such as zonula occludens-1 (ZO-1). The effect of these cytokines on endothelial cells has been confirmed for the specificity by using their specific antibodies, inhibitors or gene knockdown experiments in both cell lines and mice. Besides the role in dengue pathology by effecting increased vascular permeability of endothelial cells, a massive cytokine storm has been proposed to be involved in organ injuries by increasing the infiltrated immune cells to the infected sites and leading to excessive injured and apoptotic cells, as found in case of higher induction level of IL-8, RANTES, MIP-1α, and MIP-1β (86), (11).

3.6.4 Complement activation

Several studies have suggested that complement system is involved in the transient plasma leakage phenomenon in DHF/DSS patients. Bokisch et al. have demonstrated the remarkably reduction of C3, C4, and C5 levels in DHF patient sera and the most remarkable abnormalities have been found in higher grades of DHF (87). These observations are corresponded to Malasit et al. who also detected the elevated levels of products of complement activation, C3a and C5a, in plasma of patients with DHF/DSS (88). In addition, the end product of complement activation, C5b-9, have also been found in circulation of severe dengue patients and on the cell surface of DENV-infected endothelial ECV304 cell line (88), (10). The latter observation also proved that this phenomenon is dengue antibody-dependent. The complement cascade might be activated by immune complexes, formed by circulating dengue antigen and dengue virus-specific antibodies, such as pre-existing heterologous anti-NS1 antibodies form an immune complex with either circulating NS1 or NS1occupied on the surface of infected cells. Thereby, the complement activation in this aspect leads to

cytolysis of the infected cells and causes dengue pathology, such as hepatic injury (dengue-infected hepatic cells) and plasma leakage (dengue-infected endothelial cells) (89).

3.6.5 Autoantibody

Some antibodies against DENV antigens can be cross-reactive to the components of human. It has been reported that anti-NS1 antibodies could cross-react with fibrinogen and thrombocytes and might contribute to the development of thrombocytopenia, found in severe dengue patients (90). Furthermore, anti-NS1 antibody is also cross-reactive with endothelial cells, whilst anti-E antibody cross-reacts with human plasminogen (91), (92).

The proposed mechanisms of immunopathogenesis of the severity of DENV infection in secondary infection is shown in figure 3.6.

3.7 Cytokine expression profile of dengue patients and *in vitro* cell line studies

The increased levels of several cytokines are associated with the severity of dengue disease, as described previously. It is believed that the massive production of cytokines produced mainly by memory T cells, monocytes/macrophages and endothelial cells is primarily responsible for the critical pathogenic events, especially in increasing the vascular permeability of endothelial cells, hallmarks of DHF. Recently, several research groups have studied inflammatory cytokine expression profiling both in cellular and fluid samples isolated or collected from DENV-infected patients and DENV fatal cases, respectively. Despite, the lack of an animal model for DENV infection and the limitations of the study in primary target cells, much evidence has obtained from DENV infection in a cell line system. Herein, the increased levels of many different cytokines have been observed in dengue infection, both in samples from DHF/DSS patients and in *in vitro* cell lines. The examples of DENV-infected cytokines are shown in Table 3.1 and Table 3.2.

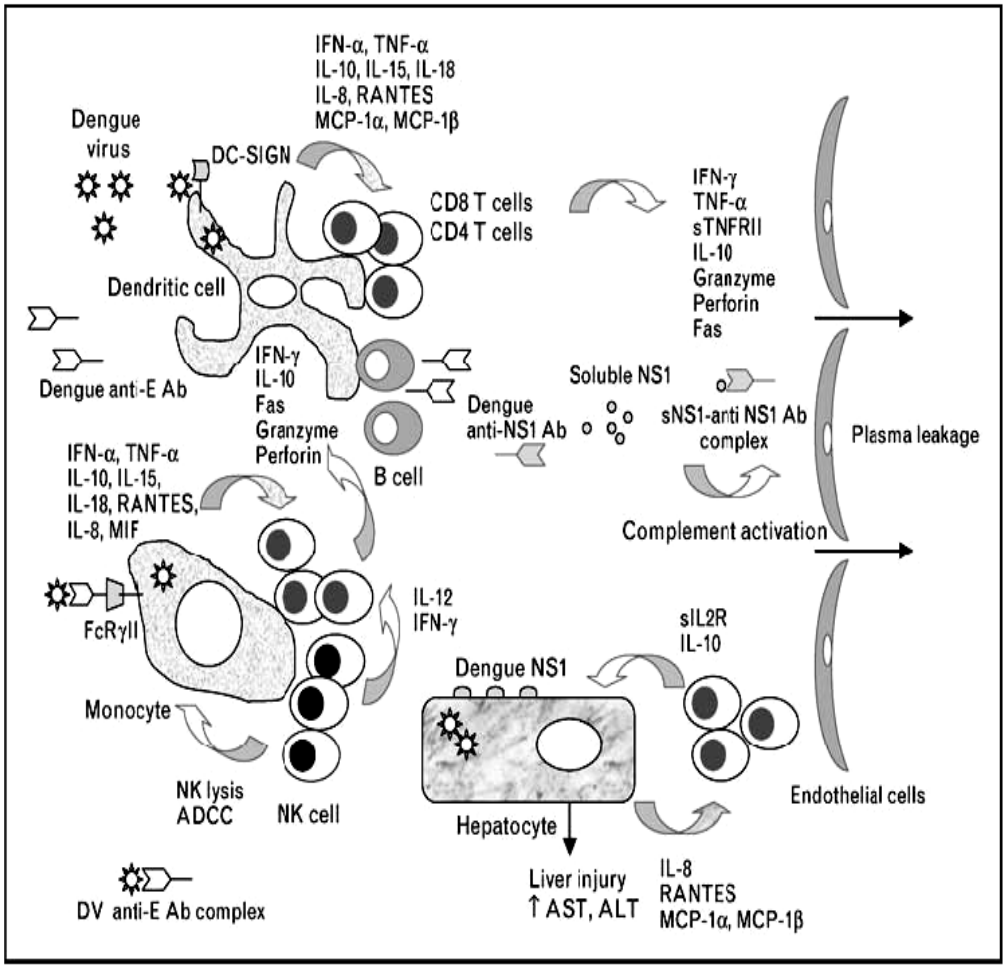

Figure 3.6 **A proposed model of the immunopathogenesis of dengue hemorrhagic fever: interactions of dengue virus with the innate, humoral and cellular immune systems during secondary dengue virus infection (89).**

Table 3.1 Cytokine expression profile of DENV infection obtained from DENV-infected patients.

Source of sample/specimen	Methods	Cytokine profile	Reference
Serum/Dengue-infected patients (not mention about the serotype)	ELISA	IL-8, RANTES	Lin, Y.L. et al. Virology (2000):276;114-26 (93)
Serum/Dengue-infected patients (not mention about the serotype)	Bead-based ELISA	Cytokines:IL-1β, IL-1ra, IL-2, IL-4, IL-5, IL-6, IL-9, IL-10, IL-12, IL-13, IL-15, IL-17, IL-18, IFN-γ, TNF-α Chemokines: Eotaxin, IL-8, IP-10, MCP-1, MIP-1α, MIP-1β, RANTES	Rathakrishnan, A. et al. PLOS ONE (2012):7;1-9 (94)
Hepatic tissue of dengue fatal cases (DENV-3)	Immunohistochemistry assay	Increased number of RANTES positive cells from ¾ of fatal cases mainly in lymphocyte, Kupffer cells and sinusoidal endothelium	De-Oliveira-Pinto, L.M. et al. PLOS ONE (2012):7;1-13 (95)

Table 3.2 Cytokine expression profile of DENV infection obtained from DENV-infected cell lines and an animal model.

Source of sample/specimen	Methods	Cytokine profile	Reference
Total RNA/Human primary hepatocytes, Human HepG2 cell line (DENV-2;16681)	qRT-PCR	TRAIL, MIP-1α, MIP-1β, MCP-1, IFN-β, IL-1β, IL-6, IL-8, RANTES	Suksanpaisan, L. et al. Journal of Medical Virology (2007):79;300-07 (96)
Total RNA and culture supernatant /Human primary endothelial HDMEC cells, Human ECV304 cell line (DENV-2;16681)	qRT-PCR and ELISA	IL-8, RANTES, MCP-1	Avirutnan, P. et al. The Journal of Immunology (1998):161;6338-46 (10)
Total RNA/Human hepatic cell lines; Chang, Hep3B,HuH-7 cells (DENV-2;PLO146)	qRT-PCR	RANTES	Lin, Y.L. et al. Virology (2000):276;114-26 (93)

Table 3.2 Cytokine expression profile of DENV infection obtained from DENV-infected cell lines and an animal model (cont.).

Source of sample/specimen	Methods	Cytokine profile	Reference
Total RNA/Human monocyte-like properties (K562) cell line and T cell lymphoblast-like cell line (Jurkat) (DENV-2 Singapore strain)	RT^2Profiler™ PCR Array (Superarray: 84 genes related to the three classes of helper T cells)	Th1, ThI2, and Th1/Th2-related genes	Chen, J. et al. Virology Journal (2008): 5; 165 (97)
Culture supernatant/Human embryonic kidney epithelial cell line or HEK293 (DENV-2;NGC)	ELISA	IL-8, RANTES	Medin, C.L. et al. Journal of Virology (2005):75;1053-61 (11)
Liver homogenates and spleen homogenates/C57BL/6 mice (DENV-2;P23085)	ELISA	MCP-1, MIP-1α, RANTES (both liver and spleen)	Guabiraba, R. et al. PLOS ONE (2010):5;1-11 (98)

3.8 Dengue viral proteins and cytokine stimulation

DENV induces high level expression of several cytokines both *in vivo* and *in vitro*, but little is known which DENV proteins operate this action. During this decade, several studies have been reported about the role of individual DENV proteins in cytokine induction. First of all, it was demonstrated by Rothman et al., who performed an experiment by separately transfecting a plasmid expressing 10 individual proteins into the HEK 293A cell line and showing that NS5 has a predominant role than other DENV proteins in secretion of IL-8, as shown in figure 3.7 (11). In the same year, Chua et al. have reported that NS1 could induce high level production of TNF-α and IL-6 in NS1-transfected murine DC cells (figure 3.8) (99). The last evidence of DENV proteins in cytokine production almost focuses on the role of NS5 in IL-8 induction and showed that nuclear accumulation of NS5 reduces IL-8 production to help DENV replication (22), (21). Recently, Kelly et al. (12) studied by transfecting all of NS proteins (NS1 to NS5) of DENV into the monocytic THP-1 cell line and showed that THP-1 cells, expressing NS5 as well as NS4B, secrete higher levels of IL-6, IL-8, and IP-10 than other NSs, while only NS5 showed a significantly induced IFN-γ production (figure 3.9). Furthermore, NS5 activated NF-κB activity in TNF-α-treated HEK 293 cells (figure 3.10). There is, thus, strong evidence that NS5 might cause the excessive cytokine production during DENV infection.

3.9 Dengue virus nonstructural protein 5 (DENV NS5)

3.9.1 Molecular biology of DENV NS5

NS5 is the largest and most conserved protein among *Flavivirus* proteins. The NS5 gene is approximately 2.7 kb in length and encodes 900 amino acids (~100-105 kDa) of protein (14), (15). The NS5 gene contains four functional domains, which encode three functional enzymes and two signal proteins (figure 3.11A). The N-terminus (amino acid 1-272) contains a methyl transferase (MTase) domain, which comprises of N-7, 2'-*O*- methyltransferase or 2'-*O*-MTase (16), (17) and guanylyltransferase (18) enzymatic activities, both of them are required for capping

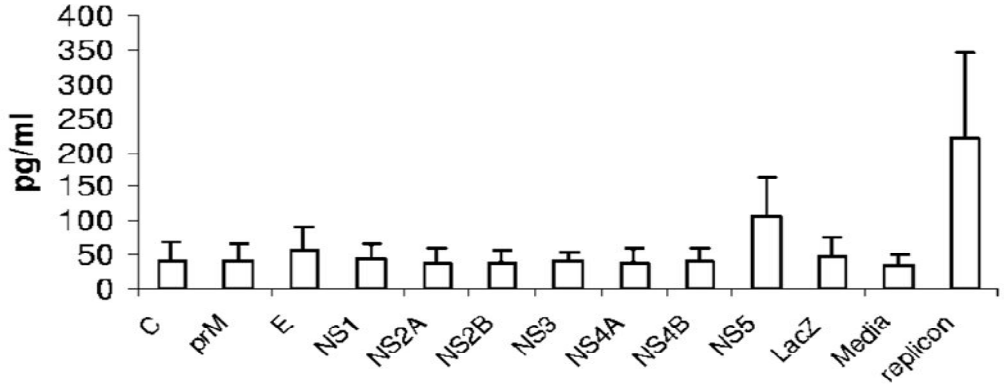

Figure 3.7 DENV NS5 predominantly induces IL-8 production in HEK 293A cells (11).

Plasmids expressing ten individual NS proteins of DENV or replicon (contains all of NS proteins, NS1-NS5, as a control) were separately transfected into HEK 293A cells. Supernatants were harvested at 48 h p.t. and analyzed for IL-8 protein by ELISA.

A.

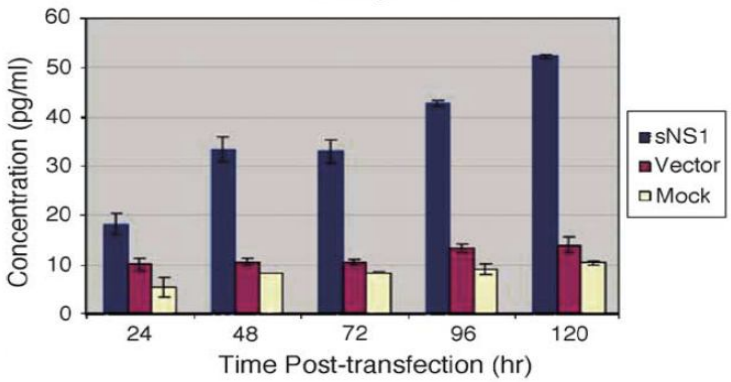

B.

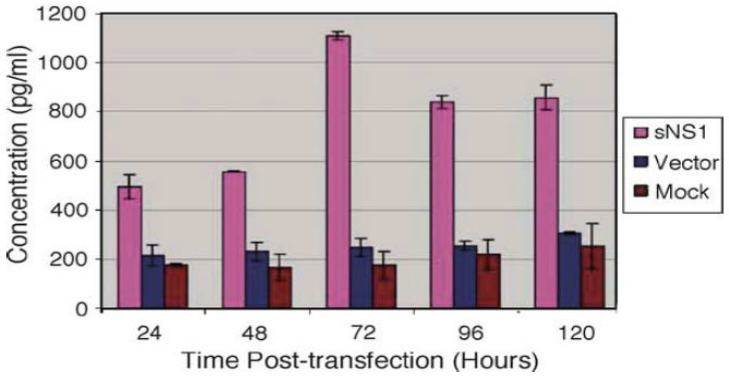

Figure 3.8 DENV NS1 induces the production of IL-6 and TNF-α in murine DC cells (99).

A plasmid, expressing NS1 protein with endogenous NS1 signal peptide sequence (sNS1), was transfected into murine DC cells. The transfected culture supernatant was collected for measuring of IL-6 (A) and TNF-α (B), using ELISA in continuous times over a 120 h-period after transfection. The differences between the induced levels and the control levels were significant with $p \leq 0.05$. Mock-transfected cells or empty plasmid-transfected cells were used as negative controls.

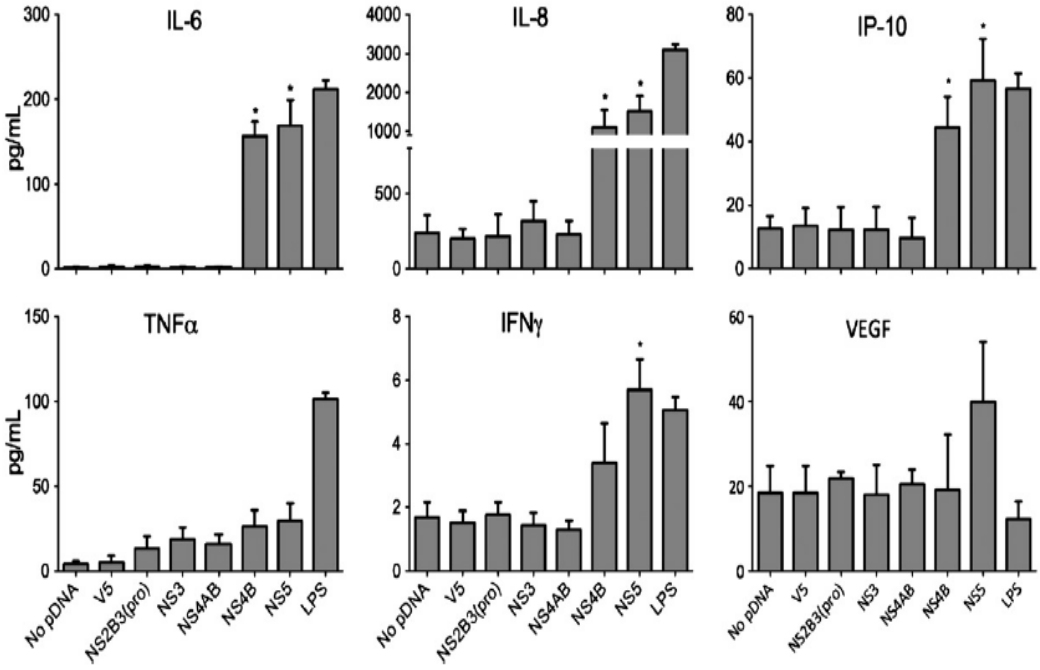

Figure 3.9 DENV NS4B and NS5 induces the high level of DHF-mediated mediators in THP-1 cells (12).

THP-1 cells were electroporated with plasmid, expressing DENV NS both in single mature form and the combination of adjacent protein, as described in legend. After 40 h, culture supernatants were measured for induction at protein level by Luminex® multiplex technology. The asterisk (*) indicates statistical significance at pb0.05, as compared to vector controls. VEGF = Vascular endothelial growth factor.

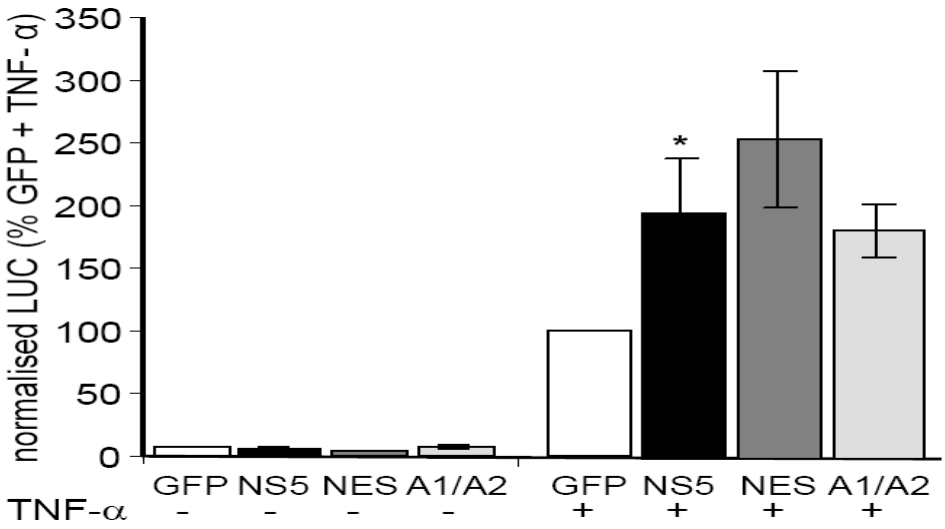

Figure 3.10 DENV-2 NS5 enhances TNF-stimulated NF-κB activation in HEK 293 cells (100).

HEK 293 cells were co-transfected with an NF-κB- responsive firefly LUC, control non-responsive *renilla* LUC reporter constructs and constructs expressing GFP-NS5 (NS5), NS5-NES mutants (NES), A1+A2 mutant (A1/A2) or control GFP expression vector alone. At 48 h p.t., cells were treated without or with TNF-α (50 ng/ml) for 6 h prior to lysis and quantitation of firefly luciferease, normalized against *renilla* luciferase control in the luminometer. Values represent mean ± SEM; * denotes significantly; $p<0.05$, Students unpaired *t-test*.

of DENV RNA genome. Capping of the RNA genome protects RNA from exoribonuclease and promotes the binding of the eukaryotic translation initiation factor 4E (eIF4E) for viral protein translation (101). while the C-terminal domain (amino acid 273-900) contains RNA-dependent RNA-polymerase (RdRp) activity that is required for newly synthesizing nascent viral RNA genome of DENV (19). The interdomain between amino acid 320 and 405 contains two adjacent nuclear localization sequences (NLSs), including bNLS or βNLS (amino acids 320 to 368) and a/bNLS or α/βNLS (amino acid 369 to 405) (20) and a nuclear exporting sequence or NES (amino acids 327-343) (21). The bNLS region is recognized by a nuclear import protein family, namely importin β (Imp β) to transport NS5 to the nucleus. In addition, bNLS has been reported to interact with DENV NS3 helicase and functions in DENV RNA replication. The binding of Imp β and DENV NS3 to bNLS is a competitive activity (20), (102): a/bNLS is a classical bipartite NLS, comprising two clusters of basic residues (amino acids 371 to 372 and 387 to 389), which are recognized by importin α/β heterodimer (Imp α/β) (103). The a/bNLS is a critical domain for NS5 nuclear translocation, of which mutation abrogates nuclear translocation of NS5, whereas bNLS contributes to maximal accumulation (22). As described previously, NS5 contains NES, which is recognized by well-known nuclear exportin protein named CRM-1 (chromosomal regional maintenance 1) to export proteins to the cytoplasm (21). The shuttle of NS5 protein between nucleus and cytoplasm is regulated by the phosphorylation status mediated by casein kinase II (CK-II or CK-2) (20), (104). NS5 is phosphorylated in at least four sites of serine residues. Furthermore, a fractionation experiment of DENV-infected cells has demonstrated that only hypophosphorylated NS5 was found in the cytoplasm and associated with NS3 within the replication complex (RC) in order to fulfill its role in DENV replication, whereas a hyperphophorylated form was found predominantly in the nucleus (23). The phosphorylation-regulated subcellular localization of DENV NS5 is shown in figure 3.11B. *Flavivirus* replication, including DENV, occurs in the cytoplasm of the host cells within membranous structure, called “vesicle packets” or VPs. This vesicle is induced by virus and budded from the host ER/Golgi (105). Within these structure, NS5 associates with other NS proteins including NS1, NS2A, NS3, and NS4A as well as some putative host cellular proteins to form the RC (106). Based on the

characterized role of NS5 in DENV RNA replication, NS5 has to occur exclusively within the cytoplasm of the host cell. However, the observation that several *Flavivirus* proteins, including DENV NS5, are found mainly in the nucleus of the host cells suggests that DENV NS5 might have additional roles or auxiliary functions, besides its RdRp activity, to support DENV replication or pathogenesis. Thereby, it is needed top clarify the exact role of DENV NS5 further. There is ample evidence demonstrating that some viruses, predominantly replicating in cytoplasm, often utilize the nucleus for functions, such as the modulation of host cell defenses, manipulation of host gene expression and regulation of the cell cycle (25), (24). There is some evidence implying the possible role in the nucleus of DENV NS5 in cytokine modulation, the details of which are given in topic 3.9.10.

3.9.2 The roles of DENV NS5 in dengue replication

As described previously, the major role of NS5 in DENV RNA replication is due to its RdRp activity and should be strictly occur in the cytoplasm. In the past a study suggested that up to 20% RdRp activity was found within the nucleus of infected cells and implied that replication may occur in the nucleus. In addition, Pryor et al. and Rawlinson et al. have reported the corresponding results that the accumulation of NS5 in nucleus enhances DENV RNA replication both after a/bNLS mutation or using a CRM-1 nuclear exporting inhibitor, respectively (22), (21). Recently, several controversial data have demonstrated that nuclear localization of DENV NS5 is not exclusive required for DENV RNA replication. Those experiments were performed by expressing a/bNLS NS5 mutant both from NS5 plasmid constructs and from DENV infectious clones in several cell lines and measuring the correlation with viral production (107), (108), (109). Furthermore, Hannemann et al. have demonstrated for the first time that not all of 4 serotypes of DENV NS5 exclusively accumulate in the nucleus. There are only two serotypes of DENV NS5 including DENV-2 and DENV-3 which have been shown that NS5 predominantly accumulates in the nucleus, both in transfected cells and infected cells, whereas DENV-1 and DENV-4 was shown exclusively to be localized in the cytoplasm (108). Nevertheless, all of the four serotypes showed a comparable RNA replication.

In addition to its role in RdRp activity, NS5 indirectly enhances DENV RNA replication by inhibiting type I IFN. DENV-2 NS5 was found to have type I IFN antagonism by mediating STAT2 degradation. The cleavage form of NS5 either interacts with STAT2 and target STAT2 to E3 ligase or might interact with both STAT2 and E3 ligase before targeting STAT2 degradation by the proteasome pathway (110). Furthermore, in a study performed by generation of various types of NLS NS5 mutations, it was found that the decrease of NS5 nuclear accumulation did not affect the efficient STAT2 degradation, suggesting that this role of NS5 exclusively exists in the cytoplasm (107).

3.9.3 The role of DENV NS5 in dengue cytokine production

Although the role of DENV NS5 in the nucleus is not clear, the studies of its nuclear localization in the production of inflammatory cytokine have been demonstrated. The first evidence of DENV NS5 in cytokine production was demonstrated by Rothman et al.; they reported that among 10 individual, NS5 has a predominant role as compared to other DENV proteins in IL-8 induction in HEK 293A cells (11). At that time it was not mentioned, in which compartment of the cellNS5 was localized. The later studies focused more on the role of NS5 in the nucleus. In addition to study the replication aspect, Pryor et al. have observed the production of IL-8 in the same experiment as well. Site-specific mutation study of either aNLS, bNLS, or both in NS5 plasmid constructs and DENV-2 infectious clone in HEK 293 cell line revealed that mutagenesis of both clusters of aNLS (K371A/K372A and K387A/K388A/K389A) abolished NS5 nuclear localization, increased IL-8 production and reduced virus production, whereas the bNLS is required for its maximal activity, implying that NS5 suppresses IL-8 production in the nucleus to enhance DENV RNA replication (22). Similar results were obtained in the same cell line showing the inhibition of NS5 nuclear exporting by CRM-1 inhibitor. The antibiotic leptomycin B

A.

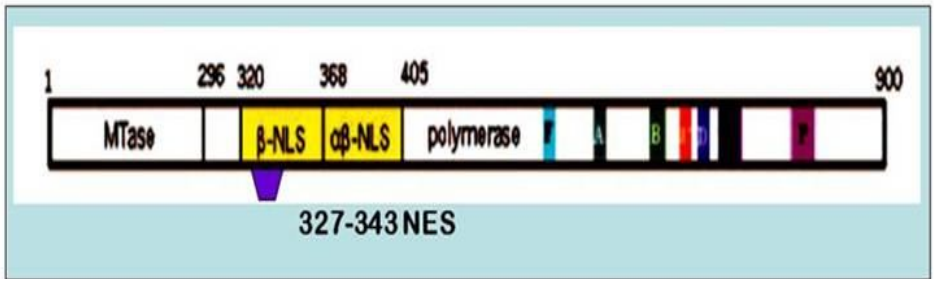

B.

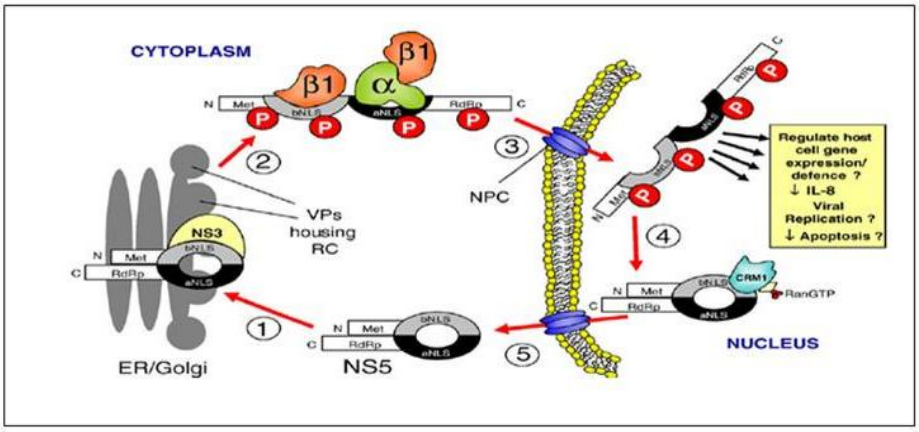

Figure 3.11 Functional domains (modified from (111), (14) and subcellular localization regulated by the phosphorylation status of DENV NS5 (26).

A. The four functional domains of DENV NS5 include MTase, NES, NLSs, and RdRp polymerase from N- to C-terminus, respectively. (B) The localization of DENV NS5 is regulated by phophorylation. Hypophosphorylated NS5 localizes in cytoplasm due to the conformational autoinhibition of both NLSs, preventing binding of importins for nuclear importing. (1) NS5 associates with NS3 in the replication site. (2) Dissociation of NS5 from NS3, stimulated by phosphorylation of NS5; NLSs are exposed and allow importins to bind, leading to transport of NS5 to the nucleus (3). (4) Within the nucleus, unknown phosphatase dephosphorylates NS5 to facilitate recognition by CRM-1 (5) and export to the cytoplasm.

(LMB), which is able to bind CRM-1 specifically and to prevent CRM-1-NES interaction, was used to inhibit NS5 nuclear export both in NS5 transfection and DENV-infected cells. The results showed that inhibition of CRM-1 activity results in an increased nuclear NS5, reduced IL-8 induction and increased virus production (21). These data were conflicted by a later report, which states that the ability of IL-8 induction was lower in two types of a/b NLS mutants, including K397A/K398A and K396A/K397A/K398A, even though theses mutants remarkably reduced nuclear accumulation of NS5. In addition, they also found that reduced IL-8 level correlates with the lower replication competence of DENV suggesting that the IL-8 induction by NS5 was due to the replication competence rather than the abundance of NS5 in nucleus, or the multiple factors influencing both the replication competence and the nuclear NS5 accumulation (107). However, the involvement of NS5 in cytokine induction has been reported in several studies. Kelley et al. demonstrated this involvement of NS5 by transfecting seven NS proteins (NS1 to NS5) of DENV into the monocytic THP-1 cell line showed that THP-1 cells, expressing NS5 secrete higher levels of IL-6, IL-8, and IFN-γ-induced protein 10 (IP-10) than other NSs, even though NS4B also had this effect but a lesser extent (12). The luciferase reporter gene assay also showed that DENV NS5 activates NF-κB activity in TNF-α-treated HEK 293 cells (100). Since all of the NS5-induced cytokines are NF-κB-dependent, it might suggest the involvement of NS5 in cytokine induction, especially NF-κB-regulated cytokine genes. Some evidence has demonstrated that NS5 induces the IL-8 promoter by activating CAAT/enhancer-binding protein or c/EBP (seven fold), activating protein 1 or AP-1 (fivefold), and nuclear kappa B or NF-κB (less than twofold) over that of the control plasmid (11) but DENV-induced IL-8 production is a cell type-dependent mechanism (112). Although DENV NS5 have been reported for the induction of several cytokines, but how NS5 regulates these cytokine production and the mechanisms are not yet completely understood. Furthermore, there are many cytokines, which are induced and related with the severity of DENV infection, but there is no direct evidence for DENV protein involvement. Thereby, all need to be studied further.

3.10 The CC chemokine ligand 5/Regulated upon activation, normal T-cell expressed and secreted/ (CCL5/RANTES)

3.10.1 Molecular biology and functions of RANTES

CCL5 or RANTES is a low-molecular-mass chemokine (7.8 kDa) (113), which belongs to the CC or β chemokine subfamily (114). It was first identified to be expressed by human T lymphocytes only after 3 to 5 days of antigen stimulation (115). Chemokines are the specialized small secreted cytokines with the size of 70-130 amino acids with chemotaxis-inducing property and secreted by leucocytes and tissue cells. Chemokines are classified depending on the presence of the four conserved cysteine residues or the spacing between first two cysteine residues: C, CC, CXC or CX_3C chemokines. The difference in structure will determine the type of receptor recognition and specific leucocyte migration(116). As mentioned earlier, RANTES is a CC or β subfamily in which the first two cysteines are adjacent (117). The members of CC chemokine in the same group as RANTES are MCP-1 (prototype), MCP-2, MCP-3, MIP-α, MIP-β, whereas the members of CXC chemokines which also have the important roles in inflammatory responses are IL-8 (prototype), IP-10, Gro-α, Gro-β, Gro-γ (118). The expression of RANTES was first thought to be limited to activate T lymphocytes, but recent data have been confirmed that it can be produced by a variety of tissue types, such as fibroblast (118), renal tubular epithelium (119) and renal mesangial cells (120), thrombin-stimulated platelets (121) in response to specific stimuli.

1. The functions of RANTES in inflammatory responses to invading pathogens

(a) Leucocyte recruitment in inflammatory responses

The migration of immune cells, including leucocytes, to inflamed or injured sites is a hallmark of inflammation. At these sites, immune cells are activated to destroy the microorganisms, cellular debris and to remove the injured or degraded tissue. The chemotactic activity of RANTES, as well as other

chemokines, is mediated by firstly inducing the expression and a conformational change in the integrins, molecules expressed on leucocytes, to adhere the endothelial cells and, secondly by promoting the migration of adherent leucocytes to cross the endothelial junction or vascular wall basement membrane, and through the extracellular matrix to inflamed or injured sites (122) (figure 3.12). RANTES induces the chemotaxis of T lymphocytes (113), NK cells (123), monocyte/macrophage cells (113), dendritic cells (124) basophils (125), eosinophils (114). Furthermore, the chemotaxis of RANTES to T cells has been reported that it selectively attracts memory or helper T cell population and does not influence B cells thereby it is proposed to be involved in immunologic memory (113). RANTES exerts its actions via interacting with a member of seven -transmembran-spanning G-protein-coupled receptors (GPCRs), CCR-1, CCR-3 and CCR-5 (126), (127), which are expressed on the surface of effecter cells and via a glycosaminoglycan (GAG) chain bound to heparin sulfate proteoglycan (HSPGs), presented on the endothelial cell surface (128). The CCR-1 and CCR-5 are the main receptors of RANTES. Actually there was a study to confirm that deletion of CCR-5 allowed RANTES to bind to CCR-1 (127). Besides the binding with RANTES, CCR-5 binds to MIP-1α and MIP-1β as well (124).

(b) Leucocyte activation

In addition to leucocyte recruitment, RANTES is a regulator of leucocyte activation as well. RANTES enhances T cell proliferation and activation by increasing the expression of B7 membrane protein on antigen-presenting cells for binding to CD28 on T cells (129) and increasing the production of IL-2 from activated T cells (130).

2. The functions of RANTES in immune-mediated diseases

(a) RANTES in tumors

It is already known that both monocytes and lymphocytes can be a major component of the mass of certain solid tumors (131). Grave et al. reported that two solid tumor cell lines of rhabdomyosarcoma, RD and MG63, showed the

expression of RANTES mRNA, even though it is far less than the expression in T cells, but they could explain the association of lymphocytes with certain tumors and their chemokines (132).

(b) RANTES in atherosclerosis

RANTES is proposed to be involved in atherosclerosis, because it is highly expressed in lymphocytes and macrophages, in *in situ* hybridization of normal carotid plaque and in heart transplant atherosclerosis (133).

(c) The possible role of RANTES in rheumatoid arthritis

The rheumatoid synovial environment is characterized by the accumulation of inflammatory cells, including lymphocytes and mononuclear cells. Schall et al. (118) has detected the expression of RANTES and other chemokines (MCP-1, IL-8) in fibroblasts cultured from rheumatoid joints. It is possible that the presence of a large number of inflammatory cells could be the result of a chemotactic activity of these chemokines.

3.10.2 The regulation of RANTES gene expression

As described previously, RANTES can be expressed in a variety of cell types. RANTES is expressed in the "late stage" (3-5 days) after stimulation of peripheral blood T cells with mitogen or antigen (115) whereas the increased expression of RANTES mRNA in monocytes/macrophages, normal fibroblasts and renal epithelial cells can be found as an "immediate early" gene in a minute or hour after stimulation with TNF-α, IFN-γ, and IL-1β (118), (120), (134), (135). These observations suggest that there are different mechanisms regulating transcription of RANTES in different cell types. The RANTES gene is about 7.1 kb in length, which is composed of three exons (133, 112 and 1075 bases) and two introns (1.4 and 4.4 kb), in which the position of intron/exon boundaries is conserved with other CC chemokine family members (136). Approximately 1 kb of the immediate 5'-upstream region of the RANTES gene was found to contain the potential transcriptional consensus elements for DNA-binding factors or *cis*-regulatory elements to control the expression of RANTES (Table 3.3). There are several trials to explain the differences in regulation

of RANTES expression. Song et al. (137) has reported that Rel proteins, p65 and p50, are sufficient for transcriptional induction of RANTES expression in fibroblast, renal epithelial cells and monocytes/macrophanges, whereas known transcription factors including nuclear factor of interleukin 6 (NF-IL6) and nuclear factor of activated T cells 1 (NFAT1) play major roles to control the expression of RANTES within first 2 days after T cell activation (139). Furthermore, in addition, acetylation, phosphorylation, and methylation of chromatin are required for RANTES expression regulation (140). At best we understand regulation of RANTES expression in T lymphocyte and this is shown in figure 3.13. For the expression of RANTES in other cells, the activated signaling molecules and transcription factors, which play a critical role in RANTES expression, are different depending on the stimuli. The well characterized transcription factors, which are crucial for RANTES regulation expression, are roughly classified into cytokine-induced and virus-induced RANTES transcription factors.

In cytokine-induced RANTES expression, Casola et al. (141) have demonstrated the mechanisms, that control RANTES induction in TNF-α and/or IFN-γ-treated lung epithelial A549 cells. They found that TNF-α and IFN-γ have a synergistic effect in induction of RANTES mRNA expression and protein secretion in A549 cells. By using promoter deletion/mutagenesis and electrophoretic mobility shift assay (EMSA), they found that NF-κB is the most important *cis*-regulatory element for controlling RANTES expression in TNF-α-treated cells, whereas NF-IL-6, cyclic AMP-responsive element or CRE, and interferon-stimulated responsive element or ISRE also play a significant role but to a lesser extent. Surprisingly, IFN-γ does not activate the RANTES promoter, but enhances RANTES expression by RANTES mRNA stabilization. Furthermore, Moriuchi et al. (142) studied the RANTES expression regulation in HVS/$CD8^+$ T cells ($CD8^+$ T cells), and H9 cells ($CD4^+$ T cells), in which it has been reported that a high expression of RANTES occurs and other CC chemokines, including MIP-1α and MIP-1β in HIV infection. They stimulated these with TNF-α and IL-1β and found that the RANTES promoter was activated through NF-κB activity. The p65/p50 heterodimer of NF-κB binds to its

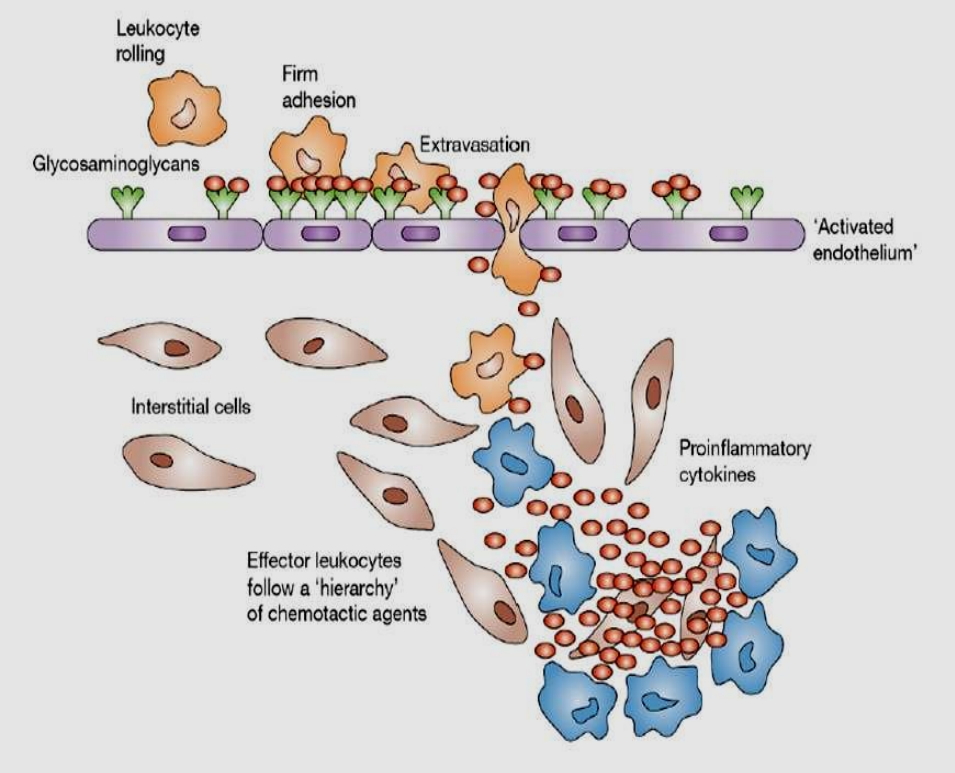

Figure 3.12 The chemotactic activity of RANTES (138).

Leucocytes are initially induced to roll along the vascular endothelial cells by interacting with selectins (primary adhesion or non-signaling interaction). RANTES chemokines (red ovals) present on glycosaminoglycan (green) of endothelial cell surface engage with G protein couple receptors (might be CCR-1, CCR-3 or CCR-5) on leucocytes, resulting in the conformation activity of integrins from low-affinity to high-affinity adhesion (secondary adhesion) or signaling interaction. Leucocytes migrate across the endothelial junction (diapedesis) to the inflammatory site along the chemotactic gradient to kill the invading pathogens.

typical sites (NF-κB1 and NF-κB2 sites) and other 2 atypical binding sites, including CD28RE and NF-AT, which is a critical binding site for RANTES induction in this situation.

In viral-induced RANTES expression, the study in Sendai virus-infected HEK 293 cells by using *in vivo* genomic footprinting analysis and overexpression of dominant- negative mutants demonstrated that RANTES mRNA was induced and was mediated via the cooperation between NF-κB and IFN-regulatory factor. The disruption of either pathway abolished the ability of the other pathway to activate the RANTES promoter (149). Furthermore, Thomas et al. (150) demonstrated that NF-κB has a predominant role also in RANTES production, induced by Respiratory syncytial virus (RSV) in A549 and HEK 293 cells. However, it was reported that for RANTES induction in the same virus and cell type infection r ISRE plays a crucial role, but all of them, i.e. NF-κB, C/EPB, CRE, and ISRE are needed for full activation of RANTES induction (151). The previous evidence was reported in other viral infections as well. For DENV infection, RANTES is induced both in patient's samples and in *in vitro* cell lines, as described in Table 3.3 and Table 3.4. Several studies also try to elucidate the mechanisms of RANTES expression in DENV infection. First evidence was done in DENV-2 infection of human umbilical cord vein endothelial cell line (ECV304). They found that DENV selectively induced RANTES and IL-8 production. In addition, DENV induced RANTES promoter activity. The immunofluorescence and EMSA assays showed the nuclear translocation of p65 and the increased p65 binding. Although this study has not shown the involvement of other transcription factors, it is enough to suggest that NF-κB might play role in this RANTES induction (10). The second study was performed in Chang liver cell line and it was found that NF-IL-6 and an unidentified protein, which bind to NF-κB sites, not NF-κB itself, plays a major role in controlling RANTES expression (93). The most recent evidence has reported in 2011 by Tsai et al. (152) who demonstrated that the STAT3 signaling pathway controls RANTES expression in the HepG2 liver cell line. They gained this evidence by suppressing STAT3 activity using JAK2 inhibitor and short hairpin RNA (shRNA) targeting STAT3 and found the decrease of RANTES

Table 3.3 The potential transcriptional consensus elements found in the 1961 bases of the immediate upstream region of RANTES gene

Consensus	Position	Tissue specificity/Features	References
TATA	-12	Ubiquitous/initiation complex	(143)
MyoD	-21	Myoblasts	(144), (145)
CTCF	-27	Muscle/fibroblast, erythrocyte	(144)
NF-κB	-30	Ubiquitous/binds re1 family members	(143), (144)
C/EBP	-47	Ubiquitous/can bind to CCAAT box	(144)
AP-3	-47	Ubiquitous/interacts with AP-2	(144), (146)
CCAAT	-70	Ubiquitous/initiation complex	(143), (147)
NF-IL-6	-92	Ubiquitous/C/EBP like, involved in inflammation	(144), (148)
PEA-3	-186	B and T cell bind Ets-1 like factor	(144)
TCF-1	-192,-541, -785,-936	T cell specific/related to Ets family	(144)
NF-AT	-213	-	(136)
NF-S	-227	Unknown binds to MHC class II *a*	(144)
STAT3	-248	-	
myb	-310	Hemopoietic proliferation, late T cell expressed	(144)
AP-1	-327,-345, -354	Ubiquitousbinds fos/jun family members	(144)
NFE-2	-349	Myeloidbinds AP-1 like factors	(144)
Ets-1	-372	B and T cell binding is phosphorylation dependent	(144)
MEF-2	-428	Muscle/enhancer	(144)
CD28RE	-579	T cell/activates IL-2 promoter	(144)
TEF-1	-797	Unknown part of the SV40 enhancer	(144)
GATA	-754,-785	Erythroid, megakaryocyte, T cells/enhancer	(144)
CF-1	-765	Ubiquitous	(144)

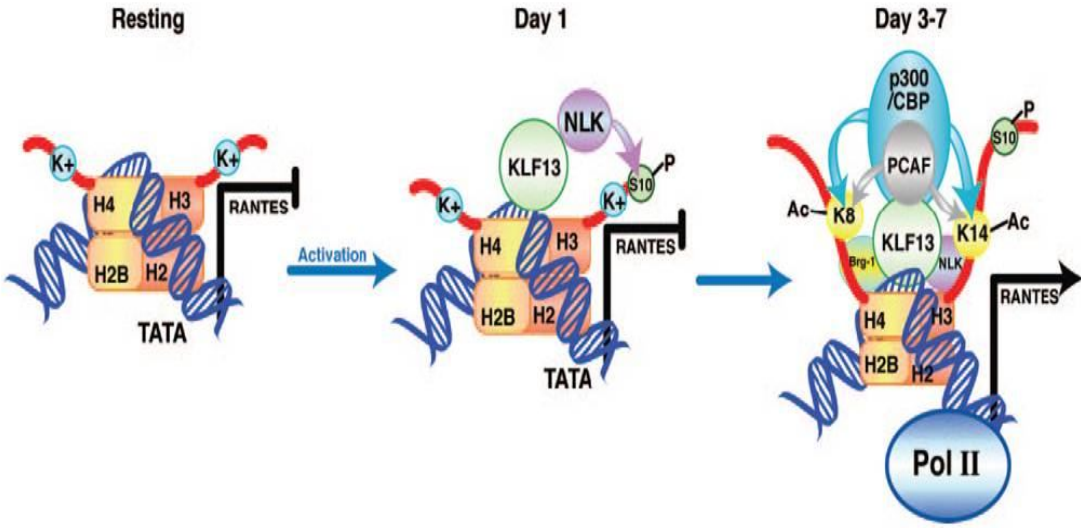

Figure 3.13 The model of late RANTES expression mechanism in T lymphocytes (140).

In the resting state, RANTES is not expressed in which its chromatin is in closed structure. After 1 day of activation, KLF13 binds to an element on the RANTES promoter and then NLK binds to KLF13 to phosphorylate on serine residue of histone H3. KLF13 recruits p300/CBP and P/CAF to the RANTES promoter and leads to both phosphorylation and acetylation of chromatin. This acetylation causes the recruitment of many molecules needed for transcriptional initiation on the RANTES promoter, opening of the chromatin structure, starting of polymerase II binding, leading to RANTES transcription on day 3-7 approximately. H = histone, KLF13 = Krueppel-like factor 13, CBP/p300 = cyclic AMP response element-binding protein/p300, NLK = Nemo-like kinase, P/CAF = p300/CBP-associated factor kinase.

production as well as of DNA binding of STAT3. Furthermore, knocking down STAT3 also decreased NF-κB and AP-1 binding activity, suggesting that STAT3 might play a role in RANTES production upstream to NF-κB and AP-1 in HepG2 cells. From all this evidence we try to explain the mechanisms for controlling RANTES expression in viral infection, even though there are the differences in transcription factors that control the induction, it seems that RANTES needs a nuclear protein complex as "enhanceosome" in T lymphocytes, but NF-κB still plays an important role in almost virus-induced RANTES production.

3.10.3 The role of RANTES in viral infection

As described previously, RANTES plays a role in both protective and pathogenic aspects. It is the same in viral infection. The protective role of RANTES in viral infection was predominant in HIV infection. RANTES and other members of CC chemokines, including MIP-1α and MIP-1β, could suppress HIV-1 replication. The antiviral action was mediated via a competitive binding with HIV-1 envelope to CCR-5, viral co-receptor of HIV-1 on target cells (153), (154), (155). In DENV infection, RANTES induction seems to be involved in pathogenic mediation, in which the high level of RANTES expression was rather found in DHF/DSS patients than DF patients. Moreover, it has been proposed to be involved in two major pathogeneses of DENV infection, including liver injury and increase of vascular permeability of endothelial cells. The evidence of RANTES-mediated liver injury was demonstrated by the finding that time point of highest RANTES induction was parallel to viral replication and viral-induced CPE in a liver cell line. In addition, serum from DHF/DSS patients, which showed a high RANTES level also showed abnormally higher level of liver transaminases (AST and ALT), even though these up-regulated levels were not significant (93). The result from a study using an immunochemistry assay demonstrated that three of four of hepatic tissues from dengue fatal cases showed remarkably RANTES-positive cells (95). The role of RANTES in increase of vascular permeability was reported by Appanna et al. (156). They found that RANTES and other cytokines were induced in the serum of DF and DHF patients. Those sera, containing induced cytokines, including RANTES, were used to directly incubate human umbilical vein endothelial cells (HUVEC) and were responsible for

perturbation of the tight junction protein ZO-1 and adherens junction protein VE-catherin, as detected by immunofluorescence analysis. Immunofluorescence staining showed that monolayers of RANTES-treated HUVEC were altered and shown highly irregular shaped cells, compared with HUVEC treated with media. This result was confirmed by incubating HUVEC with recombinant human RANTES and these morphological alterations of HUVEC could be reversed by adding anti-RANTES antibody.

3.11 Regulation of NF-κB-mediated cytokine gene expression by viruses

Besides the induction of RANTES, DENV also induces other NF-κB-regulated cytokines such as TNF-α, IL-1β, IL-2, IL-6, IL-8, MCP, MIP-1α, MIP-1β, IP-10, and IFN-γ (Table 3.1 and Table 3.2). The mechanisms in which viruses evolve to manipulate the expression of NF-κB-regulated cytokines have been widely studied in several viral systems, such as the resposible proteins, which can activate NF-κB, including NS5A (157) and core protein (158) of hepatitis C virus (HCV) ,hepatitis B virus x protein (HBx) (159), and NS5 of DENV (100). The interaction with host cellular proteins is a mechanism of viruses to manipulate their benefits in replication and pathogenesis. Influenza NS51 protein was found to interact with IKKα and IKKβ of the IκB kinase complex, resulting in inhibition of IκBα degradation, NF-κB activation, and innate cytokine production (160). Kim et al. have also demonstrated that HBx physically interacts with VHL binding protein 1 or VBP1 (a binding factor for VHL tumor suppressor protein). This interaction activates NF-κB activation and cell perforation, which leads to hepatocellular carcinoma development of HBV (161). For DENV, NS1 has been reported to interact with STAT3 protein and this interaction might influence to the latter's ability of STAT3 to form homo- or heterodimers, thereby affecting the regulation of gene expression. In addition, NS1-transfected DC cells induce TNF-α and IL-6 production (99). NS5 also interacts with NF-κB inhibitor protein, Daxx (human death domain-associated protein), as evidenced by using yeast-two hybrid screening (13). Daxx was first identified as a Fas-binding protein and plays

a predominant role in Fas-mediated apoptosis (162). The inhibition of NF-κB activity by Daxx has been reported in the study of interaction between Daxx and p65 of NF-κB. The results showed that Daxx interacts with p65 in the nucleus of TNF-α-treated cells and this interaction inhibits acetylation of p65, thereby suppressing NF-κB transcriptional activity and reducing inflammatory cytokine production, including IL-8 (163). NS5 may interact with Daxx protein to liberate NF-kB and results in the activation of it. Since NS5 has been reported to activate NF-κB activity, it induces several cytokines including IL-6, IL-8 and IP-10, all of them being NF-κB-regulated genes. Thereby, confirmation of the aggregation of NS5 and Daxx in the mammalian system might be beneficial for further studies in the mechanism of NS5 in cytokine regulation.

3.12. Research questions and hypotheses

3.12.1 Rationale

Since the massive cytokine production or cytokine storm, which correlates with the severity of DENV infection, has been observed and proposed in immunopathogenesis, several studies have attempted to explain how DENV induces those massive cytokine productions. All of the DENV proteins have been studied to determine which protein plays a predominant role in this cytokine induction. Among ten DENV proteins, NS5 shows a predominant role in the induction of several cytokines, including IL-6, IL-8, IP-10 and IFN-γ. In addition, NS5 shows the evidence of activating NF-κB, which is a major key regulator of inflammatory cytokine production, and NS5 also interacts with the known NF-κB inhibitor protein, Daxx. However, mechanisms how NS5 regulates those cytokines are still unknown. Nevertheless, several remaining DENV-induced cytokines have not been characterized in which DENV proteins operate the induction. Thereby, this study aims to identify the effect of NS5 on the expression of other DENV-induced cytokines and investigate how NS5 regulates the cytokine production and test whether the regulation of NS5 is mediated through activation of NF-κB.

3.12.2 Research questions

-Main questions:

1. Does DENV NS5 regulate the production of other host inflammatory cytokines besides IL-6, IL-8, IP-10 and IFN-γ?
2. What is the mechanism how DENV NS5 regulates the cytokine production?

-Specific questions:

2.1 Does DENV NS5 influence the promoter of induced-cytokines?

2.2 Is DENV NS5-activated cytokine promoter mediated through NF-κB activation?

2.3 Does DENV NS5 influence the DNA-binding activity of NF-κB?

3.12.3 Hypotheses

-Main hypotheses:

1. DENV NS5 regulates the production of other inflammatory cytokines besides IL-6, IL-8, IP-10 and IFN-γ.
2. DENV NS5 affects directly or indirectly the promoter of such genes, or DENV NS5 manipulates the host cellular proteins to regulate the production of host inflammatory cytokines.

-Specific hypotheses:

2.1 DENV NS5 direct or indirectly activates the promoter of such genes.

2.2 DENV NS5 increases the DNA-binding activity of NF-κB to promoter of such genes.

2.3 Interaction between DENV NS5 and Daxx might be involved in the DENV NS5-induced cytokine production.

CHAPTER IV
MATERIALS AND METHODS

4.1 Materials

4.1.1 Chemicals and reagents

The chemicals and reagents used in the experimental studies in the thesis are listed in appendix.

4.1.2 Enzymes

(1) Restriction endonucleases

-*Dpn*I, New England Biolabs, Beverly, USA

-*Bam*HI, New England Biolabs, Beverly, USA

-*Xho*I, New England Biolabs, Beverly, USA

-*Fnu*4HI, New England Biolabs, Beverly, USA

-*Kpn*I HF, New England Biolabs, Beverly, USA

-*Nhe*I HF, New England Biolabs, Beverly, USA

(2) Polymerase enzymes and other modifying enzymes

-*pfx* DNA polymerase, Invitrogen, Carlsbad, USA

-T4 DNA ligase, New England Biolabs, Beverly, USA

-HS Prime Taq DNA polymerase, GENET BIO, Seoul, Korea

4.1.3 DNA and protein markers

(1) DNA markers

-100 bp DNA Ladder, Fermentas, Hanover, MD, USA

-*Hae*III digested ϕx 174 DNA, Promega, Madison, USA

-The ZipRuler^{TM} Express DNA ladder, Fermentas, Hanover, MD, USA

-λ-*Hind*III digested DNA markers, New England Biolabs, Beverly, USA

(2) Protein marker

-PageRuler^{TM} prestained protein ladder, Fermentas, Hanover, MD, USA

4.1.4 Mammalian expression vectors

(1) pGL3-basic vector

This vector was purchased from Promega, Madison, USA. Its' physical map is shown in figure 4.1.

(2) pRL-SV40 vector

This vector was purchased from Promega, Madison, USA. Its' physical map is shown in figure 4.2.

(3) pcDNA3.1/Hygro expression vector

This vector was purchased from Invitrogen, Carlsbad, USA. Its' physical map is shown in figure 4.3.

(4) Plasmid expressing p65 subunit of NF-κB

This plasmid was kindly gifted from Dr. Karen Heyninck, Research Group LEGEST, Department of Physiology, Ghent University, Belgium.

4.1.5 *E.coli* DH5α competent cells

The genotype of this *E. coli* strain is supE44 [Delta] lacU169 ([Phi] 80 lacZ [Delta] M15) hsdR17 recA1 endA1 gyrA96 thi-1 relA1.

4.1.6 DENV and DENV propagation

Dengue virus serotype 2, DENV-2, (strain 16681) was propagated at 28ºC in the mosquito C6/36 cells according to the following protocol. Twelve million cells of C6/36 were seeded onto a 162-cm^2 tissue culture flask and maintained under the culture condition as described above until reaching 80%-90% confluence (generally 24 h after seeding). The culture medium was removed and then replaced with DENV-2 at a multiplicity of infection (MOI) of 0.01 in Leibovitz's L-15 medium supplemented with 1 % FBS, 10% Tryptose phosphate broth (TPB), 36 µg/ml of penicillin and 60

µg/ml of streptomycin (maintenance medium) with the total volume of 10 ml for 3 h on a rocking platform at room temperature. Subsequently, the cells were supplemented with 30 ml of fresh maintenance medium and incubated at 28°C for approximately 5-7 days. On the day at which CPE was initially observed, supernatant was collected and centrifuged at 1,500 rpm for 5 min at 4°C to remove cellular debris. The clear supernatant was aliquoted and stored at -70°C. DENV in the culture supernatant was titrated by a focus forming unit (FFU) assay on Vero cells. Vero cells were seeded onto a 96-well plate at a concentration of $2.5x10^4$ cells/100µl/well in Minimum Essential Medium (MEM) medium containing 10% FBS, 2 mM L-glutamine, 36 µg/ml penicillin and 60 µg/ml streptomycin, and cultured at 37°C in a 5% CO_2 incubator for 24 h to obtain approximately 90% confluence of the cell monolayer. Thereafter, the medium (80 µl) was removed from each well. DENV was serially diluted by 10-fold in MEM medium containing 3% FBS, 2 mM L-glutamine, 36 µg/ml penicillin and 60 µg/ml streptomycin, added to each well (100 µl/well) and incubated at 37°C in a 5% CO_2 incubator for 2 hr. Overlay medium (MEM containing 3% FBS, 10% TPB and 1.5% gum tragacanth) was then added to each well (100µl/well) and the culture was further incubated for 3 days at the same condition. On the third day post infection, the medium was discarded from DENV-infected cell culture and the adherent cells were washed three times with 200 µl of PBS. Thereafter, the cells were fixed with 3.7% formaldehyde in PBS and permeabilized with 1% Triton X-100 in PBS at room temperature for 10 min in each step (100 µl/well). Following three washes, the cells were then incubated with mouse anti-DENV E monoclonal antibody (clone 4G2; 50 µl/well) at room temperature for 1 h. After that, the cells were washed three times and incubated with HRP-conjugated rabbit anti-mouse antibody at a dilution of 1:500 in PBS containing 2% FBS and 0.05% tween-20 in the dark at room temperature for 30 min. To develop an enzymatic reaction, the cells were incubated with a substrate solution (50 µl/well) containing 0.6 mg/ml diaminobenzidine (DAB), 0.03% H_2O_2 and 0.08% $NiCl_2$ in PBS at room temperature in the dark for 5 min. The enzymatic reaction was terminated by washing with PBS three times. Dark brown foci of the DENV-infected cells were enumerated under a light microscope. Virus titers

were calculated from the duplicated samples and reported as focus forming unit (FFU)/ml according to the following formula.

$$\text{Virus titer (FFU/ml)} = \frac{(A+B+C+\ldots+D)}{\text{Total volume of virus (µl)}} \times 10^{y} \times 10^{3}$$

A = number of foci counted in the first dilution

B = number of foci counted in the second dilution

C = number of foci counted in the third dilution

D = number of foci counted in the last dilution

Y = the first dilution of virus at which the foci are counted

4.1.7 Cell lines

(1) C6/36 cell line

C6/36, a mosquito cell line from *Aedes albopictus* (ATCC CRL-1660), which was used for DENV propagation, was cultured in Leibovitz's L-15 medium supplemented with 10% FBS, 10% TPB, 36 µg/ml of penicillin, and 60 µg/ml of streptomycin (growth medium) at 28°C in an incubator.

(2) Vero cell line

Vero, an African green monkey kidney cell line, used for DENV titration, was cultured in MEM containing 10% FBS, 2 mM L-glutamine, 36 µg/ml penicillin and 60 µg/ml streptomycin at 37ºC in a 5% CO_2 incubator with humidified atmosphere.

(3) Human embryonic kidney 293 (HEK 293) cell line

HEK 293 cell line was generated by transformation of cultures of normal human embryonic kidney cells with sheared adenovirus 5 DNA. HEK 293 cells were grown in Dulbecco's Modified Eagle Medium (DMEM) supplemented 10% heat-inactivated FBS supplemented with 2 mM L-glutamine, 1% NEAA, 1mM sodium pyruvate, 36 µg/ml penicillin and 60 µg/ml of streptomycin. The cells were maintained in the same medium at 37°C with 5% CO_2 and subcultured twice per week. To detach

the cells for subculturing and harversting, 2.5 mM EDTA/PBS was added and incubated for 1-2 min after washing once with PBS.

(4) Human embryonic kidney 293T (HEK 293T) cell line

HEK 293T cell line is a derivative of HEK 293 cell line. It was latterly generated by expressing the large T-antigen of SV40 that allows for episomal replication of transfected plasmids containing the SV40 origin of replication. HEK 293T cells were grown and maintained in the same medium as HEK 293 cells.

4.1.8 Oligonucleotide primers

(1) Primers for construction of pcDNA3.1/Hygro containing WT-NS5 or MT-NS5 constructs (Table 4.1)

(2) Primers for cytokine expression screening (Table 4.2)

(3) Primers for construction of pGL3-Basic containing WT-RANTES and NF-κB-mutated RANTES promoter (Table 4.3)

4.1.9 Antibodies

(1) Primary antibodies

-ANTI-FLAG® M2 Monoclonal antibody, Sigma, Saint Lois, USA

-Goat anti-Daxx antibody, Santa Cruz Biotechnology, Santa Cruz, USA

-Rabbit anti-Daxx antibody, Santa Cruz Biotechnology, Santa Cruz, USA

(2) Secondary antibodies

-Rabbit anti-mouse antibody conjugated with horseradish peroxidase (HRP), Dako, Denmark

-Swine anti-rabbit antibody conjugated with HRP, Dako, Denmark

-Rabbit anti-mouse antibody conjugated with Alexa Fluor® 488,

Molecular probes, Eugene, USA

-Goat anti-mouse antibody conjugated with FITC, Molecular probes, Eugene, USA

-Donkey anti-rabbit antibody conjugated with Cy3, Jackson Immunoresearch Laboratories, West Grove, PA, USA

4.1.10 Miscellaneous materials

-Lipofectamine™ 2000, Invitrogen, Carlsbad, USA

-Protease inhibitor cocktail, Roche, Mannheim, Germany

-Protran nitrocellulose membrane, Schleicher & Schuell, Keene, USA

-SuperSignal® West Pico Chemiliminescent Substrate, PIERCE, Rockford, USA

-Hoechst 33342, Molecular Probes, Eugene, USA

-Anti-fade agent, Dako, Denmark

-High Pure RNA Isolation Kit, Roche, Mannheim, Germany

-TRIzol® Reagent, Invitrogen, Carlsbad, CA

-SuperScript ®III First-Strand Synthesis System, Invitrogen, Carlsbad, CA

-Light Cycler® 480 SYBR Green I master kit, Roche, Mannheim, Germany

-Human RANTES Instant ELISA®, eBioscience, CA, USA

-Protein G-Sepharose 4B bead, GE Healthcare, Uppsala, Sweden

-Dual-Luciferase® Reporter Assay System, Promega, Madison, USA

-SimpleChIP® Emzymatic Chromatin IP Kit: Agarose Beads,

-Cell signaling technology, MA, USA

-QIAquick Gel Extraction Kit, Hilden, Germany

-QIAquick PCR purification Kit, Hilden, Germany

-QIAprep Spin Miniprep Kit, Hilden, Germany

-TNF-α, Sigma, Saint Lois, USA

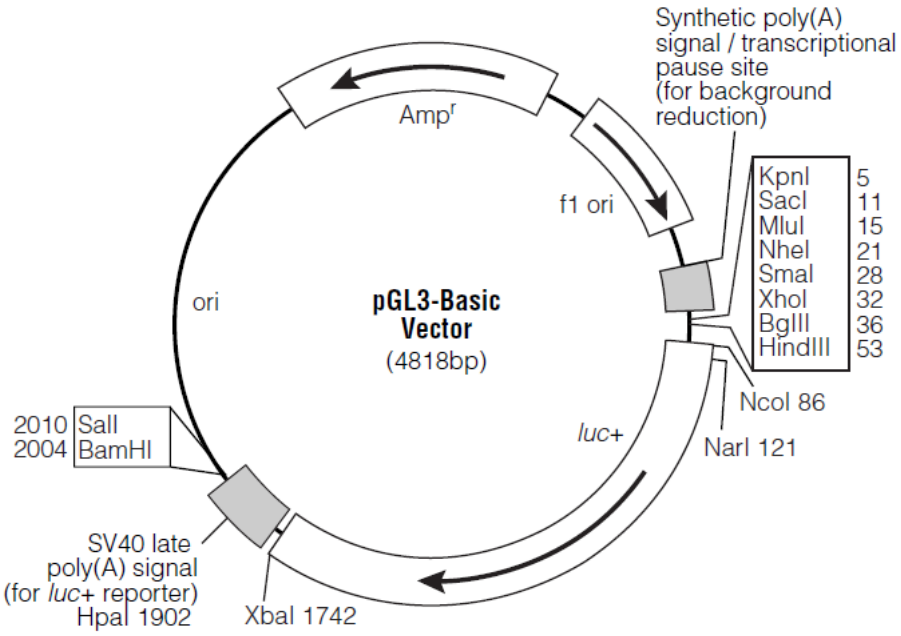

Figure 4.1 Physical map of pGL3-basic luciferase reporter.

This pGL3-basic plasmid lacks eukaryotic promoter and enhancer sequences thereby the expression of luciferase activity in cells transfected with this plasmid depends on a functional promoter inserted upstream from *luc*$^+$. The wild-type (WT) RANTES promoter or NF-κB-mutated (MT) RANTES promoter was inserted into *Kpn*I and *Nhe*I sites, respectively. Arrows within *luc*$^+$ and *Amp*^{r} indicate the direction of transcription.

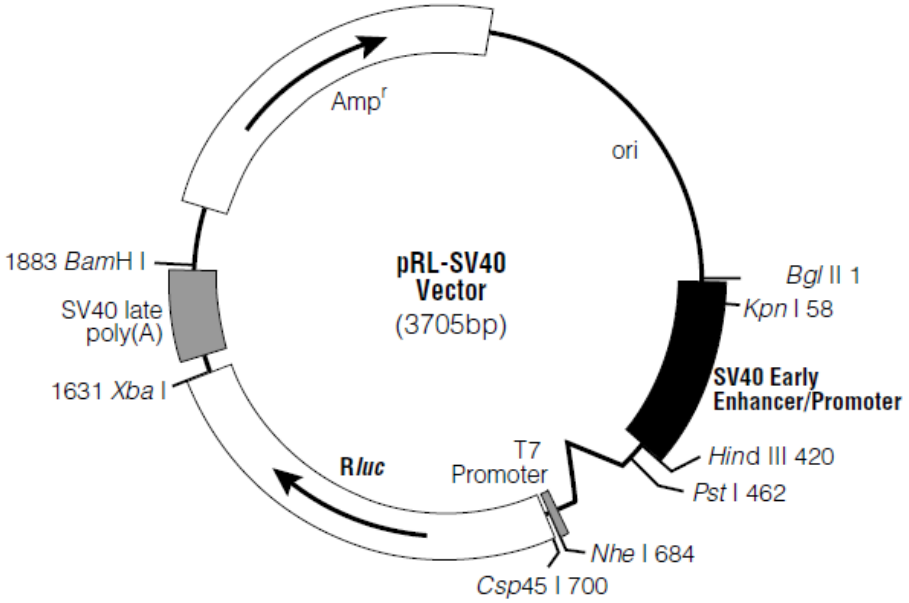

Figure 4.2 **Physical map of pRL-SV40 *Renilla* luciferase reporter.**
pRL-SV40 is commonly used for an internal control plasmid for luciferase reporter gene assay. It contains SV40 enhancer and early promoter elements to provide a high expression of *Renilla* luciferase in transfected mammalian cells.

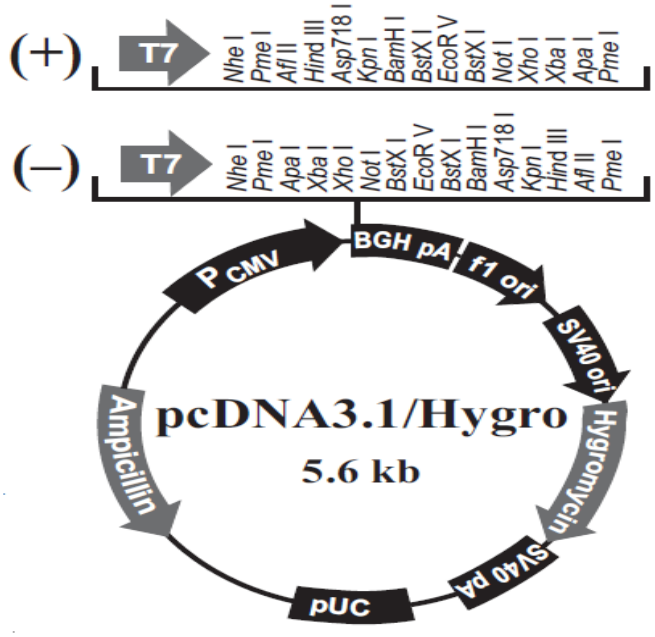

Figure 4.3 Physical map of pcDNA3.1/Hygro.

This mammalian expression plasmid, pcDNA3.1/Hygro, was used to express WT-NS5 MT-NS5 protein. WT-NS5-FLAG or MT-NS5-FLAG fragment was inserted into this plasmid in *Bam*HI and *Xho*I sites, respectively

.

Table 4.1 The list of primers for construction of pcDNA3.1/Hygro containing WT-NS5 or MT-NS5 constructs.

Primers	Orientation	Sequences (5' to 3')	Length (bp)	Melting temperature (T_m) °C
NS5 *Bam*HI	Forward	ACAGGATCCACCATGGGAACTGGCAAC ATA GGA GAG ACG	39	69.7
NS5-FLAG *Xho*I	Reverse	TGTCTCGAGTTACTTGTCATCGTCATCCTT GTAATCCCACAGAACTCCTGCTTCTTCC	58	68.6
A1 mutant_F	Forward	CCGAAAGAAGGCACGGCGGCACTAATG AAAATAAC	35	65.6
A1 mutant_R	Reverse	GTTATTTTCATTAGTGCCGCCGTGCCTTCT TTCGG	35	65.6
A2 mutant_F	Reverse	GGAAAGAATTAGGGGCGGCAGCGACACCC AGGATGTG	37	69.9
A2 mutant_R	Forward	CACATCCTGGGTGTCGCTGCCGCCCCTAAT TCTTTCC	37	69.9

Table 4.2 The list of primers for cytokine expression screening.

Primers	Orientation	Sequences (5' to 3')	Length (bp)	Melting temperature (T_m) °C
MIP-1β_F	Forward	CCTCTTTGCCACCAATACCA	20	60.4
MIP-1β_R	Reverse	AGCAGAGGCTGCTGGTCTC	20	64.5
IL-8_F	Forward	TCCTGCAGAGGATCAAGACA	20	55.5
IL-8_R	Reverse	GAGCACTTGCCACTGGTGTA	20	57.5
TNF-α_F	Forward	TGCTTGTTCCTCAGCCTCTT	20	56.5
TNF-α_R	Reverse	ATGGGCTACAGGCTTGTCACT	21	58.6

Table 4.2 The list of primers for cytokine expression screening (cont.).

Primers	Orientation	Sequences (5' to 3')	Length (bp)	Melting temperature (T_m) °C
IP-10_F	Forward	GAATCGAAGGCCATCAAGAA	20	58.4
IP-10_R	Reverse	AAGCAGGGTCAGAACATCCA	20	60.4
RANTES_F	Forward	TCCTGCAGAGGATCAAGACA	20	60.4
RANTES_R	Reverse	GTTATTTTCATTAGTGCCGCCGTGCCTTCTTTCGG	35	62.4
CXCL-9_F	Forward	CAGATTCAGCAGATGTGAAGGA	22	54.7
CXCL-9_R	Reverse	GAAATTCAACTGGTGGGTGGT	21	55.6
β-actin_F	Forward	AGAAAATCTGGCACCACACC	20	57.3
β-actin_R	Reverse	CTCCTTAATGTCACGCACGA	20	57.3

Table 4.3 The list of primers for construction of pGL3-Basic containing WT-RANTES and NF-κB-mutated RANTES promoter.

Primers	Orientation	Sequences (5' to 3')	Length (bp)	Melting temperature (T_m) °C
RANTES *Kpn*I_F	Forward	GTGGTACCCCAGTATTTATTGAGTTTCCTC	30	64.3
RANTES *Nhe*I_R	Reverse	CTAGCTAGCACGTGCTGTCTTGATCCTC	28	67.9
NF-κB 1_F	Forward	CTATTTTGGAAACTCAACGTAGGGGATGCCCCTCAAC	37	64.9
NF-κB 1_R	Reverse	GTTGAGGGGCATCCCCTACGTTGAGTTTCCAAAATAG	37	64.9
NF-κB 2_F	Forward	GAAACTCCCCTTAGGCCTTGAACCTCAACTGG	32	64.5
NF-κB 2_R	Reverse	CCAGTTGAGGTTCAAGGCCTAAGGGGAGTTTC		64.5

Table 4.3 The list of primers for construction of pGL3-Basic containing WT-RANTES and NF-κB-mutated RANTES promoter (cont.)

Primers	Orientation	Sequences (5' to 3')	Length (bp)	Melting temperature (T_m) °C
NF-κB 1+2_F	Forward	CTATTTTGGAAACTCAACGTAGGCCTTGAACCTCAACTGGCCCT	44	67.5
NF-κB 1+2_R	Reverse	AGGGCCAGTTGAGGTTCAAGGCCTACGTTGAGTTTCCAAAATAG	44	67.5

4.2 Methods

4.2.1 DENV infection of HEK293 cells

HEK 293 $3x10^5$ cells were seeded for 2 days. On infection day, cells with the confluence 70-80% were infected with DENV-2 at multiplicity of infection (MOI) at 1 in serum free DMEM for 2 h. After 2 h, viruses were removed and infected cells were replaced with 10% FBS DMEM medium. DENV-infected HEK 293 cells were further cultured for 24 and 48 h and then harvested.

4.2.2 Measurement of percentage of cell viability by trypan blue exclusion dye assay

Ten μl of cell suspension was mixed with 10 μl of trypan blue dye and the 10 μl of mixture was applied to hematocytometer. The numbers of viable cells was calculated as formula shown below.

$$\text{Percentage of cell viability} = \frac{\text{number of viable cells x100}}{\text{Total cell number}}$$

Total cell number = number of viable cells plus dead cells

4.2.3 Indirect immunofluorescence staining for flow cytometry

Cells were detached with serum free DMEM and transferred into flow cytometry tube. Then, cells were washed twice with 2 ml filtrated PBS and pelleted by centrifugation at 2,000 rpm for 5 min at room temperature. One ml of 2% formaldehyde in filtrated PBS was used to fix the cells for 30 min at room temperature before centrifugation and removal. Cells were permeabilized with 0.5 ml of 0.1% Triton-x in filtrated PBS for 10 min at room temperature and centrifuged at 2,000 rpm for 5 min before discarding. The permeabilized cells were washed twice with 1 ml of filtrated PBS and blocked with 50 μl of 1% BSA in filtrated PBS for 30 min at room temperature. After 30 min of blocking, cells were pelleted by centrifugation at 2,000 rpm for 5 min and discarded the blocking solution. Fifty μl of primary antibody diluted in 0.1% Triton-x in PBS was added to the cells and incubated for 1 h at room temperature and then washed twice by adding 2 ml of chilled DMEM containing 1%

BSA before centrifugation and discard. Then, cells were incubated with 25 μl of secondary antibody conjugated with fluorescence dye for 1 h in dark and washed twice with chilled DMEM containing 1% BSA. Three hundred and fifty μl of 1% formaldehyde was added and then cells were analysis by using FACSort™ flow cytometer.

4.2.4 Total RNA isolation

Two methods were used for total RNA isolation in this study. First method was RNA isolation using High Pure RNA Isolation Kit and the second is TRIzol® Reagent-based RNA isolation method.

(1) Total RNA isolation by High Pure RNA Isolation Kit

All of the following steps were performed according to the High Pure RNA Isolation Kit manufacturer's instruction. Briefly, cells ($1x10^6$) were washed with DEPC-treated PBS twice during cell harvesting. Cells were resuspended in 200 μl of DEPC-treated PBS and followed by 400 μl of Lysis/Binding buffer, vortex for 15 sec. The sample was transferred into High Pure Filter tube already inserted into collection tube and centrifuged at 8,000 g for 15 sec at room temperature. After centrifugation, the filter tube was removed from collection tubes to discard flow through and returned back to the collection tubes. One hundred μl of DNase I solution containing of 10 μl DNase I enzyme and 90 μl of DNase I incubation buffer was added onto the glass fiber fleece in the upper reservoir of each filter tube and incubated for 15 min at room temperature. Then, 500 μl of Wash buffer I was added into the filter tubes before centrifugation at 8,000 g for 15 sec at room temperature. The flow through was discarded and 500 μl of Wash buffer II was added. Centrifugation was performed at the same condition and then 200 μl of Wash buffer II was added and centrifuged for 2 min to ensure removal of residual wash buffer. After flow through discarding, the filter tube was transferred into new sterile 1.5 ml microcentrifuge tube. Thirty to 50 μl of Elution buffer was added onto the filter glass to elute RNA. The isolated RNA cloud be immediately subjected of purity and concentration measurement or kept at -70°C for further use.

(2) RNA isolation by TRIzol® Reagent

These steps of RNA isolation were followed the manufacturer's instruction of TRIzol® Reagent RNA isolation. After removal of 10% FBS DMEM from cultured plate, cells were washed once with DEPC-treated PBS and then added with 1 ml of TRIzol® Reagent directly on the cells. Cells were lysed by pipetting the cells up and down several times. The homogenized sample was incubated at room temperature for 5 min to permit the complete dissociation of nucleoprotein complex. Then, 200 μl of chloroform was added to the homogenized sample and the mixture was shaked vigorously by hand for 15 sec before incubating for 2-3 min at room temperature. The sample was centrifuged at 12,000 g for 15 min at 4°C. After centrifugation, the sample was separated into 3 layers; a colorless upper aqueous phase contains RNA, an interphase, and a lower red phenol-chloroform phase contains DNA and proteins. The isolated RNA in an aqueous phase was remove carefully into a new sterile microcentrifuge tube by angling the tube at 45° and pipetting the aqueous phase and avoiding the disruption any of interphase and lower phase. To precipitate the RNA in an aqueous phase, 500 μl of 100% isopropanol was added and incubated for 10 min at room temperature. The mixture was centrifuged at 12,000 g for 10 min at 4°C to pellet RNA and then supernatant was removed. The RNA pellet with gel-like pellet was washed with 1 ml of 75% ethanol and vortex briefly. The mixture was centrifuged at 7,500 g for 5 min at 4°C and completely removed the supernatant. The RNA pellet was dried at room temperature for 5-10 min before resuspending in 50-100 μl of RNase-free water. The suspension was heated in water bath or heat block at 55-60°C for 10-15 min to dissolve the RNA. RNA was ready for downstream application or kept at -70°C.

4.2.5 Reverse-transcription

Two different commercial kits were used to reverse transcribe RNA into cDNA including RT^2 First Strand Kit and SuperScript ®III First-Strand Synthesis System. After total RNA isolation, the purified RNA was reverse-transcribed into cDNA using RT^2 First Strand Kit. The steps of cDNA synthesis were followed according to the manufacturer's instruction.

(1) RT^2 First Strand Kit for RT^2 Profiler™PCR Array system

Briefly, 1μg of total RNA was firstly subjected of genomic DNA elimination by mixing of 1μg of total RNA with 2 μl of 5x genomic DNA elimination buffer and nuclease-free water up to 10 μl. The mixture was mixed gently and followed by brief centrifugation. The mixture was incubated at 42°C for 5 min and immediately chilled on ice at least 1 min. Ten μl of RT cocktail which containing 4 μl of 5x RT buffer 3, 1 μl of Primer and External control Mix, 2 μl of RT enzyme Mix 3, and nuclease-free water up to 10 μl was added to the RNA mixture from previous step. The mixture of RNA and RT cocktail was mixed gently and subjected of reverse transcription by incubating at 42°C for exactly 15 min and then immediately stopped the reaction by heating at 95°C for 5 min. Then, 91 μl of nuclease-free water was added to 20 μl of cDNA synthesis reaction mixture and incubated on ice until the next step or stored at -20°C.

(2) SuperScript ®III First-Strand Synthesis System for conventional real-time polymerase chain reaction (qPCR)

Briefly, 1μg of total RNA was firstly mixed with 1 μl of 50 μM oligo$(dT)_{20}$, 1 μl of 10 mM dNTPs, and up to 10 μp with DEPC-treated water. The mixture was incubated at 65°C for 5 min and placed on ice for at least 1 min. Then, the mixture was added with 10 μl of cDNA synthesis master mix consisting 2 μl of 10xRT buffer, 4 μl of 25 mM $MgCl_2$, 2 μl of 0.1 M DTT, 1 μl of RNaseOUT™, and 1 μl of Superscript ®III RT. Each RNA/primer mixture in cDNA synthesis master mix was mixed gently and brief centrifuged before incubating at 50°C for 50 min and followed by 85°C for 5 min to terminate the reaction. The mixture was incubated on ice, brief centrifuged and added with 1 μl of RNaseH before incubating at 37°C for 20 min. The cDNA could be stored at -20°C or used for qPCR immediately.

4.2.6 Real-time PCR or qPCR

The synthesized cDNA was used to be a template for qPCR using Light Cycler® 480 SYBR Green I master kit. The reaction contained 1 µl of the cDNA diluted in 2 µl of DEPC-treated water, 5 µl of 2X SYBR Green PCR Master Mix and 1 µl each of primer pairs specific for gene of interest. The real-time PCR was performed by LightCycler 480 II with (i) pre-incubation at 95°C for 10 min, (ii) 45 amplification cycles of denaturation at 95°C for 10 sec, annealing at 60°C for 10 sec and extension at 72°C for 20 sec, (iii) melting curve analysis by heating the product at 95°C for 5 sec, cooling at 65°C for 1 min and increasing the temperature to 97°C with 5 acquisitions of continuous florescence detection followed by cooling steps at 40°C as recommended by the manufacturer. The relative mRNA expression of gene of interest was determined by normalization to human actin mRNA levels according to the $2^{-\Delta\Delta Ct}$ method (164) as the following formulation:

$$\text{Fold change} = 2^{-\Delta\Delta Ct}$$

$\Delta Ct = Ct(GOI)-Ct(HKG)$

$\Delta\Delta Ct = \Delta Ct(Experiment)-\Delta Ct(control)$

GOI = Gene of interest

HKG = Housekeeping gene

4.2.7 Host inflammatory cytokine gene expression profiling by RT^2 Profiler™PCR Array system: Human Inflammatory Response and Autoimmunity PCR Array (96-well format)

This RT^2 Profiler™PCR Array system is designed to analyze a panel of genes in the same biological pathway or disease state. It takes the advantages of real-time PCR performance combined with the ability of microarray to analyze the expression of many genes simultaneously both rare and abundance genes in the same sample. All of the steps were followed according to the manufacturer's instruction. Briefly, 102 µl of obtained cDNA from step 4.2.5 was mixed with RT^2 qPCR master mix consisting of 1,350 µl of 2x SABiosceinces RT^2 qPCR Master Mix, and 1,248 µl of nuclease-free water. Then, 25 µl of this experimental cocktail was added to each well of PCR Array and performed real-time PCR using LightCycler 480 II with (i) pre-incubation at 95°C for 10 min, (ii) 45 amplification cycles of denaturation at 95°C for 15 sec, annealing at 60°C for 1 min, (iii) melting curve analysis. To determine the relative gene expression and fold change, Ct data from the qPCR results were analyzed using PCR Array Data Analysis Web Portal supported by SABiosceinces. The array chosen in this study was 96-well plate format containing a primer set of 84 relevant genes in Human Inflammatory Response and Autoimmunity pathway (PAHS-0772) plus five housekeeping genes and three RNA and PCR quality controls to help in the interpretation of results as shown below. Full name of each gene is showed in appendix.

	1	2	3	4	5	6	7	8	9	10	11	12
A	BCL6	C3	C3AR1	C4A	CCL11	CCL13	CCL16	CCL17	CCL19	CCL2	CCL21	CCL22
	A01	A02	A03	A04	A05	A06	A07	A08	A09	A10	A11	A12
B	CCL23	CCL24	CCL3	CCL4	CCL5	CCL7	CCL8	CCR1	CCR2	CCR3	CCR4	CCR7
	B01	B02	B03	B04	B05	B06	B07	B08	B09	B10	B11	B12
C	CD40	CD40LG	CEBPB	CRP	CSF1	CXCL1	CXCL10	CXCL2	CXCL3	CXCL5	CXCL6	CXCL9
	C01	C02	C03	C04	C05	C06	C07	C08	C09	C10	C11	C12
D	CXCR4	FASLG	FLT3LG	FOS	HDAC4	IFNG	IL10	IL10RB	IL18	IL18RAP	IL1A	IL1B
	D01	D02	D03	D04	D05	D06	D07	D08	D09	D10	D11	D12
E	IL1F10	IL1R1	IL1RAP	IL1RN	IL22	IL22RA2	IL23A	IL23R	IL6	IL6R	IL8	IL8RA
	E01	E02	E03	E04	E05	E06	E07	E08	E09	E10	E11	E12
F	IL8RB	IL9	ITGB2	KNG1	LTA	LTB	LY96	MYD88	NFATC3	NFKB1	NOS2	NR3C1
	F01	F02	F03	F04	F05	F06	F07	F08	F09	F10	F11	F12
G	RIPK2	TIRAP	TLR1	TLR2	TLR3	TLR4	TLR5	TLR6	TLR7	TNF	TNFSF14	TOLLIP
	G01	G02	G03	G04	G05	G06	G07	G08	G09	G10	G11	G12
H	B2M	HPRT1	RPL13A	GAPDH	ACTB	HGDC	RTC	RTC	RTC	PPC	PPC	PPC
	H01	H02	H03	H04	H05	H06	H07	H08	H09	H10	H11	H12

Housekeeping genes | Genomic DNA control | Reverse transcription | Positive PCR control

4.2.8 Transformation of plasmid into *E.coli* competent cells

The *E.coli* strain DH5α was used to be the competent cells for cloning and amplifying a number of plasmids in this study. Plasmid was added to 100 μl of competent cells and mixed gently before incubating on ice for 30 min. Then, the mixture was heat- shocked at 42°C in water baht for 45 sec and immediately placed on ice for 3-5 min. The 900 μl of LB broth was added into the transformed cells and incubated at 37°C for 1 h with shaker. The mixture was centrifuged at 3,000 rpm for 5 min to pellet the cells. The supernatant was removed to leave the volume about 100 μl. The transformed cell pellet was resuspended homogeneously before spreading on LB agar plate containing 100 μg/ml amplicillin and incubating at 37°C for 12-16 h.

4.2.9 PCR-based site-directed mutagenesis

The PCR-based site directed mutagenesis in this study was performed according to the protocol of Stratagene's QickChange^{TM} Site-Directed Mutagenesis Kit Instruction Manual (Stratagene). In each mutagenic generation, sense and anti-sense strands of mutagenic primer annealed to its complementary strand of denatured plasmid template. Then, *pfx* DNA polymerase extended the new mutated DNA strands from the mutagenic primers during temperature cyclings and resulted in nicked circular strand products. Following temperature cyclings, the product was subjected of *Dpn*I endonuclease treatment which is specific for methylated and hemimethylated DNA to digest the parental DNA template and to select mutation-containing synthesized DNA (nonmethylated DNA). The nicked circular mutated dsDNA was transformed in *E.coli* DH5α competent cells, which repaired the nicked ends to generate complete circular plasmid. The mutant was confirmed by digestion with the restriction endonuclease enzyme, which was design to select wild-type template from mutant.

4.2.10 Transient transfection and co-transfection by liposome-mediated transfection

HEK 293 $1.3x10^5$ cells were seeded in 12-well plate or $3x10^5$ cells in 6-well plate for 2 days before transfection. On transfection day, a transfection complex was prepared by diluting lipofectamine^{TM} 2000 in serum free DMEM (50 μl for 12-well plate or 100 μl for 6-well plate) and incubated at room temperature for 5 min. At the same time, plasmid or co-transfected plasmids was added into serum free DMEM-diluted lipofectamine. Then, transfection mixture was mixed thoroughly and incubated at room temperature for 30 min before adding on the cells. The transfection complex was incubated with the cells at 37°C with 5% CO_2 incubator with humidified atmosphere for 4-6 h. before replacing with 10% FBS DMEM. During the 30 min of transfection complex formation, cells cultured in 10% FBS DMEM were rinsed once with serum free DMEM and then added with serum free DMEM: 400 μl for 12-well and 900 μl for 6-well plate transfection scale.

4.2.11 Conventional sodium dodecyl sulfate polyacrylamide gel electrophoresis (SDS-PAGE) for analyses of protein expression

To lysis the cells in this study, HEK 293 cells were lysed by using 2 lysis buffers for different purposes. The sample buffer in final 1x concentration was used to lyse the cells for conventional testing of the expression of protein by adding directly on the cells and then scraping homogeneously. In contrast to RIPA lysis buffer, it was added to the cells after pelleting and washing the cells with PBS for Co-IP assay. Cell lysate from both those lysis buffer was heated at 95°C for 10 min and then loaded with an equal amount or volume in 10% acrylamide gel. The electrophoresis was undergone with 1x running buffer at room temperature for 90 min by using constant voltage at 150 volts. After electrophoresis, proteins were transferred to a sheet of nitrocellulose membrane using a SemiPhor semi-dry transphor unit at 75mA/membrane with Towbin buffer for 90 min. The membrane was blocked with 5% skim milk in PBS or TBST (TBS with 0.1% Tween 20) for 1 h and then incubated with a specific primary antibody diluted in 5% skim milk in PBS or TBST for 1 h or overnight. After washing 3 times for 5 min each with PBS or TBST, membrane was incubated with secondary antibody conjugated to horseradish peroxidase (HRP)

diluted in 5% skim milk in PBS or TBST for 1-2 h and then washed 3 times with PBS or TBST. The immunoreactive band of protein of interest was detected by adding SuperSignal® West Pico Chemiliminescent Substrate for 5 min according to manufacturer's instruction and washing for 3 times. To detect a chemiluminescence signal, the membrane was analysed by using a G:BOX chemiluminescence imaging system.

4.2.12 Indirect immunofluorescence staining for confocal microscopy

The transfected cells grown on coverslips were washed with PBS for 3 times and then fixed with 0.1 or 3.7% formaldehyde in PBS for 10 min. Fixed cells were permeabilized with 0.1 % Triton-x in PBS for 10 min and washed with PBS for 3 times before incubating with 1% BSA in PBS blocking solution for 30 min. Then, cells were incubated with primary antibody for 1 h and then removed. Cells were washed with 1% FBS in PBS for 3 times before incubating secondary antibody conjugated with fluorescence dye combined with Hoechst 33342 dye for nuclear staining. The coverslips were washed 3 times with 1% FBS in PBS and then mounted with anti-fade reagent. Fluorescence images were captured by confocal laser scanning microscope model LSM 510 Meta (Carl Zeiss).

4.2.13 Enzyme-linked immunosorbent assay (ELISA)

To confirm the differential expression of cytokines, Human RANTES Instant ELISA®was used to be a tool for this. The Instant ELISA® was developed by Bender MedSystems to represent an improvement of the established sandwich ELISA. This technique provides more an advantages and accuracy than that of conventional sandwich ELISA. A kit is needed just the addition of samples to the microwells, which already contains the lypholilized pellets of coating anti-human RANTES antibody adsorbed onto microwells, biotin-conjugated RANTES detection antibody, streptavidin-HRP. There is no need to add antibody or do serial dilution of standards thereby reducing of handling means less error and more consistent results and saving the time. In addition, this kit also contains a ready-to-use RANTES standard curve sample with 7 serial dilutions.

The Instant ELISA® steps were performed following the manufacturer's instruction. Both RANTES standard curve samples and experimental samples were assayed in duplicate. One hundred and fifty μl of distilled water was added into all 7 serial dilutions of RANTES standard curve sample and bank wells strips whilst just 140 μl of distilled water was added to experimental sample wells. Then, 10 μl of each supernatant from cell culture was added to experimental sample wells contained coating antibody. Microwells were covered with the plate cover and incubated at 18-25°C for 3 h. Four hundred μl of Wash Buffer was added per wells and allowed to sit in the wells for a few seconds. The microwell strips were placed upside down quickly to discard the washing buffer. This washing step was repeated 5 more times. After the last wash, the microwell strips were placed upside down on a wet absorbent paper for no longer than 15 minutes or the wells dry to remove all of remaining washing buffer. A hundred μl of TMB Substrate Solution was added to all wells and incubated at 18-25°C for 10 min in dark area. After adding the substrate, the color development was started immediately. The reactions were stopped by adding 100 μl of Stop Solution into each well and mixing throughout the microwells to inactive enzyme completely. The stopped reaction samples were subjected of absorbance reading immediately using a spectrophotometer at 450 nm. The absorbance values of each experimental sample including RANTES standard curve samples were used for plotting a standard curve. The concentration of RANTES was calculated as described in its product information and manual.

4.2.14 Luciferase reporter gene assay

This technique is widely used to study eukaryotic gene expression regulation, receptor activity, transcription factors, and intracellular signaling etc. Dual-Luciferase® Reporter Assay System was chosen to be the tool for this study. The term of "dual reporter" refers to "experimental reporter" which correlates with the effect of specific experimental conditions and "control reporter, which provides an internal control served as the baseline response. These 2 reporters are simultaneous co-transfected, expressed and measured within single sample. The experimental reporter activity is normalized to control reporter activity to minimize experimental variability caused by differences in cell viability or transfection efficiency. The experimental

reporter activity is due to the activity of firefly (*Photinus pyralis*) luciferase whist control reporter activity is due to the activity of *Renilla* (*Renilla reniformis)* luciferase. In this system, fiefly luciferase and *Renilla* luciferase are engineered in pGL3-basic plasmid (figure 4.1) and pRL-SV40 plasmid (figure 4.2), respectively.

All of steps of luciferase reporter gene assay were performed according to the manufacturer's instruction. Briefly, cells were lysed with sufficient volume of Passive Lysis Buffer (PLB) by adding directly on the cells in cultured plate. Then, cultured plate was placed on the rocking platform with gently rocking and incubated at room temperature for 15 min. To ensure the complete lysis, cells were gently scraped and homogenized by pipetting cells up and down before transferring to the new sterile tube. The luciferase activities are measured sequentially in which fiefly luciferase is firstly measured by adding its substrate (LAR II reagent). After quantifying the firefly luminescence, this reaction is quenched, and the *Renilla* luciferase reaction is simultaneously initiated by adding Stop & Glo® Reagent to the same tube. The Stop & Glo® Reagent stops the activity of fiefly luciferase and also is a substrate for *Renilla* luciferase. The experimental reporter activity was calculated as the formula shown below and the activity presents as a relative light unit (RLU).

$$\text{Experimental luciferase activity (RLU)} = \frac{\left.\dfrac{\text{Fiefly luciferase luminescence}}{\textit{Renilla} \text{ luciferase luminescence}}\right\}\text{Test}}{\left.\dfrac{\text{Fiefly luciferase luminescence}}{\textit{Renilla} \text{ luciferase luminescence}}\right\}\text{Control}}$$

4.2.15 Chromatin immunoprecipitation (ChIP) assay

To study the interaction between protein and DNA, ChIP assay is a powerful and versatile technique used for studying protein-DNA interactions within the natural chromatin context of the cells (165). This assay can be used to identify multiple proteins associated with a specific region of the genome, or the opposite, to identify the regions of the genome associated with a particular protein or protein of interest (166), (167). In this study, SimpleChIP® Emzymatic Chromatin IP Kit: Agarose Beads was applied for study the interaction between p65 subunit of NF-κB

and RANTES promoter. There are 7 steps of ChIP assay in which all of the steps were followed according to the manufacturer's instruction but they were scaled down (10 fold less than the manufacturer's instruction).

(1) *In vivo* cross-linking, nuclei preparation, and nuclease digestion of chromatin

Cells cultured in 6-well plate were replaced 10% FBS DMEM with 2 ml of serum free DMEM. Cells were further subjected of DNA-protein cross-linked by adding 54 μl of 3.7% formaldehyde (1% formaldehyde in final concentration) and incubating at room temperature for 10 min. Then, the cross-link reaction was stopped by adding 200 μl of 10x Glycine, swirling shortly to mix homogeneously, incubating for 5 min at room temperature, and then removal. Cells were washed twice with 1 ml of ice-cold PBS and discarded. Cells were added with 1 ml of ice-cold PBS + PMSF, scraped and then resuspended. The suspension cells were combined into one sterile 15 ml conical tube and centrifuged at 1,500 rpm for 5 min at 4°C. The supernatant was removed and cell pellet was resuspended with Buffer A + DTT + PIC +PMSF into $4x10^6$ cells/1ml/tube. Each tube of cell suspension was incubated for 10 min on ice and mixed by inverting tube every 3 min. The nuclei were pelleted by centrifugation at 3,000 rpm for 5 min at 4°C and aspiration of supernatant. Cells were resuspended in 1 ml of Buffer B + DTT. The centrifugation and supernatant removal were repeated. Then, cells were resuspended in 200 μl of Buffer B + DTT before adding a Micrococcal endonuclease to digest the chromatin into 150-900 bp approximately in lenght. The digestion mixture was incubated at 37°C for 20 min and mixed by inverting every 3 to 5 min. After 20 min of incubation, the digestion reaction was stopped by adding 10 μl of 0.5 M EDTA and placing on ice. The nuclei were pellet at 13,000 rpm for 1 min at 4°C and the supernatant was removed. The nuclear pellet was resuspended in 500 μl of 1xChIP Buffer + PIC + PMSF and incubated on ice for 10 min. Cells were subjected for sonication to break nuclear membrane with 10 cycles of 10 sec for pulse on and 30 sec in ice box for pulse off to break nuclear membrane.. The lysate was clarified by centrifugation at 10,000 rpm for 10 min at 4°C. The supernatant was transferred carefully into new sterile tube and

stored at -70°C until further use. Fifty μl of chromatin digestion was removed for chromatin digestion analysis in step (2).

(2) Analysis of chromatin digestion and measurement of DNA concentration

Fifty μl of chromatin digestion from step (1) was added with 100 μl of nuclease-free water, 6 μl of 5 M NaCl and 2 μl f RNAse A. The mixture was mixed by vortex and incubated at 37°C for 30 min. Two μl of Proteinase K was added to the mixture and incubated at 65°C for 2 h. Then, the mixture was subjected for DNA purifying from mixture using spin column. Briefly, 600 μl of DNA binding reagent A was added to the mixture and mixed by vortex shortly. Three hundred and seventy-five μl of the mixture was transferred to the purification spin column inserted with collection tube. The sample was centrifuged at 14,000 rpm for 30 sec at 4°C and removed flow though. The remaining 375 μl of the mixture was transferred to the same spin column and centrifuged again. After discarding flow though, 700 μl of DNA wash reagent B was added and centrifuged at the same previous. Flow though was discarded from collection tube and the spin column was additional centrifuged for removing the remaining Wash Reagent B. Fifty μl of DNA Elution Reagent C was added to each spin column placed into a new sterile 1.5 ml tube and centrifuged at 14,000 rpm for 30 sec. The obtained purified DNA was subjected of chromatin digestion analysis by agarose gel electrophoresis and measured for the concentration by NanoDrop spectrophotometer.

(3) Chromatin immunoprecipitation

Before starting the immunoprecipitation (IP), 10 μl of digested chromatin prepared in steps (1) was removed and kept at -20°C as a 2 % input of the sample for step (5). In each IP reaction, the volume (μl) equal to 10 μg of each digested chromatin was diluted in 1xChIP buffer in total volume of 500 μl. Five to 10 μg of antibody against the protein of interest and 1 μl (1 μg) of normal isotype control antibody was added individually in each IP reaction. The IP samples were rotated for 4

h or overnight at 4°C. Then, 30 µl of ChIP-Grade Protein G agarose bead was added and incubated with rotation at 4°C for 2 h.

(4) Washing of the immunoprecipitated chromatin

The IP samples from steps (3) were pelleted using protein G bead by centrifugation at 6,000 rpm for 1 min at 4°C and removal of supernatant. One ml of low salt wash buffer was added to the bead and incubated at 4°C for 5 min with rotation. The samples were centrifuged and subjected of this low salt washing for 2 more times (total 3 low salt washes). Then, 1 ml of high salt wash buffer was added to the bead and incubated at 4°C for 5 min with rotation. From this step, the samples were immediately proceeded to step (5).

(5) Elution of chromatin from antibody/Protein G bead and reversal of cross-linking

The samples from step (4) were centrifuged at 6,000 rpm for 1 min to pellet Protein G bead. The supernatants were removed and 150 µl of 1xChIP buffer was added to the bead and also added to 2% input of sample from step (c). Only the bead from IP samples were subjected of DNA elution from antibody/Protein G bead by incubating at 65°C for 30 min with gently mixed every 3 min. The samples were centrifuged at 6,000 rpm for 1 min and the supernatants were carefully transferred into new sterile tubes. All of samples including 2% input of sample were subjected of reverse cross-linked by adding 6 µl of 5 M NaCl and 2 µl of Protein K, incubated at 65°C for 2 h or can be extended overnight. Then, these samples were immediately preceded in step (6) or kept at -20°C.

(6) DNA purification using spin column

The samples from step (5) were purified by using spin column as the same method in (2).

(7) Quantification of DNA by PCR

To quantify the amount of DNA which was immunoprecipitated, 1-2 μl of DNA samples eluted in step (6) was used a template for standard PCR method. The primers which are specific for DNA of interest were design for DNA amplification.

4.2.16 Co-immunoprecipitation assay (Co-IP)

Cells from triplicate of 6-well plate of the same transfection condition were detached with serum free DMEM. These detached cells were combined into one 15-ml tube and centrifuged to discard the supernatant. One ml of RIPA lysis buffer with protease inhibitor cocktail was added to cell pellet and then resuspened by gentle agitation for 3 sec with a vortex mixer set at a medium speed. The lysis reaction was kept on ice for 20-30 min until complete lysis. Cell lysate was centrifuged at 12,000 g at 4°C for 30 min and transferred the supernatant to new a sterile 1.5 ml tube without disturbing the pellet. Thirty μl of cell lysate was taken and kept separately as an input sample control. Then, 1 ml of cell lysate was added with 50% protein G-Sepharose 4B bead slurry which already was washed with PBS once before resuspending in RIPA buffer. Cell lysate added with protein G was rotated at 4°C for 30 min in a tube rotator. Protein G was pellet by centrifugation at 16,000 g at 4°C for 5 min and the preclear lysate was carefully transferred for preparation of Ag-Ab complex formation. Five μg of antibody specific for protein of interest was added to 500 μl of each preclear lysate and rotated at 4°C in a tube rotator for 6 h or overnight. After overnight of incubation, 30 μl of 50% BSA-blocked protein G-sepharose bead was added into Ag-Ab complex formed-lysate and further incubated for overnight. The sample was centrifuged at maximum speed for 5 sec, removed of supernatant, and then washed once with 400 μl of ice-cold washing buffer with inverting 3-4 times. Four hundred μl of ice-cold PBS was added to the immunoprecipitated complex and then centrifuged for washing again. The immunoprecipitated complex was eluted from the beads by adding 30 μl of 2xSDS buffer and incubated at 99°C for 5 min. The eluted sample was centrifuged at maximum speed for 2 min to collect the supernatant. Twenty μl of supernatant was subjected of 10% SDS-PAGE. To detection interacting proteins,

primary antibody which is specific for each protein was added and followed by its corresponding HRP-conjugated secondary antibody. Immunoreactive bands were visualized by G: BOX chemiluminescence imaging system.

4.3 Study design

The cytokine gene expression profiling was firstly observed in DENV-infected HEK 293 cells using RT^2 PCR Array to identify which gene was induced in DENV-infected HEK 293 cells and to use as a corresponding result with cytokine gene expression profiling induced by NS5. Then, DENV-induced cytokines were the candidate genes for testing in HEK 293 cells expressing NS5. Plasmid expressing either WT-aNLS NS5 or MT-NS5 protein was transfected in HEK 293 cells. The differential expression affected by WT-NS5 or MT-NS5 of selected DENV-induced cytokine genes was screened by qRT-PCR using specific primers for each gene. NS5-induced cytokines were observed the differential expression at translational levels by ELISA. The only one of NS5-induced cytokine gene was chosen for further studies. Luciferase reporter plasmid containing promoter of selected NS5-induced cytokine gene was constructed and used to investigate the influence of NS5 on such NS5-induced cytokine promoter. To clarify whether selected cytokine promoter was mediated through NF-κB, binding site of NF-κB on selected cytokine promoter was mutated and analyzed by luciferase reporter gene assay. Chromatin immunoprecipitation assay was performed to examine the binding ability of NF-κB on selected cytokine promoter in NS5-trasnfected HEK 293 cells. Furthermore, the interaction between NS5 and NF-κB inhibitor protein, Daxx, was confirmed in HEK 293 cells by Co-IP and colocalization assay to explain the mechanism of how NS5 regulates cytokine production in aspect of viral-host protein-protein interaction. Taken together, the proposed model of DENV NS5 regulating cytokine gene expression was created.

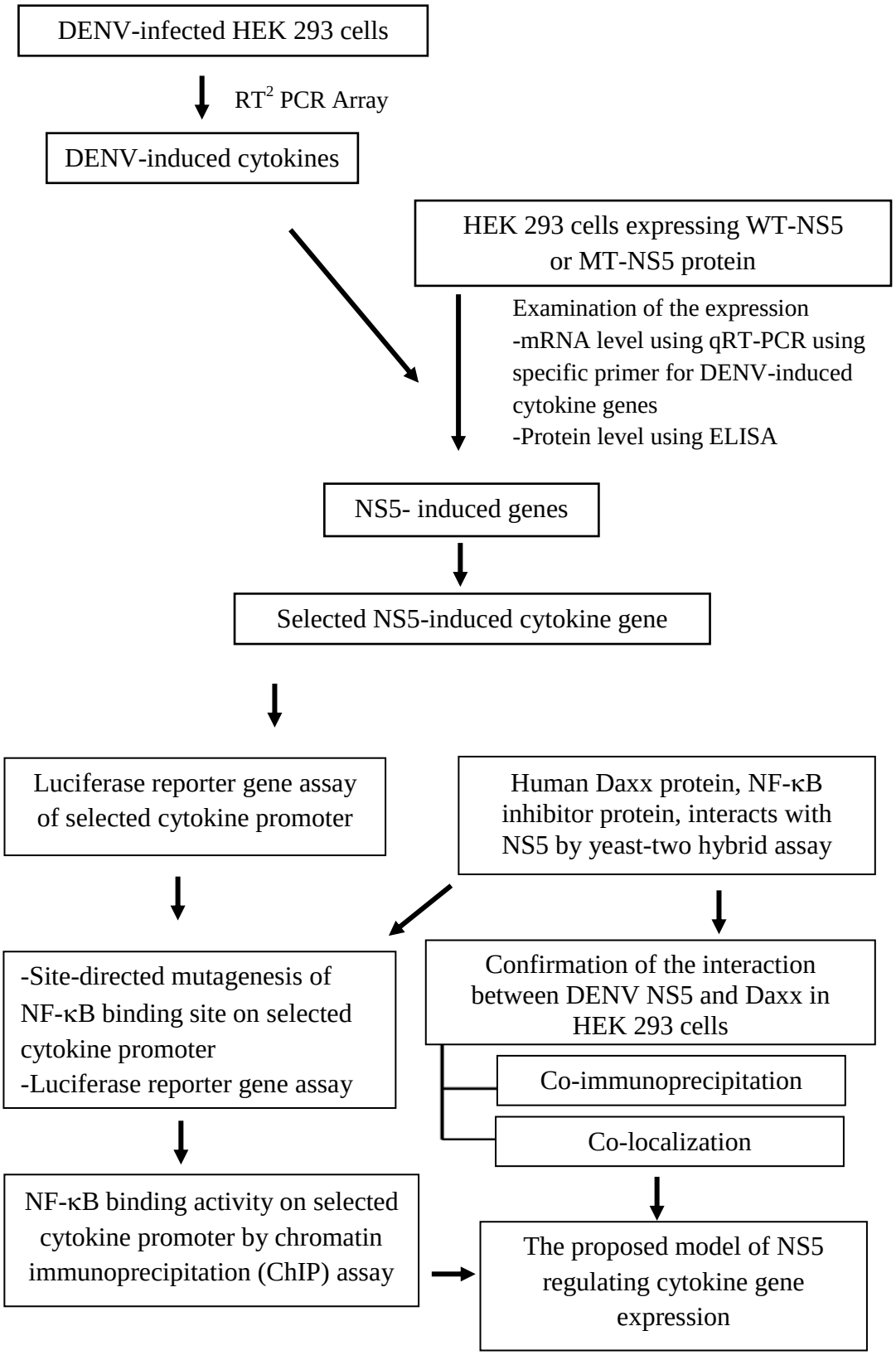

Figure 4.4 Design for this study.

4.4 Experiments

4.4.1 Study of host inflammatory cytokine gene expression profiling in DENV-infected HEK 293 cells by RT^2 Profiler™PCR Array system

(1) DENV infection and analysis of the percentage of infection

To prepare DENV-infected HEK 293 cells for inflammatory cytokine gene expression screening, HEK 293 cells were mock-infected or infected with DENV-2 at MOI of 1 for 24 and 48 h. At both time points, the infected cells were subjected of cell viability measurement by trypan blue exclusion assay. In addition, the infected cells were immunostained with mouse anti-DENV E monoclonal antibody (clone 4G2) and followed by goat anti-mouse conjugated with FITC secondary antibody. Then, the percentage of infection (% of infectivity) was analyzed by FACSort™ flow cytometery. Both data from cell viability and % infectivity were used to be criteria for choosing an appropriated time post infection (p.i.) of DENV-HEK 293 cell sample for RT^2 Profiler™PCR Array.

(2) RT^2 Profiler™PCR Array

The only one time point post infection of HEK 293 cells was further subjected to total RNA isolation using High Pure RNA Isolation Kit. The total RNA was measured for the purity and concentration by NanoDrop spectrophotometer in which the ratio of A_{260}:A_{230} should be greater than 1.7 and the ratio of A_{260}:A_{280} should greater than 1.8-2.0. Then, 1 μg of purified total RNA was reversed transcribed into cDNA using RT^2 First Strand Kit for RT^2 Profiler™PCR Array system. The obtained cDNA was subjected of RT^2 Profiler™PCR Array process and the results were analyzed by using PCR Array Data Analysis Web Portal supported by SABiosceinces as described previously.

4.4.2 Construction of mammalian expression plasmid expressing wild-type (WT)-a/bNLS NS5-FLAG protein

(1) Amplification of full length WT-a/bNLS *NS5*-FLAG cDNA

To construct the plasmid, which expresses full length WT-a/bNLS DENV-2 NS5 protein tagged c-terminally with FLAG epitope, WT-a/bNLS *NS5*-FLAG was amplified from pET21a containing full length DENV-2 *NS5* gene by polymerase chain reaction (PCR) using NS5 *Bam*HI forward and NS5-FLAG *Xho*I reverse primers exhibited in Table 4.1. A total volume of 50 μl PCR reaction was consisted of 100 ng of pET21a DENV-2 *NS5*, 10 pmole of each primer, 10 mM dNTPs, 1x *pfx* buffer, 1 mM $MgSO_4$, and 2.5 U of *pfx* DNA polymerase. After gently mixing, the reaction mixture was carried out in a thermal cycler GeneAmp® PCR System 9700. PCR cycles were set for 30 cycles of denaturation at 94 °C for 30 sec, annealing at 55 °C for 30 sec, extension at 68 °C for 3 min, and one cycle of final extension at 68 °C for 10 min. The 5 μl of PCR product was analyzed by 0.8% agarose gel electrophoresis. After ethidium bromide staining, the PCR product was visualized by Gene Genius Bio Imaging system. Then, WT-aNLS *NS5*-FLAG PCR product was purified by using QIAquick Gel Extraction Kit following manufacturer's protocol.

(2) Restriction endonuclease digestion of WT-a/bNLS *NS5*-FLAG cDNA and pcDNA3.1/Hygro

PCR product of WT-a/bNLS *NS5*-FLAG was double digested with *Bam*HI and *Xho*I restriction enzymes in a volume of 20 μl consisting of 500 ng of purified PCR product, 1x NEB buffer 2, 1x BSA, and 5 U each of *Bam*HI and *Xho*I. The digestion mixture was incubated at 37°C for 16 h and then purified by using QIAquick PCR purification Kit. In addition, 2 μg of pcDNA3.1/Hygro (figure 4.3) was firstly digested with *Xho*I at 37°C for 16 h and then purified by using QIAquick Gel Extraction Kit. The purified *Xho*I-digested plasmid was further subjected to *Bam*HI digestion and purified using the same kit as first *Xho*I digestion. Both purified-

digested PCR product and plasmid were determined the concentration and purity by NanoDrop spectrophotometer.

(3) Cloning of WT-a/bNLS *NS5*-FLAG cDNA into pcDNA3.1/Hygro

To insert WT-a/bNLS *NS5*-FLAG into pcDNA3.1/Hygro, the digested PCR product was ligated into digested pcDNA3.1/Hygro in which molar ratio of plasmid to PCR product was 1:2. The ligation mixture consisted of 100 ng of pcDNA3.1/Hygro, 100 ng of PCR product, 2 U of T4 DNA ligase and 1x ligation buffer in a volume of 10 μl. The ligation mixture was incubated at 16 °C in a water bath for overnight and then the day after the ligation mixture was transformed into *E.coli* DH5α competent cells.

(4) Screening of pcDNA3.1/Hygro containing WT-a/bNLS *NS5*-FLAG

The putative clones of *E.coli* harboring the pcDNA3.1/Hygro WT-a/bNLS *NS5*-FLAG recombinant plasmid were extracted by using QIAprep Spin Miniprep Kit. The extracted recombinant plasmids were screened to identify for WT-a/bNLS *NS5*-FLAG insertion by PCR using the same primers as the amplification step (1).

(5) DNA sequencing analysis of pcDNA3.1/Hygro WT-a/bNLS *NS5*-FLAG

Purified putative clone of pcDNA3.1/Hygro WT-a/bNLS *NS5*-FLAG was sequenced by sending to Macrogen DNA Sequencing Service (Seoul, Korea) for sequencing analysis. The recombinant plasmid with the correct sequences was renamed as pcDNA3.1/Hygro WT-*NS5*-FLAG or WT-NS5.

4.4.3 Construction of mammalian expression plasmid expressing mutated (MT)-a/bNLS NS5-FLAG protein

(1) Site-directed mutagenesis for generation pcDNA3.1/Hygro MT-a/bNLS *NS5*-FLAG recombinant plasmid

To generate pcDNA3.1/Hygro MT-a/bNLS *NS5*–FLAG containing two mutation sites in a/bNLS domain of *NS5* gene or A1+2 mutant, pcDNA3.1/Hygro WT- *NS5*-FLAG plasmid was used to be a template for amino acid substitution by using PCR-based site-directed mutagenesis. The nucleotide sequences for coding of amino lysine (K) were changed to be nucleotide sequences coding for amino acid alanine (A) at position of 371-372 (K371AK372A) and 387-389 (K387A, K388A, and K389A) related to the amino acid position in full length NS5 protein. Two mutagenic primers were designed (Table 4.1). The steps of MT-a/bNLS *NS5*-FLAG mutation generation were initiated by separately generating K371A-K372A and K387-389A with A1 and A2 mutagenic primer to obtain A1 mutant and A2 mutant, respectively. Both A1 and A2 mutants were used as the template for generating A1+2 mutant or "pcDNA3.1/Hygro MT-a/bNLS *NS5*–FLAG". The PCR was carried out in a volume of 25 μl containing 1x *pfx* DNA polymerase buffer, 2 mM dNTPs, 1mM $MgSo_4$, 0.4 mM dNTPs, 10 pmole each of primers, 0.5 U of *pfx* DNA polymerase, and 100 ng of pcDNA3.1/Hygro WT-*NS5*-FLAG template. PCR profile was 94°C for 2 min for the first round of reaction, followed by 18 cycles of 94°C for 30 sec, 55°C for 1 min, and 68°C for 18 min in a Biometra TGradient Thermal Cycler. Two U of *Dpn*I was directly added to PCR product and incubated at 37°C for 3 h. Ten μl of digested PCR mixture was transformed into *E.coli* DH5α cells.

(2) Screening of colonies harboring A1 and A2 mutants

Some putative colonies of each A1 and A2 transformant clones were picked up to grow in 5 ml of LB broth with 100 μg/ml amplicillin antibiotic at 37°C for 12-16 h. The day after, cultured LB broth of each was subjected of plasmid extraction using QIAprep Spin Miniprep Kit. All of extracted plasmids were screened for screening *NS5*-FLAG fragment insertion by PCR using *Bam*HI forward and NS5-

FLAG *Xho*I reverse primers and detected by 0.8% agarose gel electrophoresis. The PCR products exhibited the size of *NS5*-FLAG fragment were purified and further subjected of *Fnu*4HI digestion reaction consisting of 1 μg of purified PCR product, 5 U of *Fnu*4HI restriction enzyme, and 1x NEB buffer 4. The digestion mixture was incubated at 37°C for 5h and then *Fnu*4HI-digested products were analyzed by 3% agarose gel electrophoresis.

(3) Site-directed mutagenesis of pcDNA3.1/Hygro MT-a/bNLS *NS5*-FLAG or A1+2 mutant

To generate pcDNA3.1/Hygro MT-a/bNLS *NS5*-FLAG or A1+2 mutant, the obtained A1 and A2 recombinant plasmids were used as the template. The all of steps were performed the same as A1 and A2 mutagenic generation.

(4) DNA sequencing of pcDNA3.1/Hygro containing A1, A2, or A1+2 mutation

The purified putative pcDNA3.1/Hygro containing A1, A2 or A1+2 mutation were sequenced by sending to Macrogen DNA Sequencing Service (Seoul, Korea) for sequencing analysis. pcDNA3.1/Hygro, which contained the correct sequences corresponding to A1+2 mutation was renamed as pcDNA3.1/Hygro MT-*NS5*-FLAG or MT-NS5.

4.4.4 Testing of expression and sub-cellular localization of WT-NS5 and MT-NS5

(1) Transient transfection of WT-NS5 and MT-NS5 recombinant plasmid into HEK 293 cells

To examine the expression of WT-NS5 and MT-NS5 proteins from the obtained recombinant plasmids, HEK 293 cells were seeded for 2 days before transfection. A hundred μl of transfection complex in serum free DMEM consisting of 6 μl of lipofectamine^{TM} 2000 and 2 μg of WT-NS5, MT-NS5, or empty pcDNA3.1/Hygro plasmid was added to the cells on transfection day. After 6 h, cells

were replaced with 10% FBS DMEM and further incubated. Based on the previous study (100), which demonstrated that NS5 activated NF-κB activity at 48 h p. t. in TNF-α-treated condition, thereby the expression of HEK 293 cells were observed at 48 h p.t.

(2) Investigation of recombinant WT-NS5 and MT-NS5 protein expression by Western blot analysis

After 48 h p.t., cells were harvested for SDS-PAGE and Western blot analysis. Media were removed and then cells were washed with PBS once. Cells were directly added with 80-100 μl of 1x sample buffer and scraped homogenously. Cell lysates were transferred into new 1.5 microtube before heating at 95°C for 10 min. The total cell lysate of WT-NS5 and MT-NS5 were loaded into 10% acrylamid gel and then electrophoresis condition was followed as described in 4.2.4. After blocking membrane with 5% skim milk in PBS, membrane was incubated with primary mouse anti-FLAG antibody diluted in PBS (1:1000) for 1 h and then washed with PBS. The membrane was incubated with 1:1000 dilution of rabbit anti-mouse secondary antibody conjugated with HRP for 1 h and then washed with PBS. Both WT-NS5 and MT-NS5 specific bands were developed and detected as described in 4.2.11.

(3) Investigation of recombinant WT-NS5 and MT-NS5 subcellular localization in HEK 293T cell line

To examine subcellular localization of WT-NS5 and MT-NS5 proteins, HEK 293T cells were used to express both types of NS5 instead of HEK 293 cells because HEK 293 cells were almost detached during the immunofluorescence staining steps. HEK 293T $8x10^4$ cells were grown on glass coverslips in 24-well plate for 2 day before transfection. On transfection day, the transfection complex consisting of 1.5 μl of lipofectamine™ 2000 mixed with 0.5 μg of WT-NS5, MT-NS5, or empty pcDNA3.1/Hygro plasmid in 50 μl of serum free DMEM medium was added on the cells. After 48 h p.t., NS5-positive cells were stained with was mouse anti-FLAG antibody diluted in 1% FBS in PBS (1:500) and followed by Alexa Fluor® 488-conjugated rabbit anti-mouse secondary antibody with 1:1000 dilution in 1% FBS in

PBS. In addtition, Hoechst 33342 dye was used for nuclear staining with 1:1000 dilution in 1% FBS in PBS. After staining, coverslips were mounted as described previously and imaged by confocal microscopy.

4.4.5 Examination of effect of WT-NS5 and MT-NS5 on the expression of DENV-induced cytokine genes in HEK 293 cells

(1) Transient transfection of WT-and MT-NS5 recombinant plasmid into HEK 293 cells

To examine the effect of both WT-NS5 and MT-NS5 on the expression of DENV-induced cytokine genes, HEK 293 cells were seeded in 12-well plate for 2 days before transfection. Fifty μl of transfection complex in serum free DMEM consisting of 3 μl of lipofectamine^{TM} 2000 and 1 μg of WT-NS5, MT-NS5, or empty pcDNA3.1/Hygro plasmid was added to the cells on transfection day. After 6 h, cells were replaced with 10% FBS DMEM and further incubated. To observe the effect of NS5 on cytokine production that might be more predominant effect in condition which NF-κB is activated in the absence of TNF-α, cells were harvested at 48 h p.t.

(2) qRT-PCR using primer specific to DENV-induced cytokines

To investigate the effect of WT-NS5 and MT-NS5 on DENV-induced cytokine genes, HEK 293 cells expressing WT-NS5, MT-NS5 and empty pcDNA3.1/Hygro were subjected of total RNA isolation using High Pure RNA Isolation Kit. One μg of total isolated RNA was reverse-transcribed using SuperScriptIII First-Strand Synthesis System. The obtained cDNA was subjected of qPCR using primers specific for each DENV-induced cytokine genes. The components of qPCR mixture were the same as described in 4.2.6 and then qPCR mixture was pre-incubated at 95°C for 10 min and then followed by 50 cycles of denaturation at 95°C for 10 sec, annealing at 60°C for 10 sec, and extension at 72°C for 20 sec. Then, the calculation of relative mRNA expression was analyzed according to the formula as described in 4.2.6.

(3) Examination of expression of NS5-induced cytokine genes in the presence of TNF-α both mRNA and protein levels

Based on the previous study in which NS5 can activate NF-κB activity at 48 h p. t. in TNF-α-treated condition. One of NS5-induced cytokine gene from step (2) was chosen for repeating of its expression again. HEK 293 cells were transfected with the same condition as step 1. Then, cells were treated with 50 mg/ml of TNF-α diluted in 0.1% FBS DMEM at 48 h p.t. for 6 h. After 6 h of TNF-α incubation, the supernatants of each transfection condition were collected for ELISA using Instant ELISA® according to the manufacturer's instruction (described in 4.2.13) and cell pellets were harvested for total RNA isolation.

4.4.6 Study of the influence of WT-NS5 on RANTES promoter (RANTES is a selected NS5-induced cytokine gene) by using Dual-Luciferase® Reporter Assay System

To study the influence of NS5 on RANTES promoter, RANTES promoter sequence was inserted in pGL3-basic plasmid and named as RANTES promoter reporter plasmid in this study. Then, RANTES promoter reporter plasmid and its internal control plasmid, pRL-SV40, were co-transfected with WT-NS5 or empty pcDNA3.1/Hygro plasmid into HEK 293 cells. The influence of NS5 on RANTES promoter was determined by measuring the luciferase activity by luminometer.

(1) Construction of pGL3 luciferase reporter plasmid containing RANTES promoter sequence

(a) Amplification of RANTES promoter cDNA

To construct pGL3-basic luciferase reporter plasmid containing RANTES promoter with all of transcription factor binding sites for RANTES expression regulation, 881 nucleotides of 5'region immediately upstream from transcriptional start site plus 38 nucleotides of RANTES gene was amplified by PCR using genomic DNA (gDNA) extracted from human PBMC, which was kindly gift from Dr. Watip. Tangjittipokin, Department of Immunology, Faculty of Medicine

Siriraj hospital, Mahidol University, as a template. A pair of primer for RANTES promoter cDNA amplification (RANTES *Kpn*I forward and RANTES *Nhe*I reverse) is shown in Table 4.3. The PCR mixture was consisted of 100 ng of gDNA template, 10 pmole of each primer, 10 mM dNTPs, 1x *pfx* buffer, 1 mM $MgSO_4$, and 2.5 U of *pfx* DNA polymerase in a total volume of 50 μl. After gently mixing, the reaction mixture was carried out in a Biometra TGradient Thermal Cycler. PCR cycles were set at 94 °C for 5 min and followed by 35 cycles of denaturation at 94 °C for 30 sec, annealing at 55 °C for 30 sec, extension at 68 °C for 3 min, and one cycle of final extension at 68 °C for 5 min. The 5 μl of PCR product was loaded in 1% agarose gel and visualized by G:BOX chemiluminescence imaging system. Then, RANTES promoter PCR product was purified by using QIAquick Gel Extraction Kit.

(b) Restriction endonuclease digestion of RANTES promoter cDNA and pGL3-basic plasmid

Purified RANTES promoter PCR product and pGL3-basic plasmid was separately double digested with *Kpn*I HF and *Nhe*I HF restriction enzymes. The 50 μl of digestion mixture included 1 μg of purified RANTES promoter PCR product or pGL3-basic plasmid, 1x NEB buffer 4, 1x BSA, and 5 U each of *Kpn*I HF and *Nhe*I HF. The mixture was incubated at 37°c for 6 h. Then, *Kpn*I and *Nhe*I-digested RANTES promoter PCR product was purified by QIAquick PCR purification Kit whilst *Kpn*I and *Nhe*I-digested pGL3-basic plasmid was purified by using QIAquick Gel Extraction Kit. Both of them were measured for the purity and concentration by NanoDrop spectrophotometer.

(c) Cloning of RANTES promoter cDNA into pGL3-basic plasmid

To insert RANTES promoter cDNA into pGL3-basic plasmid, the digested PCR product was ligated into digested pGL3-basic plasmid in which molar ratio of plasmid to PCR product was 1:3. The ligation mixture consisted of 150 ng of pGL3-basic plasmid, 94 ng of RANTES promoter PCR product, 2 U of T4 DNA ligase and 1x ligation buffer in a volume of 20 μl. The

ligation mixture was incubated at 16 °C in a water bath for overnight. The day after, 10 μl of the ligation mixture was transformed into *E.coli* DH5α competent cells.

(d) Screening of pGL3-basic plasmid containing RANTES promoter sequence

To screen the putative clones of *E.coli* harboring the pGL3 RANTES promoter reporter plasmid, 8 colonies of transformants were picked up and subjected to *E.coli* colony PCR using RANTES *Kpn*I forward and RANTES *Nhe*I reverse primers and detected by 1% agarose gel electrophoresis. The *E.coli* clones exhibited the size of RANTES promoter PCR product were picked up to grow in 5 ml of LB broth with 100 μg/ml amplicillin antibiotic at 37°C for 12-16 h. The day after, cultured LB broth of each was subjected to plasmid extraction using QIAprep Spin Miniprep Kit. The presence of RANTES promoter fragment in the recombinant plasmid was confirmed by *Kpn*I HF and *Nhe*I HF double digestions. The digestion reaction was carried out in 15 μl of volume containing 1 μg of each putative pGL3 RANTES promoter reporter plasmid, 1x NEB buffer 4, 1x BSA, and 5 U each of *Kpn*I HF and *Nhe*I HF. The digested product was analyzed by 1% agarose gel electrophoresis.

(e) DNA sequencing of pGL3-basic plasmid containing RANTES promoter sequence

The purified putative pGL3-basic plasmids containing RANTES promoter sequence were sequenced by sending to Macrogen DNA Sequencing Service (Seoul, Korea) for sequencing analysis. The obtained construct with correct sequences was renamed as pGL3 RANTES promoter reporter plasmid.

(2) Investigation of the influence of NS5 on RANTES promoter by Dual-Luciferase® Reporter Assay System

(a) Co-transfection of pcDNA3.1/Hygro WT-NS5 plasmid and pGL3 RANTES promoter reporter plasmid in HEK 293 cells

To investigate the influence of NS5 on RANTES promoter, HEK 293 cells were seeded in 12-well pate for 2 days before transfection. On transfection day, cells were added with transcription complex consisting of 3.66 μl of lipofectamine™ 2000 mixed with 1 μg of either WT-NS5 or empty pcDNA3.1/Hygro plasmid, 200 ng of pGL3 RANTES promoter reporter plasmid, and 20 ng of pRL-SV40 internal control plasmid. After 5 h of incubation with cells, the transcription complex was removed and replaced with 10% FBS DMEM.

(b) Measurement of RANTES promoter activity by luminometer

After 48 h p.t., cells were washed once with PBS and added with 250 μl of PLB on the cells directly. The cells were incubated on the rocking platform with gently rocking for 15 min at room temperature. Twenty μl of each lysate was transferred into the tubes (flow cytometry tubes). A 100 μl of LAR II reagent was added into the lysate and mixed thoroughly. The fiefly luciferase activities were measured immediately after adding LAR II reagent by luminometer. Then, 100 μl of Stop & Glo® Reagent was added into the same sample and immediately measured for *Renilla* luciferase activity. The influence of NS5 on RANTES promoter was calculated as a formula shown below.

$$\text{RANTES promoter activity (RLU)} = \frac{\left.\dfrac{\text{Fiefly luciferase luminescence}}{\textit{Renilla} \text{ luciferase luminescence}}\right\}\text{Test}}{\left.\dfrac{\text{Fiefly luciferase luminescence}}{\textit{Renilla} \text{ luciferase luminescence}}\right\}\text{Control}}$$

Test = Sample was obtained from the co-transfection between pcDNA3.1/Hygro WT-NS5 and pGL3 RANTES promoter reporter plasmids

Control = Sample was obtained from the co-transfection between pcDNA3.1/Hygro WT-NS5 and empty pGL3-basic plasmids

4.4.7 Identification of whether NS5-activated RANTES promoter is mediated through NF-κB

(1) Generation of pGL3-basic plasmid containing RANTES promoter with NF-κB binding site mutation

To identify that NF-κB is a transcription factor in which NS5 use to induce RANTES expression, RANTES promoter reporter plasmids with the mutation in NF-κB binding sites are very necessary.

(a) PCR-based site-directed mutagenesis for generation of pGL3 RANTES promoter reporter plasmid containing NF-κB binding site mutation

To generate pGL3 RANTES promoter reporter plasmid containing the mutation in NF-κB binding sites, pGL3 RANTES promoter reporter plasmid or "WT-RANTES promoter plasmid" was used as a template. The steps of PCR-based site directed mutagenesis were performed the same as previously. There are 2 binding sites for NF-κB (NF-κB 1 and NF-κB 2) on RANTES promoter. To obtain the complete data, there were 3 different types of NF-κB binding site mutation were generated. First construct was mutated at only NF-κB 1 binding site by replacing the cytosine (C) nucleotide at position -46 and -45 relative to transcription start site with adenine (A) nucleotide and the thymine (T) nucleotide at position -43 with guanine (G) nucleotide. This mutation was called NF-κB 1 mutant. The second construct was mutated at NF-κB 2 binding site by replacing G at position -38 and -37 with C, A at position -36 with T and C at position -33 and -32 with A. This mutation

was called NF-κB 2. The last construct was mutated at both sites of NF-κB and called NF-κB 1+2 mutant by replacing nucleotides as same as in NF-κB 1 mutation or NF-κB 2 mutation. All of nucleotide replacements in both sites of NF-κB was performed by following the study of Casola et al. (141). Three pairs of primer, NF-κB 1, NF-κB 2, NF-κB 1+2 primers, were designed to mutate NF-κB 1, NF-κB 2, or both NF-κB 1 and NF-κB 2 binding sites, respectively (Table 4.3). The PCR mixture was performed separately and consisted of 1x *pfx* DNA polymerase buffer, 2 mM dNTPs, 1mM $MgSo_4$, 0.4 mM dNTPs, 10 pmole each of primers, 0.5 U of *pfx* DNA polymerase, and 100 ng of WT-RANTES promoter plasmid template. PCR profile was 94°C for 5 min for the first round of reaction, followed by 18 cycles of 94°C for 30 sec, 55°C for 30 sec, and 68°C for 12 min. Then, nicked strand PCR product was treated with *Dpn*I and subjected of all the later steps as described previously. There was the problem to amplify NF-κB1+2 mutants so that PCR intergradient's and PCR profile were modified. The enhancer buffer in final concentration of 0.5x and 1x and the varying of annealing temperature at 42, 44, 46, 48, and 50°C were applied to amplified NF-κB 1+2 mutant by using NF-κB 1+2 primers. All of the remaining PCR intergradient and PCR profile were the same. The PCR products were followed as the same steps as previous.

(b) DNA sequencing analysis of pGL3 RANTES promoter reporter plasmid containing NF-κB 1, NF-κB 1 or NF-κB 1+2 mutation

Because there was no recognition site for any restriction enzymes, which could be used to discriminate between WT-RANTES and NF-κB-mutation on RANTES promoter so the putative *E.coli* clones were subjected to plasmid extraction and DNA sequencing analysis directly. The putative plasmids were sequenced by sending to Macrogen DNA Sequencing Service for sequencing analysis. The obtained construct with expected sequences was renamed as NF-κB 1, NF-κB 2, NF-κB 1+2 RANTES promoter reporter plasmid, respectively.

(2) Examination of whether NF-κB is a major transcription factor in which NS5 use to induce RANTES expression

(a) Co-transfection of WT-NS5 plasmid and pGL3 NF-κB-mutated RANTES promoter plasmid to HEK 293 cells

HEK 293 cells were seeded on 12-well plate for 2 days before transfection. The transcription complex consisting of 1 μg of WT-NS5 plasmid with 200 ng of either WT-RANTES promoter, NF-κB 1, NF-κB 2, NF-κB 1+2 RANTES promoter mutation plasmid, or empty pGL3-basic plasmid and 20 ng of pRL-SV40 internal control plasmid mixed with 3.66 μl of lipofectamine^{TM} 2000 in 100 μl of serum free DMEM was added on the cells.

(b) Measurement of RANTES promoter activity of RANTES promoter reporter plasmid containing NF-κB mutations of by luminometer

After 48 h p.t., cells were subjected of PLB lysis. Twenty μl of cell lysates were transferred into the flow cytometry tube and then LAR II and Stop & Glo® reagents were orderly added to the samples before measuring luciferase activity of each reporter. The calculation of RANTES promoter activity of each transfection condition was followed as formula above.

4.4.8 Examination of the binding ability of NF-κB on RANTES promoter in HEK 293 cells expressing WT-NS5 protein by chromatin immunoprecipitation (ChIP) assay

(1) Optimization of the amount of Micrococcal endonuclease enzyme for chromatin digestion

To get the best condition for chromatin with expected size of DNA fragment ~150-900 bp in length, the amount of Micrococcal endonuclease was varied at 0.125, 0.25, 0.5, 0.75, and 1.0 μl and added to $1x10^6$ HEK 293 cells in which these cells were already subjected of cross-linked and other steps as described in

4.2.13 (a). The digested products were analyzed by 2% agarose gel electrophoresis. The amount which generated an appropriated product size of DNA was chosen for ChIP assay in NS5 transfection system.

(2) Transfection of WT-NS5 plasmid into HEK 293 cells

Two days before transfection, $3x10^5$ of HEK 293 cells were seeded in 6-well plate in triplicate for each immunprecipitation reacrion (~$1x10^6$ cells on the day of ChIP assay). Cells were transfected with the transfection complex consisting of 2 μg of WT-NS5 or empty pcDNA3.1/Hygro plasmid mixed and 6 μl of lipofectamine™ 2000 in 100 μl of serum free DMEM. The transfection complex was removed after 6 h of incubation and cells were replaced with 10% FBS DMEM until 48 h p.t.

(3) Determination of the binding activity of p65 subunit of NF-κB to RANTES promoter by ChIP assay

(a) Cross-linking and chromatin digestion

After 48 h p.t., cells were replaced with 2 ml of serum free DMEM and then cross-linked reaction with formaldehyde was performed. The latter steps of cross-linking reaction and chromatin digestion were followed according to 4.2.15 (1) in which triplicate of 6-well plate from the same transfection condition were combined in one tube. Then, the cell suspension was digested with the optimized amount of Micrococcal endonuclease enzyme. After digestion, cells were processed as described previously until keeping at -70°C.

(b) Analysis of chromatin digestion and measurement of DNA concentration

To examine the chromatin digestion result, 50 μl of chromatin digestion from step (a) was subjected of DNA purification and 2% agarose gel electrophoresis. The concentration and purity of DNA were measured by NanoDrop spectrophotometer.

(c) RANTES promoter immunoprecipita-tion using anti-p65 antibody

To determine the binding activity of p65 subunit of NF-κB to RANTES promoter, 5 μg of rabbit anti-p65 antibody was added to 10 μg of digested chromatin prepared in (1). In addition, 1 μl of normal rabbit isotype control antibody was added to the identical transfection condition as a control. The IP samples were subjected of adding of Protein G bead, washing, elution, and DNA purification, respectively.

(d) RANTES promoter amplification by PCR

To determine the amount of RANTES promoter, which was immunoprecipitated, 1 μl of eluted DNA, was used as a template for RANTES promoter amplification by PCR in 15 μl of total volume. The PCR mixture consisted of 1x HS buffer, 1mM of each dNTPs, 0.5 μM each of NF-κB ChIP forward and NF-κB ChIP reverse primers (shown in Table 4.3), 0.375μl of HS Prime Taq DNA polymerase, and nuclease-free water up to 15 μl. PCR profile was 95°C for 5 min for the first round of reaction, followed by 25 cycles of 95°C for 30 sec, 62°C for 30 sec, and 72°C for 30 sec. Eight μl of PCR product was analyzed for the amount of RANTES promoter by 2% agarose gel electrophoresis. Using 1μl of DNA template and 25 cycles of PCR amplification were the best conditions, which have already been optimized (data not shown).

4.4.9 Confirmation of the interaction and co-localization between NS5 and human Daxx protein in HEK 293 cells

(1) Confirmation of the interaction between NS5 and Daxx by Co-IP assay

To confirm the interaction between NS5 and human Daxx protein in mammalian cells, HEK 293 cells were transfected with 1 μg of plasmid expressing either WT-NS5 or MT-NS5. Based on the previous study has reported that the effect of Daxx on inhibition of NF-κB activity was observed only in stimulated

cells. Thereby, the interaction between NS5 and Daxx should be observed at the same condition. After 48 h p.t., cells were treated with 50 mg/ml of TNF-α diluted in 0.1% FBS DMEM for 6 h. Cells were lysed with RIPA buffer and processed following Co-IP method in 4.2.11. Briefly, the interaction complex NS5 and Daxx was immunoprecipitated by adding 5 μg of goat anti-Daxx or 5μg of mouse anti-FLAG on the lysate and subjected of SDS-PAGE electrophoresis using 10% acrylamide gel. The expression of NS5 and Daxx was detected by adding either mouse anti-FLAG antibody or goat anti-Daxx antibody following by either a rabbit anti-mouse antibody conjugated- HRP or a swine anti-rabbit antibody conjugated-HRP, respectively. Immunoreactive bands of NS5 and Daxx were generated after adding SuperSignal West Pico substrate and detected using a G:BOX chemiluminescence imaging system.

(2) Testing for the co-localization between NS5 and Daxx using co-localization assay

To confirm whether at 48 h p.t. NS5 and Daxx expressed at the same compartment of the cells, HEK 293 cells were grown on coverslips for 2 days and then transfected with plasmid expressing either WT-NS5, MT-NS5 or empty pcDNA 3.1/Hygro. At 48 h p.t., 50 mg/ml of TNF-α diluted in 0.1% FBS DMEM was added on the cells for 6 h. Cells cultured on coverslips were subjected of the processes of immunofluorescence staining using mouse anti-FLAG antibody and rabbit anti-Daxx antibody to detect NS5 and Daxx protein, respectively. An Alexa 488-conjugated rabbit anti-mouse antibody and a Cy3-conjugated donkey anti-rabbit antibody were used as secondary antibodies for NS5 and Daxx, respectively. The fluorescence images were captured by confocal microscope.

CHAPTER V
RESULTS

In order to examine the role of NS5 protein in cytokine induction, examination of the inflammatory cytokine gene expression profile in DENV infection system was performed to identify which gene was induced in DENV-infected HEK 293 cells, which could be used as a corresponding result with the cytokine gene expression profile, induced by NS5. Then, HEK 293 cells expressing WT-NS5 and MT-NS5 protein were constructed and tested for their effects on the expression of DENV-induced cytokine genes by qRT-PCR, using gene-specific primers. Twenty two cytokine genes were found to be induced by DENV. Then, 5 of the highest fold change of the DENV-induced cytokine genes were chosen for further examination in HEK 293 cells, expressing WT-NS5 and MT-NS5 protein. Furthermore, TNF-α was also included, because it has been demonstrated to be involved in DENV pathogenesis. RANTES was the single one of DENV-induced cytokine genes that showed the predominant differential expression affected by NS5. It was up-regulated in HEK 293 cells expressing WT-a/bNLS NS5, but down-regulated in MT-a/bNLS NS5. Thereby, RANTES was chosen to be a model for further study in the mechanism how NS5 regulates the cytokine production, using the luciferase reporter gene assay and chromatin immunoprecipitation (ChIP). Furthermore, the interaction between NS5 and human Daxx protein, NF-κB inhibitor protein, was subsequently confirmed by Co-IP and by a co-localization assay in order to propose that NS5 might need the cellular host proteins to manipulate its benefit in its replication and in pathogenesis. The following sections described the results of all experiments in this study.

5.1 Study of host inflammatory cytokine gene expression profile in DENV-infected HEK 293 cells by RT^2 Profiler™PCR Array system

5.1.1 DENV infection and analysis of the percentage of infection

HEK 293 cells were infected with either mock or DENV-2 at MOI of 1. After 24 and 48 h p i., cells were immunostained with anti-DENV E monoclonal antibody (clone 4G2), followed by the corresponding secondary antibody conjugated with FITC before analyzing the percentage of infection by flow cytometry. The result of flow cytometry is shown in figure 5.1. A demonstrated that, at both time points 24 and 48 h p.i., the percentage of infection or % infectivity of DENV-infected HEK 293 cells was comparable (93.05% and 94.85%, respectively.). At the same samples, the percentage of cell viability (% cell viability) of the infected cells was also measured and shown in figure 5.1B. At 48 h p.i., the % cell viability was less than at 24 h p.i. (68.3 and 85.4, respectively). Furthermore, the morphology of DENV-infected cells showed the cytopathic effect (CPE) at 48 h p.i., which could be observed under the light microscope (data not shown). Thereby, the sample of DENV-infected HEK 293 cells at 24 h p.i. was chosen for further study in the RT^2 Profiler™PCR Array system as a representative of healthy productively DENV-infected HEK 293 cells.

5.1.2 RT^2 Profiler™PCR Array

DENV-infected HEK 293 cells were subjected to total RNA isolation; the RNA was reverse-transcribed, and screened for an inflammatory cytokine gene profile, using Human Inflammatory Response and Autoimmunity PCR Array. After analysis of the result with, Data Analysis Web Portal supported by SABiosciences, 22 up-regulated genes and 7 down-regulated genes by DENV were found in HEK 293 cells. All of the up-regulated and down-regulated genes were further determined by selection from more than 1.5 fold change (> 1.5 of fold change), compared with that of mock-infected HEK 293 cells. The lists of up-regulated and down-regulated genes is shown in figure 5.2A and 5.2B, respectively. Because of the interest in the role of NS5 in cytokine production, with might be related with the cytokine storm phenomenon in

DENV infection, some of the DENV-induced cytokine genes were chosen for further studies in HEK 293 cells, expressing WT-NS5 and MT-NS5 protein.

5.2 Construction of mammalian expression plasmid expressing wild-type (WT)-a/bNLS NS5-FLAG protein

5.2.1 Amplification of full length WT-a/bNLS *NS5*-FLAG cDNA

Full length WT-a/bNLS *NS5* cDNA tagged C-terminally with a FLAG sequence was amplified from a pET21a DENV-2 NS5. The PCR product with the size of 2.7 kb is shown in figure 5.3. Purified PCR product was double digested with *Bam*HI and *Xho*I restriction enzymes and purified. The digested WT-a/bNLS *NS5*-FLAG fragment was ligated into pcDNA3.1/Hygro, doubly digested with the same enzymes to generate pcDNA3.1/Hygro WT-a/bNLS *NS5*-FLAG. The ligation mixture was transformed into *E.coli* DH5α.

5.2.2 Screening of *E.coli* clones containing recombinant pcDNA3.1/Hygro WT-a/bNLS *NS5*-FLAG

Seven putative clones were picked up for plasmid extraction using the QIAprep Spin Miniprep Kit. Then, 7 extracted plasmids were screened for *NS5*-FLAG fragment insertion by PCR and analysed by agarose gel electrophoresis. All of 7 obtained clones showed the expected size of NS5-FLAG fragment insertion as shown in figure 5.4.

5.2.3 DNA sequencing of recombinant pcDNA3.1/Hygro WT-a/bNLS *NS5*-FLAG

One purified pcDNA3.1/Hygro WT-a/bNLS *NS5*-FLAG was sent to Macrogen DNA sequencing Service (Seoul, Korea). The sequencing result showed that there were 8 positions in WT-NS5 construct at the amino acid position: 196, 325, 454, 551, 673, 674, 683, and 759, respectively, showed the variation of type of NS5 amino acid among DENV-2 strain 16681 characterized by Sittisompat et al., Kinney

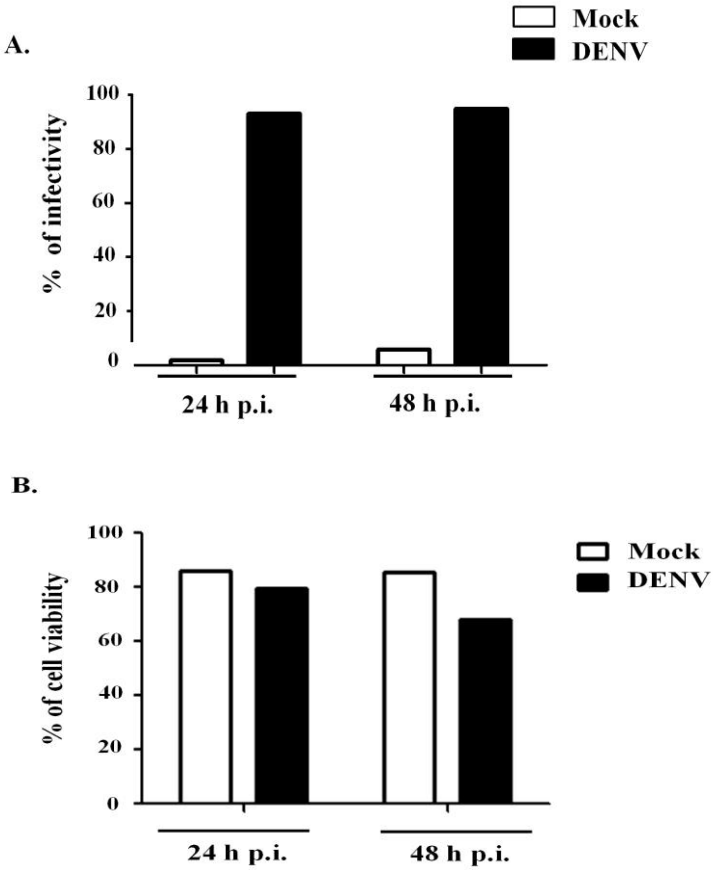

Figure 5.1 Flow cytometry analysis of percentage of DENV-infected HEK 293 cells and trypan blue exclusion assay of cell death of DENV-infected HEK 293 cells.

HEK 293 cells were mock-infected or DENV-infected for 24 and 48 h p.i. At both time points, cells were immunostained with anti-DENV E monoclonal antibody, followed by a corresponding secondary antibody conjugated with FITC. Then, the percentage of DENV-positive cells (% of infectivity) was analyzed by flow cytometry (A). At the same sample, cells were subjected of trypan blue exclusion assay to measure the % of cell viability (B).

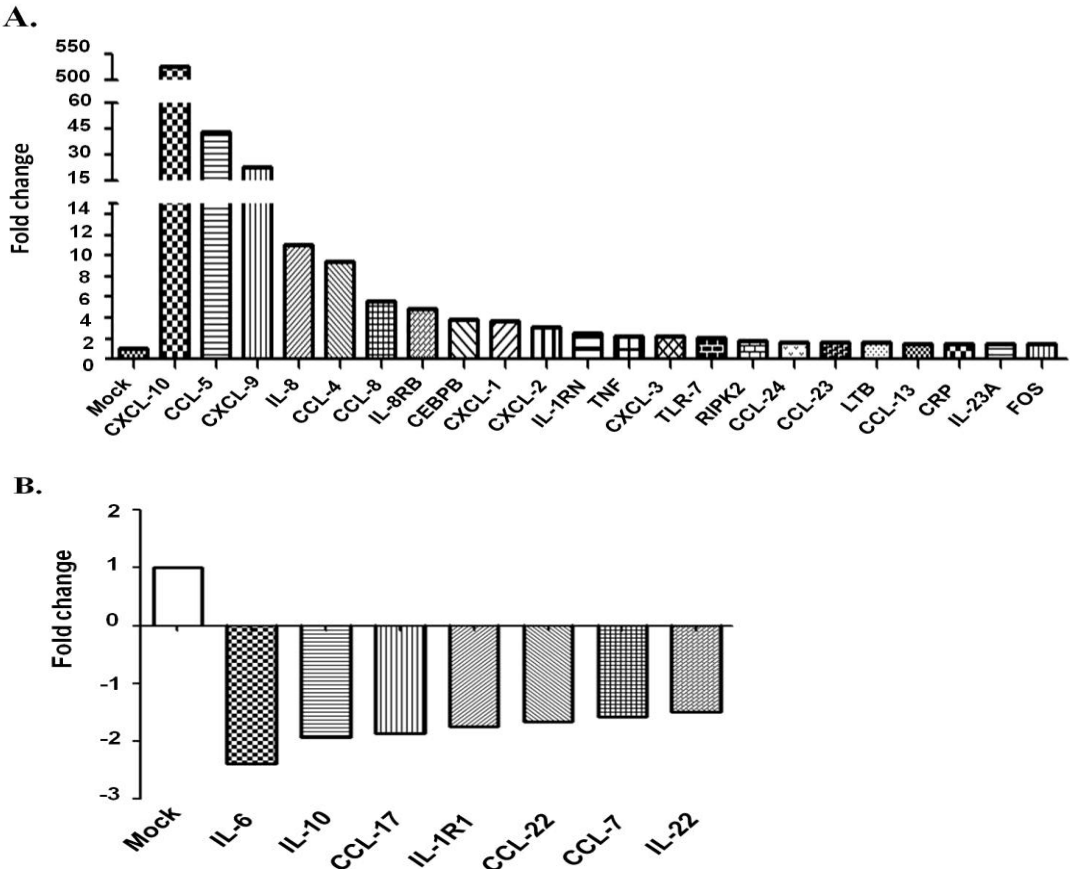

Figure 5.2 **RT^2 Profiler™PCR Array results of DENV-infected HEK 293 cells.** HEK 293 cells were infected with either mock or DENV for 24 h. Then, total RNA was isolated and reverse-transcribed into cDNA. The obtained cDNA of each transfection condition was subjected of RT^2 Profiler™PCR array screening. After analysis of relative expression (fold change) compared with mock-infected cells, both up-regulated and down-regulated genes with a fold change of more than 1.5 were chosen and represented in A and B, respectively.

et al., and, Block et al.(data of amino acid alignment and the varied amino acids are shown in bold and underline letters in an appendix 6). However, these variations found in this construct showed the homology with NS5 of DENV-2 strain 16681. This construct was renamed as pcDNA3.1/Hygro WT-NS5-FLAG or WT-NS5.

5.3 Construction of mammalian expression plasmid expressing mutated (MT)-a/bNLS NS5-FLAG protein

5.3.1 Site-directed mutagenesis

By using pcDNA3.1/Hygro WT-*NS5* FLAG as a template for site-directed mutagenesis to generate pcDNA3.1/Hygro MT-a/bNLS *NS5*-FLAG or A1+2 mutant, A1 and A2 recombinant plasmids in the form of nicked circular strands were generated by PCR as shown in figure 5.5. The products of *Dpn*I digestion for degrading the parental pcDNA3.1/Hygro WT-*NS5* FLAG template plasmid is shown figure 5.6.

5.3.2 Screening of colonies harboring A1 and A2 mutations

Only four putative colonies of A1 mutant and five colonies of A2 mutant were detected on LB agar plate as transformant clones. Then, these transformant clones were selected for plasmid extraction and subjected to agarose gel electrophosis (figure 5.7A). Three recombinant plasmids of A1 mutant and four A2 mutants were further subjected of PCR amplification to screen for an *NS5*-FLAG fragment insertion, by using the *Bam*HI forward primer and the *Xho*I reverse primer tagged with FLAG sequences (figure 5.7B). The amplicons were purified, digested with *Fnu*4HI to select the clones containing the A1 or A2 mutation and subjected to 3% agarose gel electrophoresis. There are seven recognition sites of *Fnu*4HI in WT-*NS5*-FLAG fragment, giving rise to 8 digested products with the size of 991, 790, 241, 217, 190, 133, 124, and 53 bp, whereas A1 mutation contains 8 recognition sites giving rise to 9 digested products with the size of 991, 790, 217, 190, 133 (2 fragments), 124, 108, and 53 bp, respectively. The A2 mutation contains 9 recognition sites, which gave 10

digested products with the size of 991, 790, 217, 190, 181, 133, 124, 57, 53, and 3 bp, respectively. A1 and A2 mutants were discriminated from WT-*NS5*-FLAG in which the fragment with the size of 241 bp in WT-*NS5*-FLAG was digested into 133 and 108 bp in the A1 mutant, and 181, 57, and 3 bp in the A2 mutant. There are 2 clones of each A1 and A2 mutation, that exhibited the fragment sizes as expected (figure 5.8) and were selected to be the template for an A1+2 mutation generation. Two individual clones of each A1 and A2 mutants were used as the templates to generate A1+2 mutant, using the A2 and A1 mutagenic primers, respectively. The PCR result showed that A1+2 PCR products could be amplified more, when the A2 mutant was used as a template than the A1 mutant (figure 5.9); therefore only PCR products from the A2 mutant template were used to generate A1+2 mutant further. One putative A1+2 recombinant plasmid was selected to be digested with *Dpn*I (figure 5.10) and transformed into *E.coli*. Five transformant clones were picked up to extract the plasmid and used to be a template for *NS5*-FLAG fragment amplification. The *NS5*-FLAG PCR products (figure 5.11) were then purified for further *Fnu*4HI digestion. Figure 5.12 showed .the products of *Fnu*4HI digestion to select A1+2 mutant from the A1 mutation template. *Fnu*4HI digested A1+2 mutation into10 fragments with the size of 991, 790, 217, 190, 181, 133, 124, 57, 53, 48, and 3 bp. The A1+2 mutant was discriminated from the A2 mutation template, in which a fragment with the size of 181 bp is present in the A2 mutant, and was digested in to 133, and 48 bp in the A1+2 mutant.

5.3.3 DNA sequencing of pcDNA3.1/Hygro containing A1, A2, or A1+2 mutation

Two individual putative clones of each A1, A2, and A1+2 mutants were sent to Macrogen DNA Sequencing Service for sequencing analysis. The sequencing results showed that all the plasmids contained A1, A2, or A1+2 mutations, as expected. Figure 5.13 showed partial chromatograms of DNA sequences of WT-NS5-FLAG and A1+ 2 mutant (K371-372A and K387-389A). In addition, pcDNA3.1/Hygro MT-a/bNLS *NS5*-FLAG was renamed as pcDNA3.1/Hygro MT-*NS5*-FLAG or MT-NS5.

5.4 Testing of expression and sub-cellular localization of WT-NS5 and MT-NS5

5.4.1 Investigation of recombinant WT-NS5 and MT-NS5 protein expression in HEK 293 cells by Western blot analysis

Before starting the experiments in HEK 293 cells, both WT-NS5 and MT-NS5 were tested for the expression with the corrected size in HEK 293 cells. After 48 h p.t., cells were harvested and subjected to SDS-PAGE and Western blot analysis. Figure 5.14A showed the expression of WT-NS5 and MT-NS5 with expected molecular weight about 100 kDa in which MT-NS5 could be lesser expressed than WT-NS5 protein.

5.4.2 Investigation of recombinant protein WT-NS5 and MT-NS5 sub-cellular localization in HEK 293T cells

Because of the problem in immunofluorescence staining steps, HEK 293T cells were used to demonstrate subcellular localization of WT-NS5 and MT-NS5 instead of HEK 293 cells. As described previously, almost the times during DENV-2 infection or transient transfection of NS5 recombinant plasmid showed predominant nuclear accumulation of WT-NS5 whereas MT-NS5 containing 2 mutation sites in a/bNLS almost abolished the nuclear translocation of NS5. As expected, both WT-NS5 and MT-NS5 recombinant plasmids obtained from the construction shows the expected localization in transfected HEK 293T cells. Sub-cellular localization of WT-NS5 and MT-NS5 at 48 h p.t. was chosen to be a representative of the result and shown in figure 5.14B

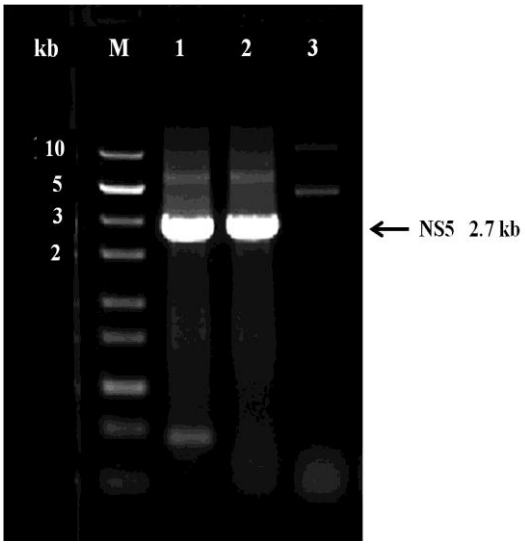

Figure 5.3 Agarose gel electrophoresis of WT-a/bNLS *NS5* cDNA amplicon. The full length WT-a/bNLS *NS5* cDNA tagged C-terminally with FLAG sequences (2.7 kb) was amplified from pET-21a, containing the DENV-2 *NS5* gene by PCR using the *Bam*HI forward primer and *Xho*I reverse primer, tagged with FLAG sequences. kb = kilobase, lane M = ZipRuler 1DNA ladder marker, lane 1 = *NS5*-FLAG amplicon was amplified by using a pair of primer used for clone of *NS5* gene in pET21a plasmid (PCR positive control), lane 2 = *NS5*-FLAG amplicon was amplified by using *Bam*HI forward primer and *Xho*I reverse primer tagged with FLAG sequences, and lane 3 = PCR negative control was amplified from empty pET21a plasmid.

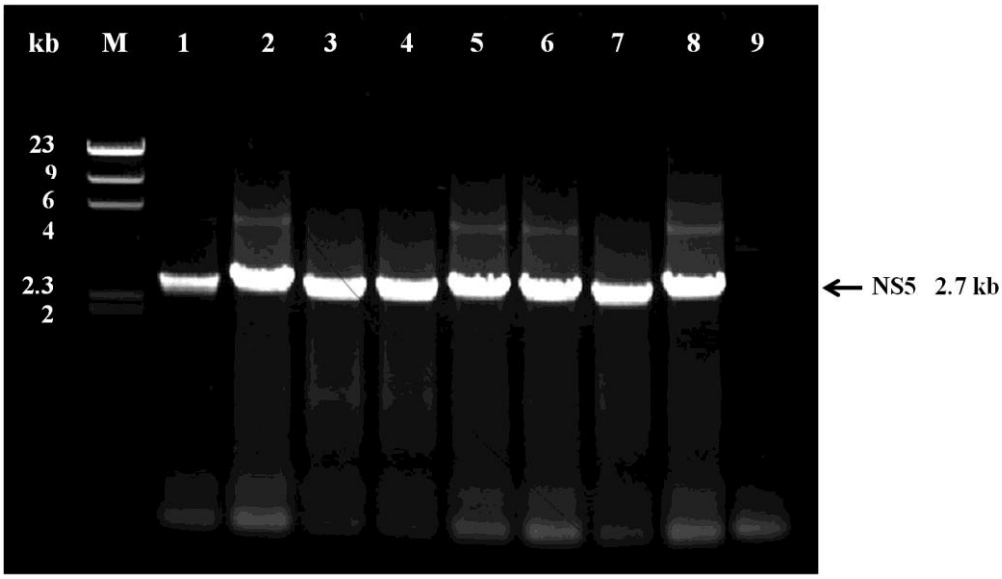

Figure 5.4 Agarose gel electrophoresis showing recombinant plasmids containing WT-a/bNLS *NS5*-FLAG fragment.

The extracted plasmids from 7 individual clones of *E. coli* DH5α were used to be the template in the PCR method for identifying pcDNA3.1/Hygro containing WT-a/bNLS *NS5*-FLAG fragment, using the *Bam*HI forward primer and *Xho*I reverse primer tagged with FLAG sequences. kb = kilobase, lane M = λ *Hind*III DNA ladder marker, lane 1 = *NS5* amplicon was amplified from pET21a containing DENV-2 *NS5* gene (PCR-positive control), lane 2-7 = *NS5*-FLAG amplicons were amplified from 7 individual *E. coli* clones, 9 = PCR-negative control using empty pcDNA3.1/Hygro as a template.

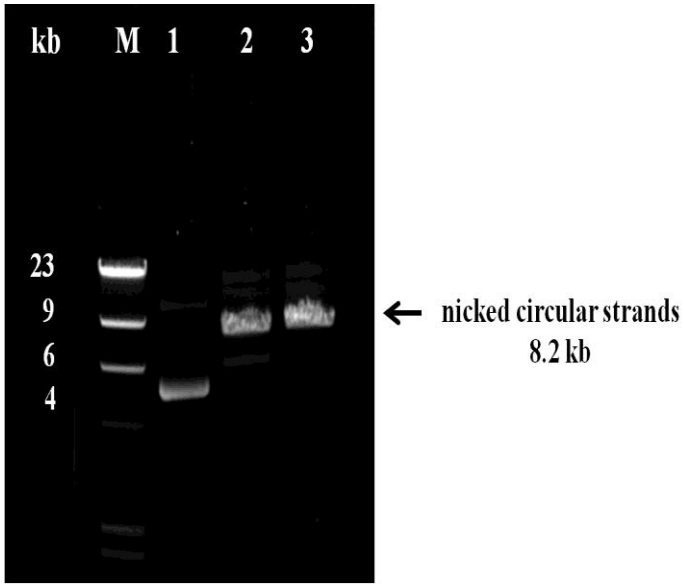

Figure 5.5 Agarose gel electrophoresis of PCR products of putative pcDNA3.1/Hygro containing A1 or A2 mutation site generated by site-directed mutagenesis.

The PCR products of A1 (lane 2) and A2 (lane 3) exhibiting a form of nicked circular strands (8.2 kb), were amplified from pcDNA3.1/Hygro WT-*NS5*-FLAG by PCR. kb = kilobase, M = λ *Hind*III DNA ladder marker, lane 1 = pcDNA3.1/Hygro WT-*NS5*-FLAG used as a loading control plasmid, lane 2 = putative pcDNA3.1/Hygro containing A1 mutation, lane 3 = putative pcDNA3.1/Hygro containing A2 mutation

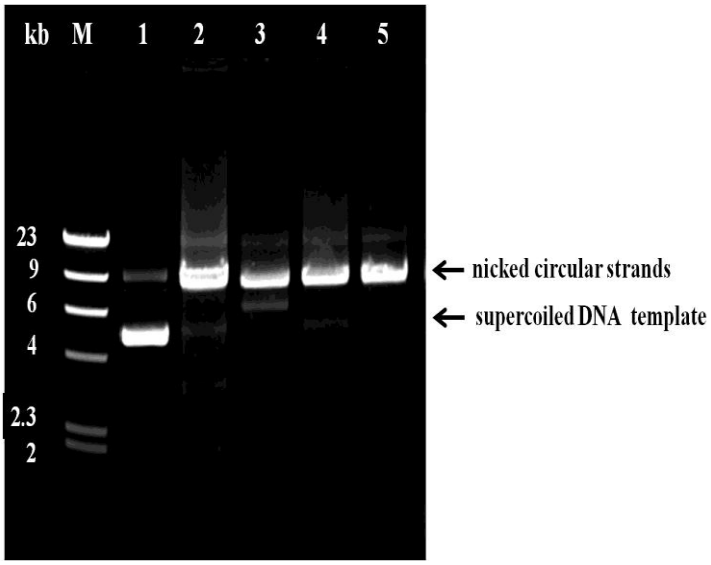

Figure 5.6 Agarose gel electrophoresis of *Dpn*I-digested products of putative pcDNA3.1/Hygro, containing the A1 or A2 mutation.

The PCR products in the form nicked circular strands (lane 2 and 4) were digested with *Dpn*I restriction enzyme (lane 3 and 5) to degrade the parental DNA template, pcDNA3.1/Hygro WT-*NS5*-FLAG (supercoiled DNA). kb = kilobase, lane M = λ *Hind*III DNA ladder marker, lane 1 = pcDNA3.1/Hygro WT-*NS5*-FLAG used as a loading control plasmid, lane 2 and 4 = putative pcDNA3.1/Hygro, containing A1 and A2 mutation, lane 3 and 5 = *Dpn*I-digested putative pcDNA3.1/Hygro, containing A1 and A2 mutations, respectively.

A.

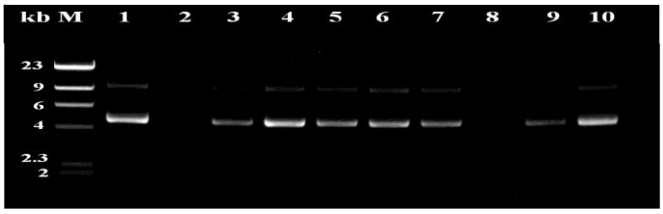

B.

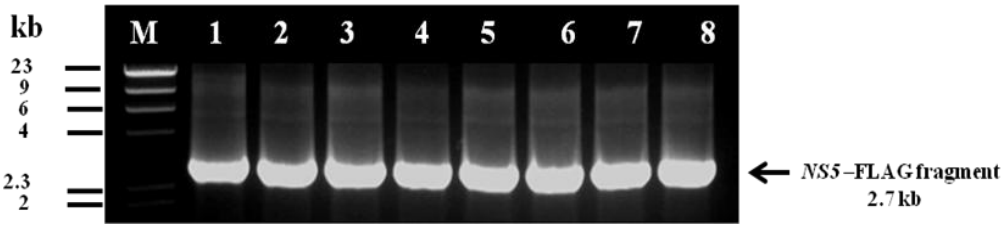

Figure 5.7 Agarose gel electrophoresis of extracted 5 putative pcDNA3.1/Hygro containing A1 or A2 mutation and *NS5*-FLAG PCR products amplified from the putative extracted plasmids.

A.Four clones of the putative A1 mutant (lane 2, 3, 4, and 5) and 5clones of the putative A2 mutant (lane 6, 7, 8, 9, and 10) were extracted and subjected of agarose gel electrophoresis. kb = kilobase, lane M = λ *Hind*III DNA ladder marker, lane 1= pcDNA3.1/Hygro WT-*NS5*-FLAG used as a loading control plasmid. B. Only 3 recombinant plasmids of the A1 mutant and 4 recombinant plasmids of the A2 mutant were further selected to be template for *NS5*-FLAG fragment amplification by PCR, using *Bam*HI forward primer and *Xho*I reverse primer tagged with FLAG sequences primers. kb = kilobase, lane M = λ *Hind*III DNA ladder marker, lane 1 = *NS5*-FLAG fragment amplified from pcDNA3.1/Hygro WT-*NS5*-FLAG as PCR appositive control, lane 2, 3, and 4 = *NS5*-FLAG fragment amplified from 3 selected clones of A1 recombinant plasmid, lane 5, 6, 7, and 8 = *NS5*-FLAG fragment amplified from 3 selected clones of A2 recombinant plasmid

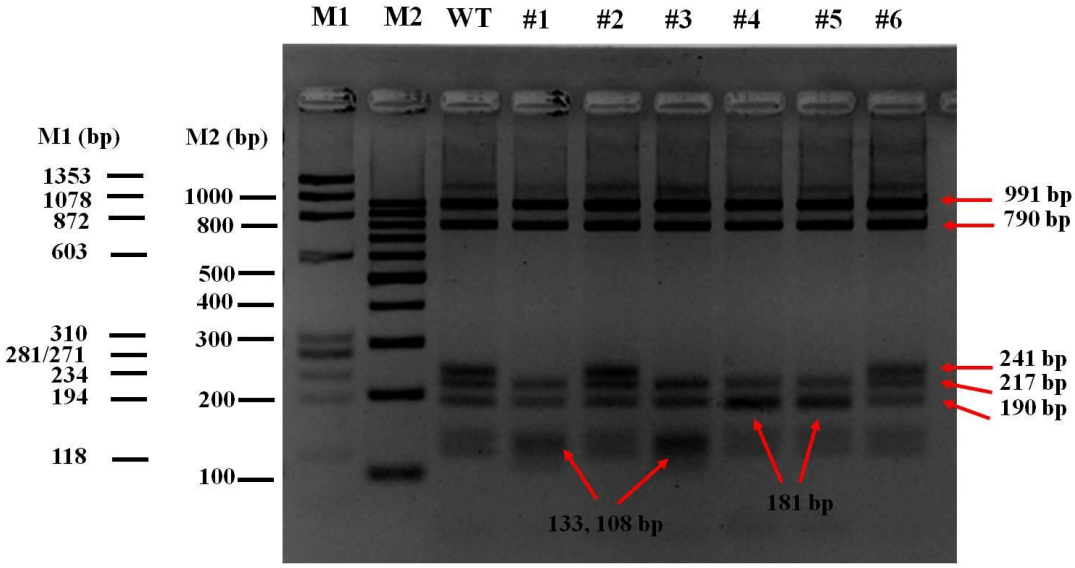

Figure 5.8 Agarose gel electrophoresis of *Fnu*4HI-digested products of A1 and A2 mutants.

The purified *NS5*-FLAG PCR products from 3 selected clones of A1 and A2 mutant were digested with *Fnu*4HI restriction enzymes and subjected of 3% agarose gel electrophoresis. *Fnu*4HI digested WT-*NS5*-FLAG fragment into 8 fragments (lane 3), used as a control, whereas *Fnu*4HI digested A1 mutant into 9 fragments (lane#1 and #3) and 10 fragments of A2 mutant (lane #4 and #5), respectively. A1 and A2 mutation are determined by the fragment with the size of 241 bp present in WT-*NS5*-FLAG was digested into 133 and 108 bp in A1 mutant and 181, 57, and 3 bp in A2 mutant. M1 = ∅x 174 DNA ladder marker, M2 = 100 bp DNA ladder marker, bp = basepair.

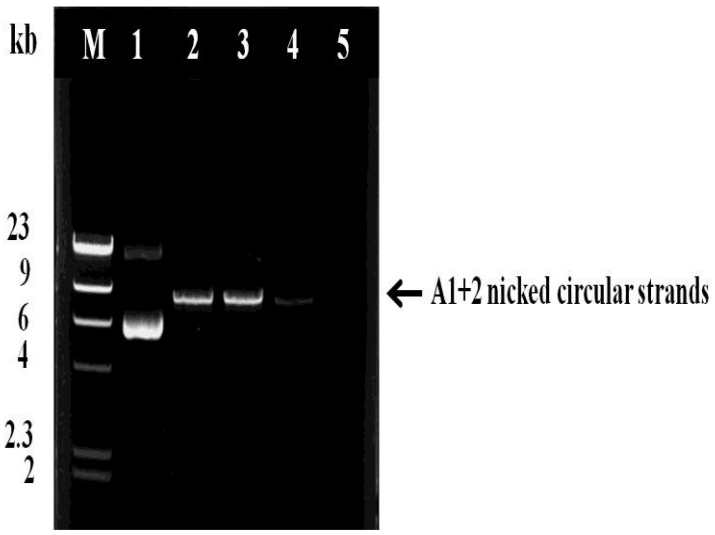

Figure 5.9 Agarose gel electrophoresis of PCR products of putative pcDNA3.1/Hygro containing A1+2 mutations using A1 and A2 mutants as the template.

The PCR products of A1+2 mutations exhibiting a form of nicked circular strands were amplified from pcDNA3.1/Hygro A2 mutation by PCR. kb = kilobase, M = λ *Hind*III DNA ladder marker, lane 1 = pcDNA3.1/Hygro WT-*NS5*-FLAG used as a loading control plasmid, lane 2 and 3 = putative pcDNA3.1/Hygro containing A1+2 mutation amplified from 2 individual clones of A2 mutant, lane 4 and 5 = putative pcDNA3.1/Hygro containing A1+2 mutations amplified from 2 individual clones from A1 mutant.

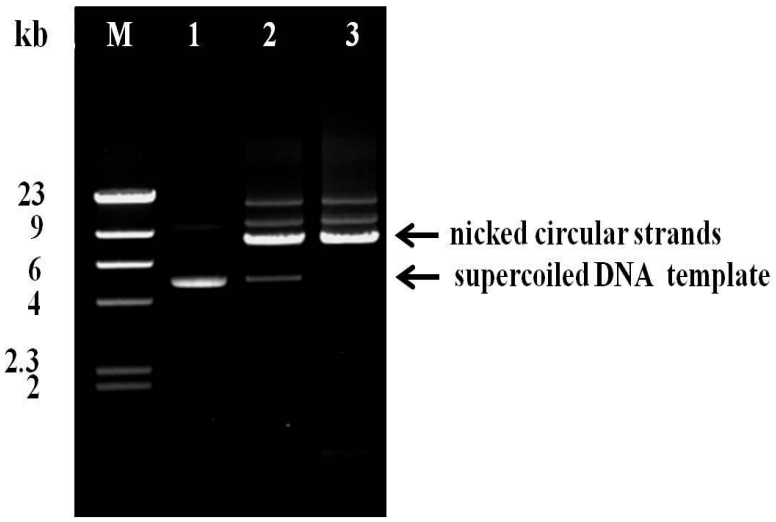

Figure 5.10 Agarose gel electrophoresis of *Dpn*I-digested products of putative pcDNA3.1/Hygro containing A1+2 mutations.

The PCR product in the form nicked circular strands was digested with *Dpn*I restriction enzyme to degrade the parental DNA template, supercoiled.pcDNA3.1/Hygro WT-*NS5*-FLAG (lane 3). kb = kilobase, lane M = λ *Hind*III DNA ladder marker, lane 1 = pcDNA3.1/Hygro A2 mutation used as a loading control plasmid, lane 2 and 3 = putative pcDNA3.1/Hygro containing A1+2 mutation without and with *Dpn*I restriction enzyme.

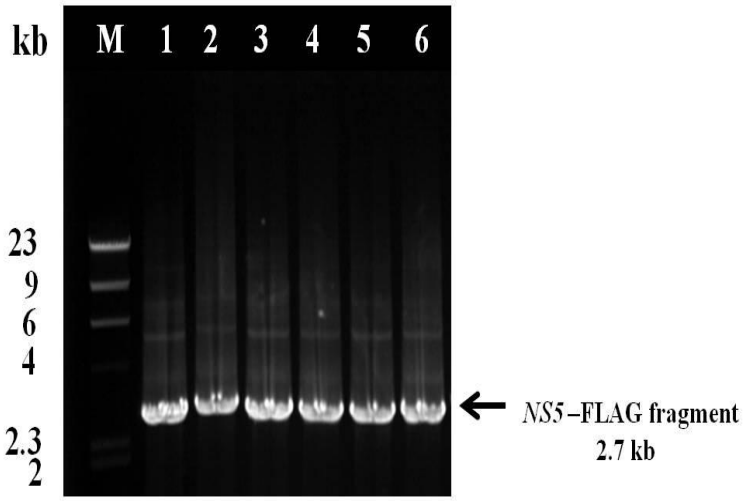

Figure 5.11 Agarose gel electrophoresis of *NS5*-FLAG PCR products amplified from extracted putative A1+2 recombinant plasmids.

The *NS5*-FLAG PCR products were amplified from 5 extracted putative A1+2 recombinant plasmids by PCR using *Bam*HI forward primer and *Xho*I reverse primer tagged with FLAG sequences primers. kb = kilobase, lane M = λ *Hind*III DNA ladder marker, lane 1 = *NS5*-FLAG fragment amplified from pcDNA3.1/Hygro A2 mutation as PCR a control, lane 2-6 = *NS5*-FLAG fragment amplified from 5 extracted putative A1+2 recombinant plasmids, respectively.

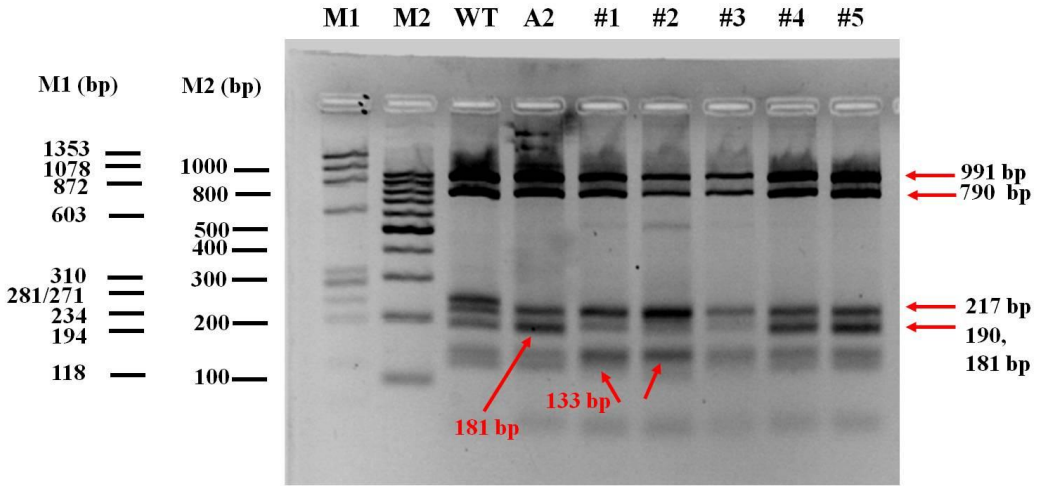

Figure 5.12 Agarose gel electrophoresis of *Fnu*4HI-digested products of A1+2 mutant generated by A1 mutant template.

Purified PCR products of A1+2 mutations generated by using A2 mutation as a template were digested with *Fnu*4HI restriction enzyme and subjected of 3% agarose gel electrophoresis. A1+2 mutants were discriminated from A2 mutation template (lane A2) in which fragment with the size of 181 bp present in A2 mutant was digested in to 133 and 48 bp in A1+2 mutant. (lane #1 and #2). M1 = ∅x 174 DNA ladder marker, M2 =100 bp DNA ladder marker, lane WT = WT-*NS5*-FLAG fragment was digested to be a control, lane A2 = *NS5*-FLAG fragment was amplified from A2 mutant as a control as well, lane #1-#5 = *NS5*-FLAG fragments were amplified from 5 putative A1+2 recombinant plasmids, bp = basepair.

A. WT-NS5

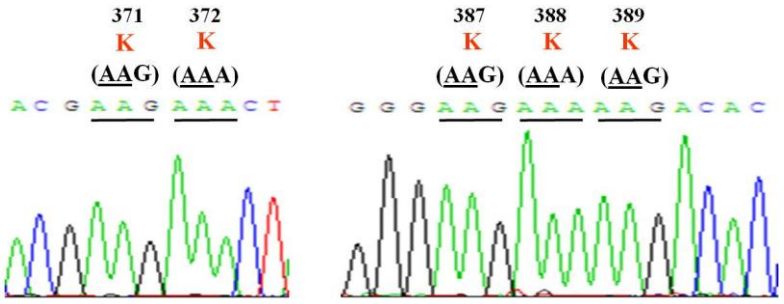

B. MT-NS5

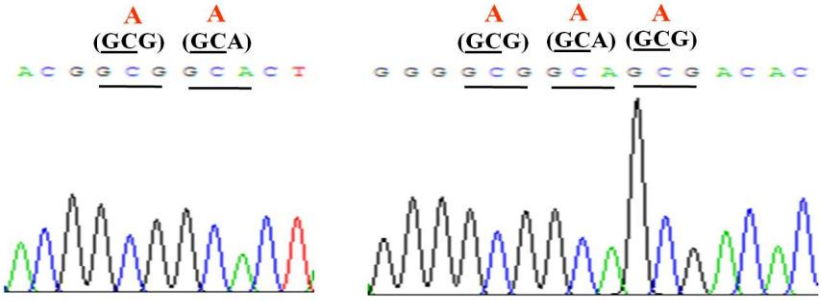

Figure 5.13 Partial sequencing profiles of WT-*NS5*-FLAG and MT-*NS5*-FLAG.

A. The partial nucleotide sequences of WT-*NS5*-FLAG. The codon AAG or AAA were coded for lysine (K).

B. The partial nucleotide sequences of MT-*NS5*-FLAG or A1+2 mutant. The codon for coding to lysine (K) was changed to alanine (A) in 2 positions which are 371-372 and 387-389 positions related to amino acid position in full length NS5 protein.

The nucleotide sequences were underlined indicating the exchanged nucleotides.

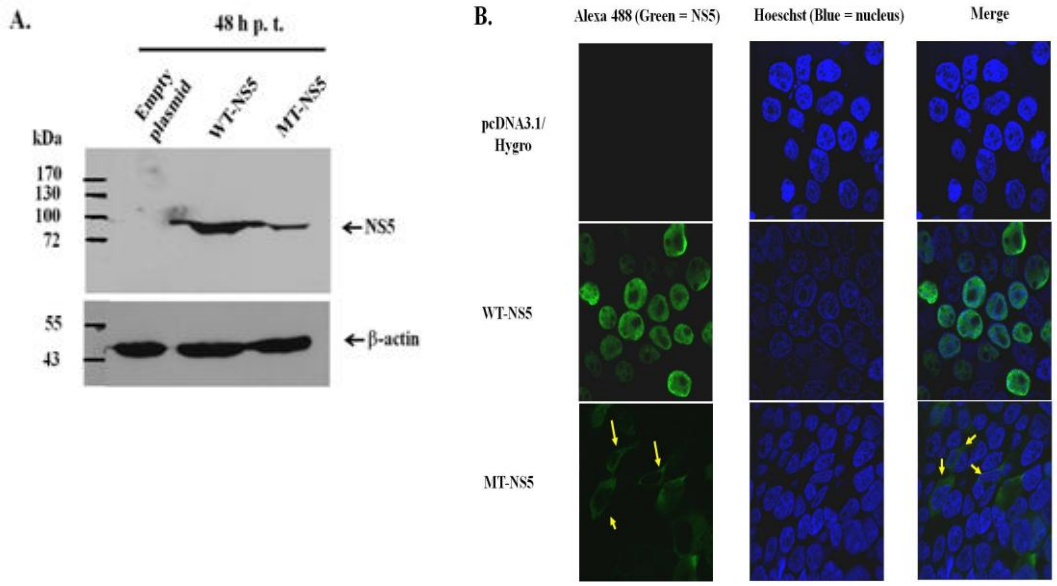

Figure 5.14 Expression and subcellular localization of WT-NS5 and MT-NS5 proteins by WB and immunoflurescence staining assay.

A.Plasmid expressing WT-NS5 or MT-NS5 tagged with FLAG sequence was separately transfected in HEK 293 cells. After 48 h p.t., the total protein of each samples were equally loaded and subjected of 10% SDS-PAGE and Western blot analysis using anti-FLAG antibody. The expected 100 kDa of NS5 in molecular weight was compared with PageRuler^{TM}prestained protein ladder. An empty pcDNA3.1/Hygro was transfected as a control. B. HEK 293T cells were transfected with plasmid expressing either WT-NS5 or MT-NS5 for 48 h. Cells were immunostained with mouse anti-FLAG antibody followed by Alexa Fluor® 488-conjugated rabbit anti-mouse antibody. Hoechst dye was used for nuclear staining. Green color represents NS5 protein staining and blue represents nucleus of the cells. The yellow arrows indicate the accumulation of NS5 protein in cytoplasm expressed from MT-NS5 recombinant plasmid. An empty pcDNA3.1/Hygro was transfected as a control.

5.5 Examination of effect of WT-NS5 and MT-NS5 on the expression of DENV-induced cytokine genes in HEK 293 cells

5.5.1 qRT-PCR using primer specific to DENV-induced cytokine genes

HEK 293 cells expressing either WT-NS5 or MT-NS5 were subjected to total RNA isolation and cDNA reverse-transcription. The synthesized cDNA of WT-NS5-and MT-NS5-transfected cells was used to examine the expression of DENV-induced cytokines. Among all of 22 up-regulated genes, the first 5 of highest fold change of DENV-induced cytokine genes including CXCL-10 (IP-10), CCL-5 (RANTES), CXCL-9, IL-8, and CCL-4 (MIP-1β) were chosen for further in NS5-trasnfected cells. Furthermore, TNF-α which involves in DENV pathogenesis was also included. qPCR was performed by using primers which are specific for these cytokine genes. Figure 5.15 shows that WT-NS5 could induce higher RANTES mRNA expression than that of MT-NS5. In contrast to the expression of IL-8 and TNF-α, MT-NS5 could induce their expressions higher than WT-NS5. Both WT-NS5 and MT-NS5 did not affect IP-10 expression. For the remaining cytokine genes including of MIP-1β and CXCL-9, it could not interpret the induction effect because Ct amplification of MIP-1β was more than 35 cycles and the technical error for CXCL-9 amplification. Since RANTES was predominantly induced by WT-NS5, which mainly localized in the nucleus of transfected cells corresponding to the rationale of this study and together with it has been reported the involving in DENV pathogenesis thereby RANTES was chosen for studies in mechanisms how NS5 regulates cytokine production.

5.5.2 Repeating the expression of RANTES expression both in mRNA and protein levels in the presence of TNF-α

Before progressing to further steps, RANTES expression was confirmed in the presence of TNF-α as reported by Wati et al. (2010). HEK 293 cells were transfected with plasmid expressing either WT-NS5 or MT-NS5 and treated with 50 mg/ml of TNF-α diluted in 0.1% FBS DMEM at 48 h p.t. for 6 h. After 6 h of TNF-α

incubation, RANTES mRNA level was measured by qRT-PCR and RANTES protein level was measured by Instant ELISA®. Figure 5.16A shows that WT-NS5 induced RANTES mRNA expression 4.2-fold more than that of MT-NS5. The corresponding result was found at RANTES protein level in which WT-NS5 induced almost 10-fold more than that of MT-NS5; 520 pg/ml and 63 pg/ml, respectively (figure 5.16B). This result suggested that either the absence or presence of TNF-α, WT-NS5 could induce RANTES production.

5.6 Study of the influence of WT-NS5 on RANTES promoter by using Dual-Luciferase® Reporter Assay System

5.6.1 Construction of pGL3 luciferase reporter plasmid containing RANTES promoter sequence

(a) Amplification of RANTES promoter cDNA

RANTES promoter fragment including 881 nucleotides of 5'region immediately upstream from transcriptional start site plus 38 nucleotides of RANTES gene (919 bp in total) was amplified by PCR using gDNA extracted from human PBMC as a template. PCR product with the expected size was shown in figure 5.17. The PCR product was purified and double digested with *Kpn*I HF and *Nhe*I HF restriction enzymes and purified again. The digested RANTES promoter fragment was ligated into pGL3-basic double digested with the same enzymes to generate pGL3 RANTES promoter reporter plasmid. The ligation mixture was transformed into *E.coli* DH5α.

(b) Screening of pGL3-basic plasmid containing RANTES promoter fragment

Eight colonies of transformant *E.coli* was picked up to screened the insertion of RANTES promoter fragment. Colony PCR was performed by using RANTES *Kpn*I forward and RANTES *Nhe*I reverse primers to amplify

RANTES promoter fragment. The 919 bp of expected RANTES promoter fragment was found in 3 of 8 screened clones (figure 5.18). Then, the insertion of RANTES promoter fragment in pGL3-basic plasmid was confirmed by *Kpn*I HF and *Nhe*I HF double digestion of 3 putative recombinant plasmids. Two of them exhibited the two expected fragments of inserted RANTES promoter fragment and linear pGL3-basic plasmid with the size of 919 and 5256 bp, respectively (figure 5.19).

(c) DNA sequencing of putative pGL3 RANTES promoter reporter plasmids

Two clones of putative pGL3 RANTES promoter reporter plasmids were sent to Macrogen DNA Sequencing Service for sequencing analysis. The sequencing results showed that there was one mismatched nucleotide at nucleotide position 400 from transcriptional start site of RANTES gene in which the nucleotide “G” (guanosine) was changed into “A” (adenosine). This mismatched nucleotide is not corresponding to the binding site of any transcription factors. The sequencing result and the references, which showed all of transcription factor binding site sequences, are shown in appendix.

5.6.2 Investigation of the influence of NS5 on RANTES promoter by Dual-Luciferase® Reporter Assay System

To investigate the influence of NS5 on RANTES promoter, HEK 293 cells were co-transfected with empty pcDNA3.1/Hygro or WT-NS5 plasmid, pGL3 RANTES promoter reporter plasmid, and pRL-SV40 internal control plasmid. After 48 h p.t., cells were subjected of luciferase activity measurement by luminometer. Figure 5.20 showed that NS5 activated RANTES promoter ~11 fold compared with that of the empty pcDNA3.1/Hygro transfection control.

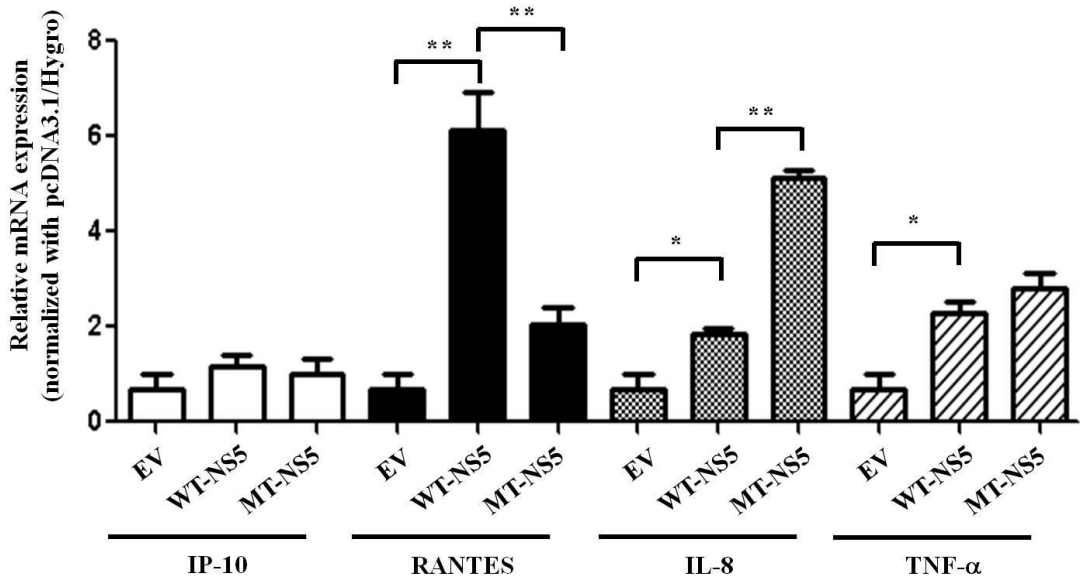

Figure 5.15 Real-time PCR result of relative mRNA expression of IP-10, RANTES, IL-8, and TNF-α in HEK293 cells transfected with either WT-NS5 or MT-NS5 plasmid.

Total RNA was isolated from HEK 293 cells transfected with either WT-NS5 plasmid, MT-NS5 plasmid or empty pcDNA3.1/Hygro for 48 h. Total RNA was reverse-transcribed into cDNA and then used to be a template for real-time PCR using the specific primers for genes as indicated. The relative mRNA expression of these cytokines was present as fold change normalized with empty pcDNA3.1/Hygro transfection control using the $2^{-\Delta\Delta Ct}$ method. Results shown are typical of three independent experiments. The significant difference was tested with an unpaired *t-test* using GraphPad Prism 5. * represents *p* value less than 0.05 whilst ** represents *p* value less than 0.005.

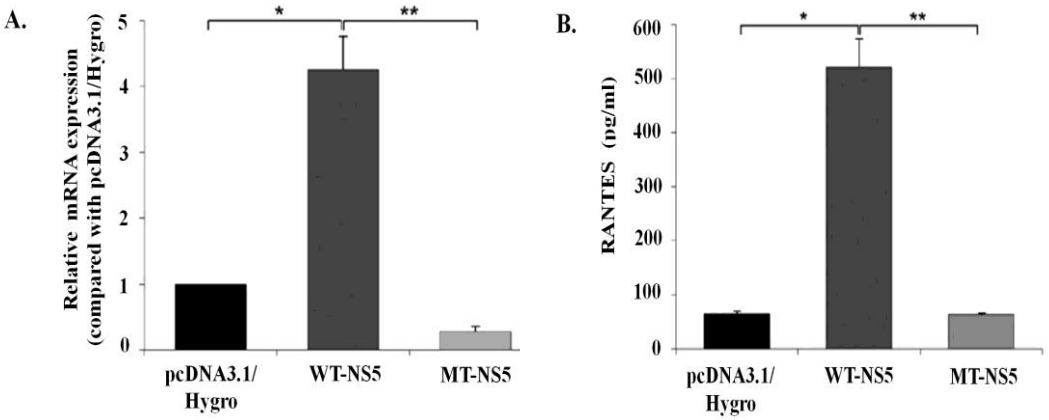

Figure 5.16 Validation of the expression of RANTES induced by WT-NS5 at both transcriptional and translational levels by qRT-PCR and ELISA.

Cell pellets and supernatants were collected from HEK 293 cells transfected with WT-NS5-plasmid or empty pcDNA3.1/Hygro and treated with 50 ng/ml of TNF-α in 0.1% FBS DMEM for 6 h at 48 h p.t. Cells were subjected of RANTES mRNA analysis by qRT-PCR using specific primers to human RANTES (A) whilst supernatants were measured for RANTES protein expression level by Instant® ELISA (B). Results shown are typical of three independent experiments. The asterisk indicates statistically significant differences tested with an unpaired *t-test* using StatView 5.0 (*$p < 0.05$, **$p < 0.01$).

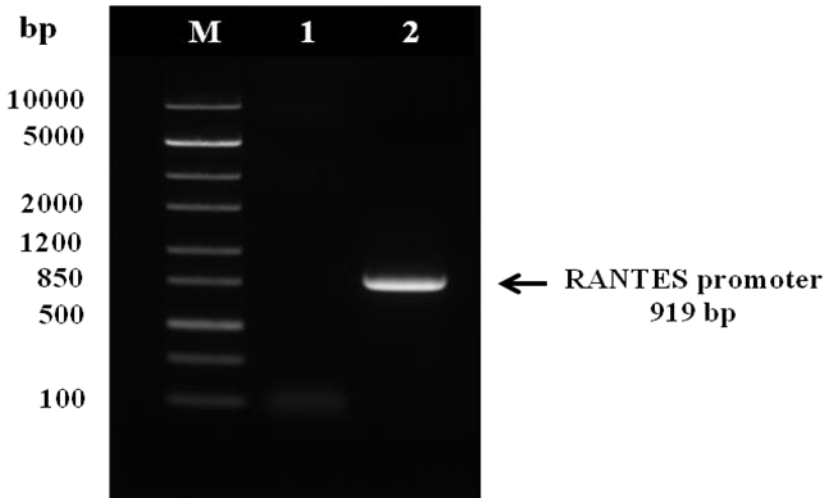

Figure 5.17 Agarose gel electrophoresis of RANTES promoter cDNA amplicon. The 919 bp of RANTES promoter which included 881 nucleotides of 5'region immediately upstream from transcriptional start site plus 38 nucleotides of RANTES gene was amplified by PCR using gDNA extracted from human PBMC as a template. bp = basepair, M = ZipRuler 1 DNA ladder marker, lane 1 = negative control for PCR, lane 2 = RANTES promoter cDNA amplicon was amplified by RANTES *Kpn*I forward and RANTES *Nhe*I reverse primers.

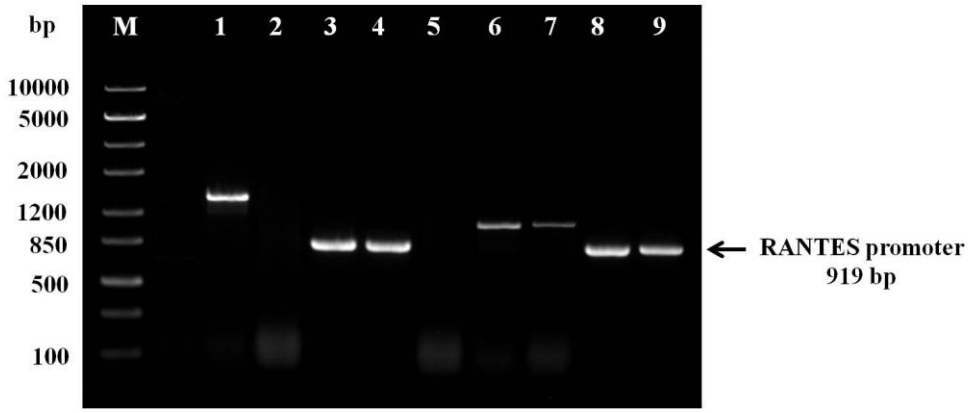

Figure 5.18 Agarose gel electrophoresis of transformed *E.coli* clones containing pGL3 RANTES promoter reporter plasmid by colony PCR.

Eight transformed *E.coli* were picked up and screened for RANTES promoter fragment insertion by PCR. Only 3 of 8 (lane 3, 4, and 8) showed the expected size of RANTES promoter fragment (919 bp). bp = basepair, M = ZipRuler 1 DNA ladder marker, lane 1-8 = amplicons were amplified from transformed *E. coli* clone number 1-8 , respectively, lane 9 = RANTES promoter amplicon was amplified from gDNA template used as a PCR positive control.

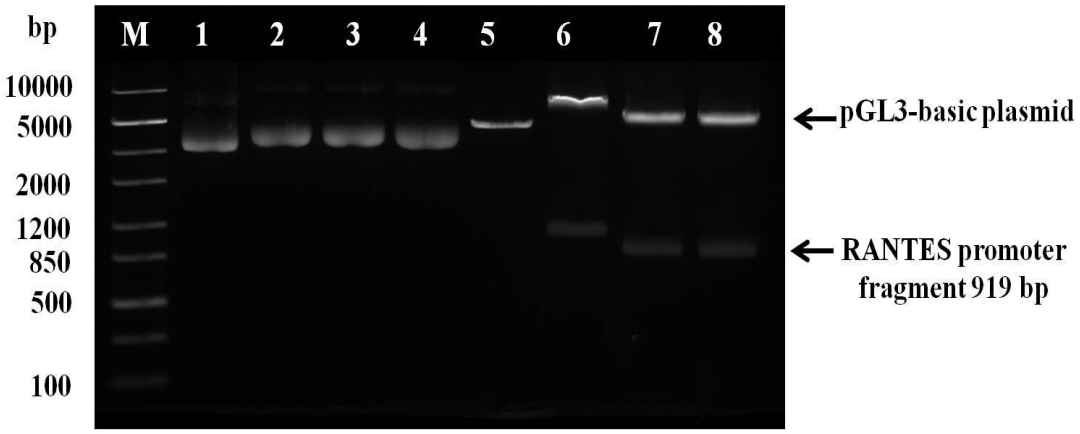

Figure 5.19 Agarose gel electrophoresis for confirming of pGL3-basic plasmid containing RANTES promoter fragment by *Kpn*I and *Nhe*I double digestion.

Three transformed *E.coli* clones which showed the insertion of RANTES promoter fragment by colony PCR were subjected of plasmid extraction. The extracted plasmids were double digested with *Kpn*I HF and *Nhe*I HF restriction enzymes. Only 2 of 3 clones (lane 7 and 8) showed two expected fragments of linear pGL3-basic plasmid with the size of 5256 bp and inserted RANTES promoter fragment with the size of 919 bp, respectively. bp = basepair, lane M = ZipRuler 1 DNA ladder marker, lane 1-4 = non-digested plasmids of empty pGL3-basic plasmid and 3 putative pGL3 RANTES promoter reporter plasmids, respectively, lane 5-8 = *Kpn*I-and *Nhe*I-digested products of empty pGL3-basic plasmid and 3 putative pGL3 RANTES promoter reporter plasmids, respectively.

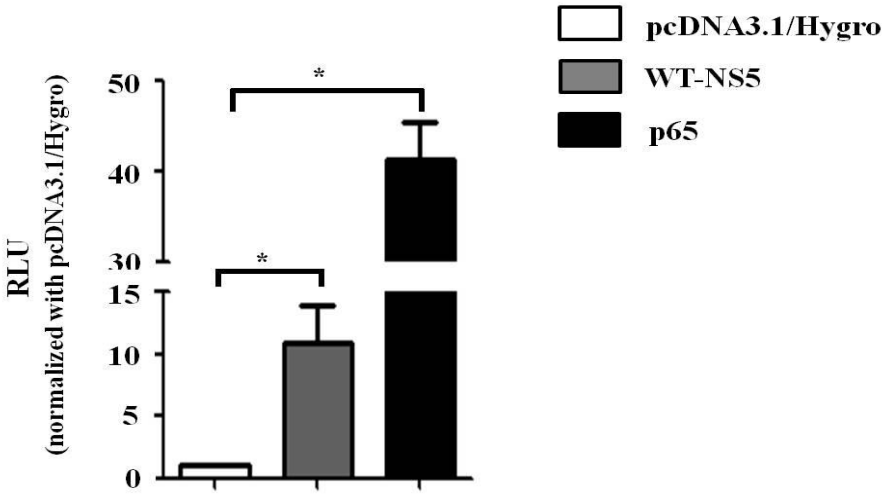

Figure 5.20 Relative light unit (RLU) of RANTES promoter activity in NS5-transfected HEK 293 cells.

An empty pcDNA3.1/Hygro or WT-NS5 plasmid was transfected in HEK293 cells. After 48 h p.t., cells were subjected of luciferase activity measurement by luminometer. RANTES promoter activity was presented in term of RLU normalized with empty pcDNA3.1/Hygro transfection control. Plasmid expressing p65 subunit of NF-κB was transfected to be a control. Results shown are typical of three independent experiments. The significant difference was tested with an unpaired *t-test* using StatView 5.0. * represents *p* value less than 0.05 whilst ** represents *p* value less than or equal 0.001.

5.7 Identification of whether NS5-activated RANTES promoter is mediated through NF-κB

5.7.1 Generation of pGL3-basic plasmid containing RANTES promoter with NF-κB binding site mutation

(a) PCR-based site-directed mutagenesis for generation of pGL3 RANTES promoter reporter plasmid containing NF-κB binding site mutations

To examine whether NF-κB is a major transcription factor for NS5-activated RANTES promoter, 2 binding sites of NF-κB on RANTES promoter were mutated using PCR-based site-directed mutagenesis as described previously. The PCR products exhibited nicked strands of NF-κB 1, NF-κB 2, and NF-κB 1+2 mutants were shown in figure 5.21 in which NF-κB 2 and NF-κB 1+2 PCR products could be amplified lesser than NF-κB 1. Then, PCR products were subjected of *Dpn*I digestion and transformed into *E.coli* DH5α. There was no transformed *E.coli* colonies from NF-κB 1+2 transformation, the adjustments of PCR condition for NF-κB 1+2 mutated amplification was performed. The final concentrations of enhancer buffer at 0.5x and 1x and the varying in annealing temperature at 42, 44, 46, 48, and 50°C were applied. Figure 5.22 shows a success in NF-κB 1+2 amplification especially in 42°C and 44°C and both in 0.5x and 1x enhancer buffer conditions. Then, the best 4 PCR products from 42°C and 44°C and both in 0.5x and 1x enhancer buffer conditions (lane 2 and 3 of both conditions) were further subjected of *Dpn*I digestion (figure 5.23). After *Dpn*I digestion, the obtained NF-κB 1+2 PCR products were transformed into *E.coli* DH5α and then subjected to plasmid extraction for further DNA sequencing.

(b) DNA sequencing of putative pGL3 RANTES promoter reporter plasmid containing NF-κB 1, NF-κB 2, NF-κB 1+2 mutation

Two purified plasmids of NF-κB 1, NF-κB 2, and 4 purified plasmids of NF-κB 1+2 mutants were sent to Macrogen DNA Sequencing Service for

sequencing analysis. The sequencing results showed that all of 3 types of mutation contain the mutated sequences as expected.
(figure 5.24).

5.7.2 Measurement of RANTES promoter activity of RANTES promoter reporter plasmid containing NF-κB mutation of by luminometer

At 48 h p.t., cells were subjected of luciferase activity measurement as the same previous. Figure 5.25 showes that when both binding sites of NF-κB on RANTES promoter were mutated, the ability of NS5 to induce the luciferase activity was decreased approximately 12 fold compared with that of WT-RANTES. In addition, the mutation in NF-κB 1 was found to be a more critical site for NF-κB than NF-κB 2 in this situation (decreasing about 8- and -5 fold compared with WT-RANTES).

5.8 Examination of the binding ability of NF-κB on RANTES promoter in NS5-transfected HEK293 cells by chromatin immunoprecipitation (ChIP) assay

5.8.1 Optimization of the amount of Micrococcal endonuclease enzyme for chromatin digestion in HEK 293 cells

To obtain the appropriated fragment (150-900 bp) of DNA for ChIP assay, Micrococcal endonuclease enzyme was varied in the amount at 0.25, 0.5, 0.75, and 1.0 μl.

5.8.2 Chromatin digestion by Micrococcal endonuclease enzyme of NS5-tranfected HEK 293 cells

HEK 293 cells were transfected with empty pcDNA3.1/Hygro, WT-NS5 plasmid or MT-NS5 plasmid for 48 h. Cells were subjected of DNA-protein cross-linking, endonuclease digestion, sonication, and DNA purification followed as the methods in 4.4.8 (3). Fifteen μl of eluted DNA was subjected of 1% agarose gel electrophoresis. The result of chromatin digestion from HEK 293 cells transfected with either WT-NS5 plasmid or empty pcDNA3./Hygro control was shown in figure 5.27. All of the samples showed the success in chromatin digestion with expected size of DNA fragment (150-900 bp).

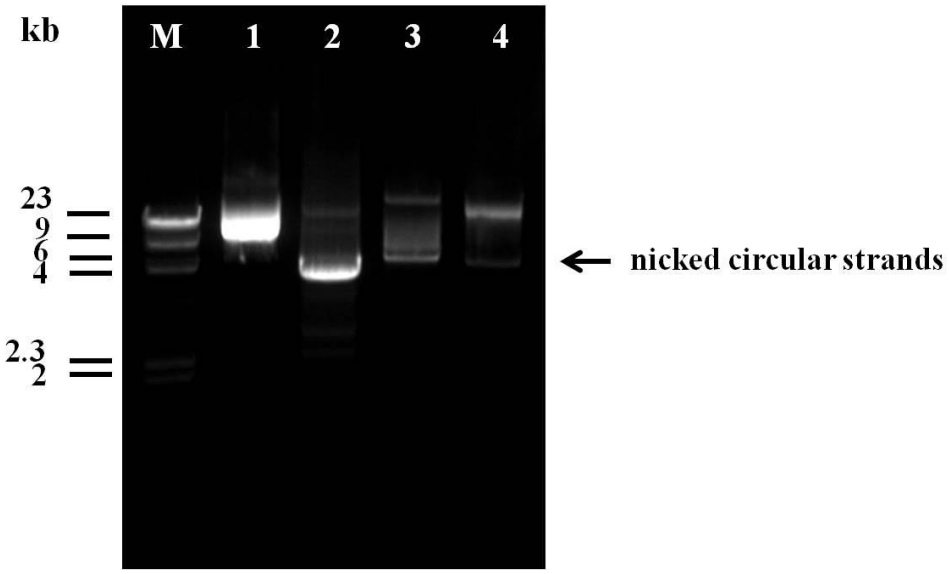

Figure 5.21 Agarose gel electrophoresis of PCR products of putative pGL3 RANTES promoter reporter plasmid containing NF-κB 1, NF-κB 2, or NF-κB 1+2 mutation site generated by site-directed mutagenesis. pGL3 WT-RANTES promoter reporter was used as a template to generate pGL3 RANTES promoter reporter plasmid containing either NF-κB 1 (lane 2), NF-κB 2 (lane 3), or NF-κB 1+2 (lane 4) mutation using a specific pair of primer for each mutated site, NF-κB 1, NF-κB 2 and NF-κB 1+2 primers, respectively. kb = kilobasepair, M = λ *Hind*III DNA ladder marker, lane 1 = pGL3 WT-RANTES promoter reporter plasmid was loaded as a control plasmid.

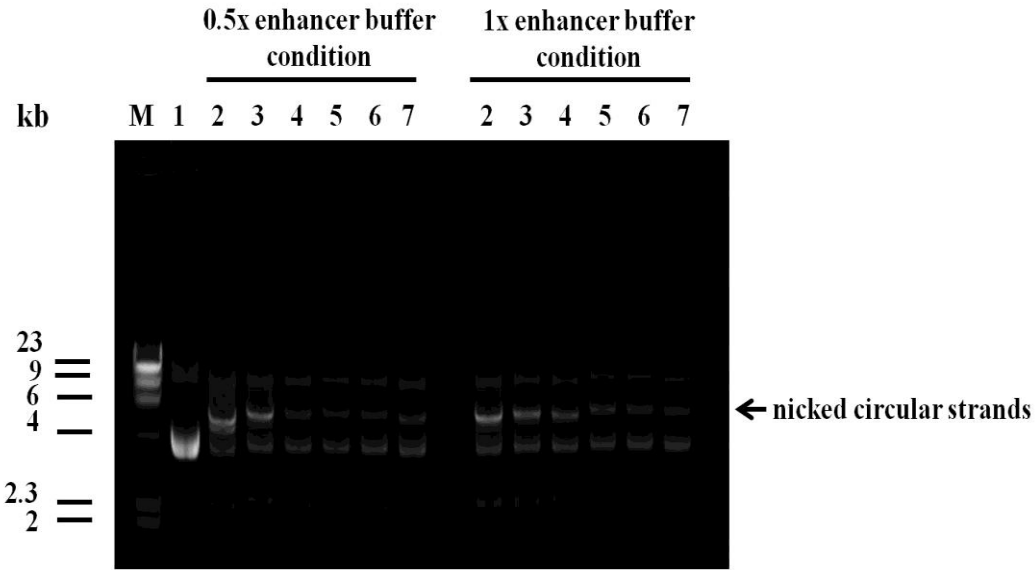

Figure 5.22 Agarose gel electrophoresis of PCR products of putative pGL3 RANTES promoter reporter plasmid containing NF-κB 1+2 mutation site amplified by adjustment the PCR conditions.

The enhancer buffer at final concentration 0.5X and 1x combined with varying of annealing temperature at 42, 44, 46, 48, and 50°C (lane 2-7, respectively) were applied to amplified RANTES promoter reporter plasmid with NF-κB 1+2 mutation site by using NF-κB 1+ 2 primer. Then, the best 4 PCR products from 42°C and 44°C and both in 0.5x and 1x enhancer buffer conditions (lane 2 and 3 of both conditions) were further subjected of *Dpn*I digestion. kb = kilobasepair, M = λ *Hind*III DNA ladder marker, lane 1 = WT-RANTES promoter reporter plasmid used as a loading control, lane 2-7 = PCR products were amplified by varying the annealing temperature at 42, 44, 46, 48, and 50°C and adding 0.5x and 1x enhancer buffer as indicated.

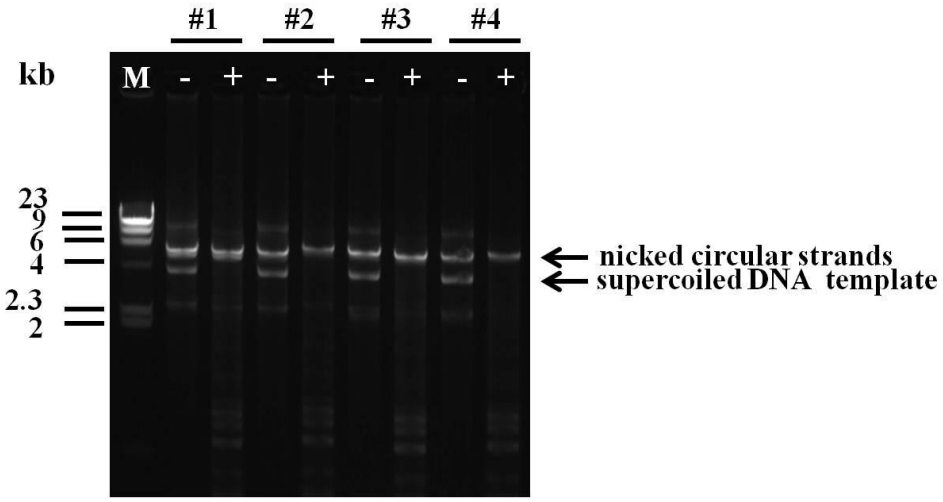

Figure 5.23 Agarose gel electrophoresis of *Dpn*I-digested putative RANTES promoter reporter plasmid containing NF-κB 1+2 mutation.

Four PCR products from 42°C and 44°C and both in 0.5x and 1x enhancer buffer conditions (#1, #2, #3, and #4, respectively) were further subjected of *Dpn*I digestion to degrade the parental WT-RANTES promoter plasmid.

kb = kilobasepair, M = λ *Hind*III DNA ladder marker, - or + = with or without *Dpn*I restriction enzyme, respectively.

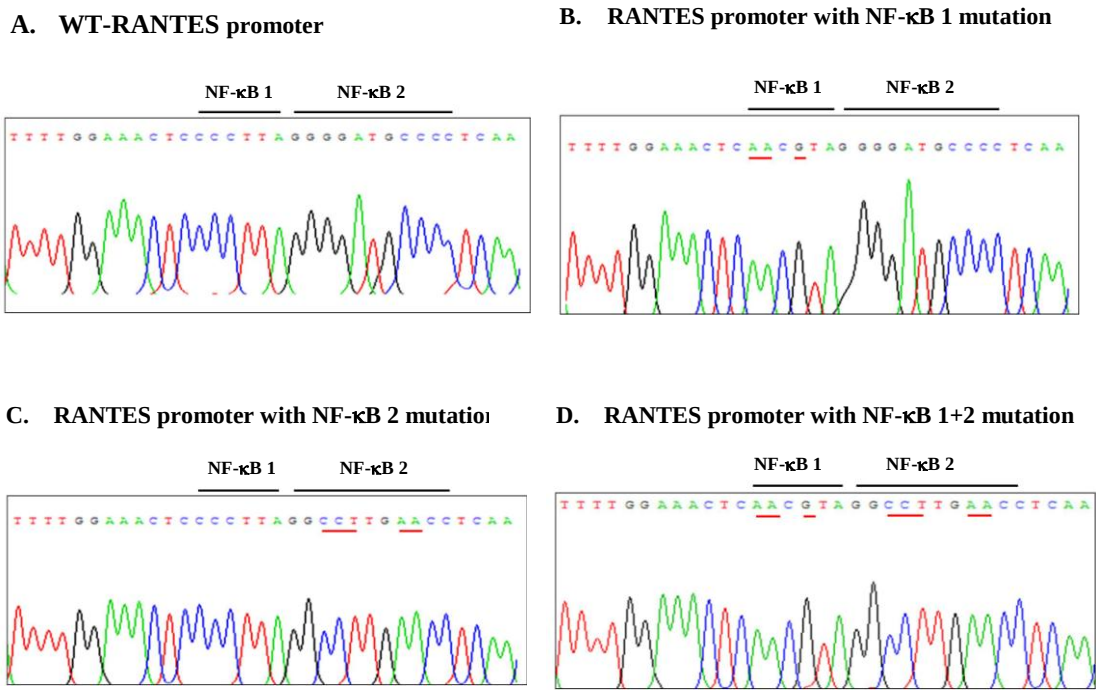

Figure 5.24 The sequencing profiles of RANTES promoter: WT-RANTES promoter, RANTES promoter with NF-κB 1, NF-κB 2, or NF-κB 1+2 binding site mutation.

The nucleotide sequences of NF-κB binding sites

A. WT-RANTES promoter. The nucleotide CCCTTA represents NF-κB 1 binding site and GGGGATGCCCC represents NF-κB 2 binding site.
B. RANTES promoter with NF-κB 1 binding site mutation.
C. RANTES promoter with NF-κB 2 binding site mutation.
D. RANTES promoter with both NF-κB 1 and NF-κB 2 binding site mutations

The nucleotide sequences were underlined indicating the exchanged nucleotides.

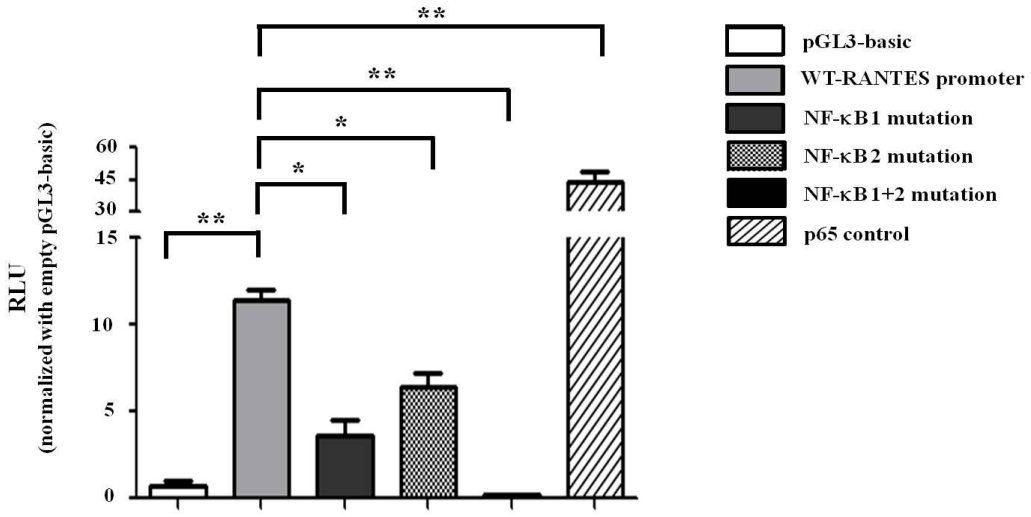

Figure 5.25 Relative light unit (RLU) of luciferase activity of WT-NS5 plasmid co-transfected with either WT-RANTES promoter or RANTES promoter reporter plasmid with NF-κB 1, NF-κB 2, or NF-κB 1+2 mutation.

WT-NS5 plasmid was co-transfected with either empty pGL3-basic, WT-RANTES promoter reporter plasmid or RANTES promoter reporter plasmid with NF-κB 1, NF-κB 2, or NF-κB 1+2 mutations, and pRL-SV40 internal control plasmid in HEK 293 cells. Plasmid expressing p65 subunit of NF-κB was transfected to be a control. After 48 h p.t., cells were subjected of luciferase activity measurement by luminometer. RANTES promoter activity was present in term of RLU normalized with WT-NS5 co-transfected with empty pGL3-basic (1). Results shown are typical of three independent experiments. The significant difference was tested with an unpaired *t-test* using GraphPad Prism 5. * represents *p* value less than 0.05 whilst ** represents *p* value less than 0.005 and 0.0005.

5.8.3 PCR amplification of RANTES promoter sequence from immunoprecipitating complex

Ten μg of chromatin digestion was incubated either with 5 μg of rabbit anti-p65 antibody or 1μg of normal rabbit isotype control antibody. Then, RANTES promoter was isolated from those complexes and subjected to PCR amplification. RANTES promoter PCR products were amplified and analysed by 2% agarose gel electrophoresis. The ChIP assay was performed in 3 independent experiments and result shown in figure 5.28A is a representative one. The result showed that in NS5-transfected HEK 293 cells, NF-κB could bind to its binding sites on RANTES promoter better than empty pcDNA3.1/Hygro transfection control. Furthermore, these 3 independent results were calculated for the intensity of RANTES promoter PCR product by Image J public domain software. Figure 5.28B shows that the intensity band of RANTES promoter PCR product in NS5-transfected HEK 293 cells was significantly more than that of empty pcDNA3.1/Hygro-transfected HEK 293 cells.

5.9 Confirmation of the interaction and co-localization between NS5 and human Daxx protein in HEK 293 cells

5.9.1 Confirmation of the interaction between NS5 and Daxx by Co-IP assay

Result of Co-IP assay confirmed that NS5 really interacts with human Daxx protein (figure 5.29). In addition, transfection with either WT-NS5 or MT-NS5 into HEK293 cells and tested for the interacting with Daxx could obtain more the information that only nuclear NS5 (WT-NS5) interacts with Daxx. The same result could be observed even though using a reciprocal immunoprecipitating antibody.

5.9.2 Testing for the co-localization between NS5 and Daxx using co-localization assay

Besides the confirmed interaction by Co-IP assay, co-localization assay also shows that WT-NS5 co-localized with Daxx in the nucleus of transfected cells (figure 5.30).

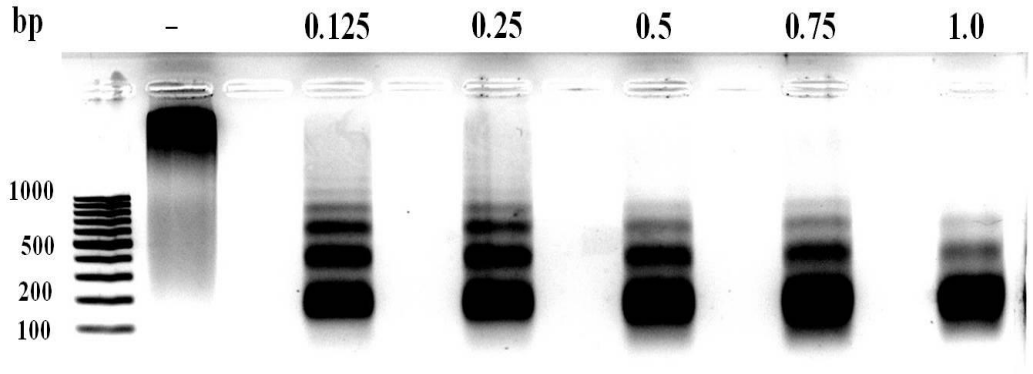

Figure 5.26 Agarose gel electrophoresis of chromatin-digested products from Micrococcal endonuclease enzyme at various amounts.

Chromatin from HEK293 $1x10^6$ cells were subjected of Micrococcal endonuclease digestion at various amounts. The numbers of 0.125, 0.25, 0.5, 0.75, and 1.0 represent the amount in μl of adding enzyme. The populations of small product size were increased when the amount of enzyme was increased. bp = basepair, M = ZipRuler 1 DNA ladder marker, - = no Micrococcal endonuclease enzyme.

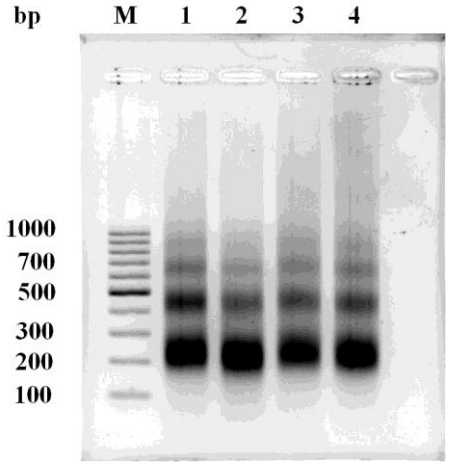

Figure 5.27 Agarose gel electrophoresis of chromatin-digested products of Micrococcal endonuclease enzyme from HEK 293 cells transfected with WT-NS5 plasmid or empty plasmid.

HEK 293 $1x10^6$ cells transfected with WT-NS5 plasmid or empty plasmid were subjected of DNA-protein cross-linking, and then digested with 0.5 μl of Micrococcal endonuclease enzyme. Before going to the next steps, digested chromatin should be tested for the optimized digestion. The appropriated fragments were 150-900 bp in length. bp = basepair, M = ZipRuler 1 DNA ladder marker, lane 1 and 2 = chromatin digested products from empty pcDNA3.1-transfected cells in duplicate, lane 3 and 4 = chromatin digested products from WT-NS5-transfected cells in duplicate

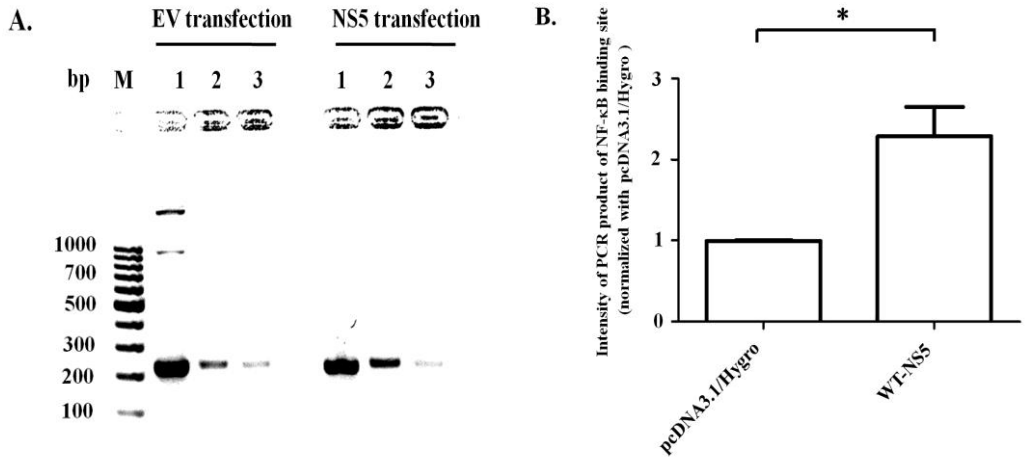

Figure 5.28 Agarose gel electrophoresis of NF-κB binding site PCR product (A) and comparison of intensity of NF-κB binding site PCR products by using ImageJ software (B).

HEK 293 cells were transfected with empty pcDNA3.1/Hygro (EV transfection) or plasmid expressing WT-NS5 (NS5 transfection). After 48 h p.t., cells were subjected of DNA-protein cross-linking, chromatin digestion (150-900 bp of size), and cell sonication. Anti-p65 antibody was used to immunoprecipitate the NF-κB-RANTES promoter complex. Then, RANTES promoter fragments were purified and subjected of PCR. Primer which is specific for NF-κB binding sites on RANTES promoter was used in the amplification. A is the representative of three independent experiments. B is calculated from three independent experiments. Lane 1 = RANTES PCR product was amplified from 2% input, lane 2 = RANTES PCR product was amplified from immunoprecipitation with rabbit anti-p65 Ab, lane 3 = RANTES PCR product was amplified from immunoprecipitation with normal rabbit isotype control Ab.

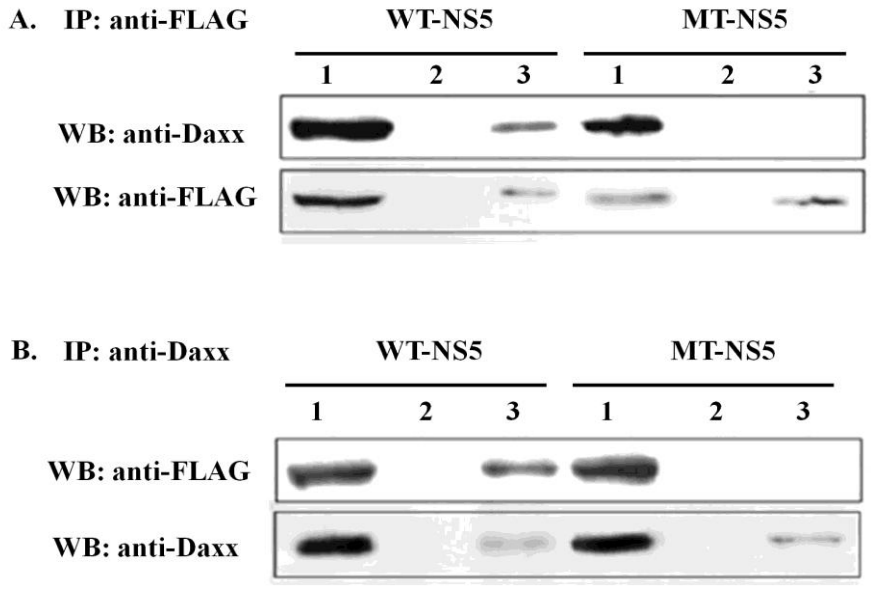

Figure 5.29 Western blot analysis of the interaction between NS5 and human Daxx protein by Co-IP assay.

Cell lysates from HEK 293 cells transfected with either WT-NS5 or MT-NS5 plasmid for 48 h before treating with 50 ng/ml of TNF-α in 0.1% FBS DMEM for 6 h were subjected of immunoprecipitation (IP) with either mouse anti-FLAG (upper panel: A) or a reciprocal rabbit anti-Daxx (lower panel: B) antibody. The immunoprecipitated complexes were detected by Western blot analysis using the antibodies as indicated. Lane 1 = input lysates, lane 2 = lysate from IP with no antibody, and lane 3 = lysate from IP indicated antibody.

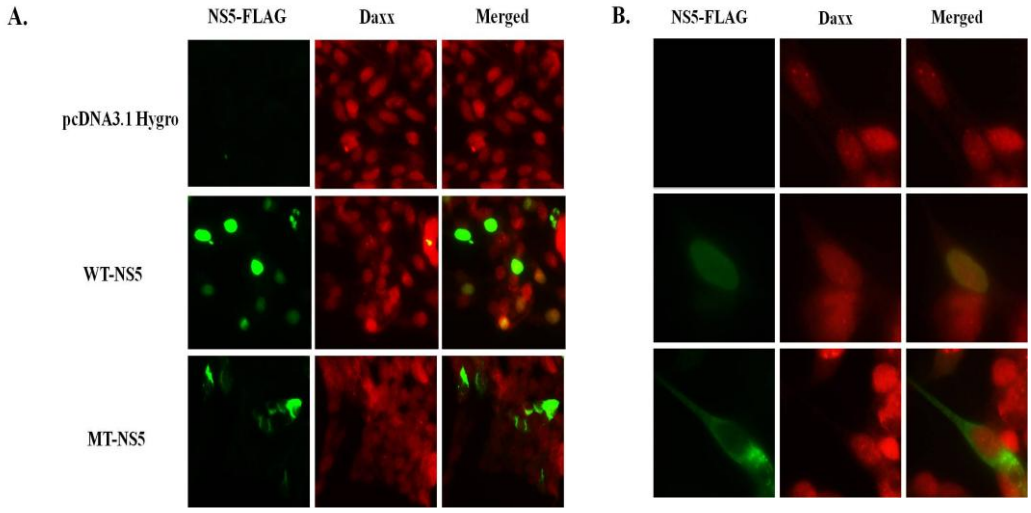

Figure 5.30 Fluorescence images of the co-localization between NS5 and human Daxx by co-localization assay.

HEK 293 cells were grown on coverslips before transfection with either WT-NS5, MT-NS5, or empty pcDNA3.1/Hygro plasmid for 48 h. Cells were treated with 50 ng/ml of TNF-α in 0.1% FBS DMEM for 6 h and subjected of immunostaining by using mouse anti-FLAG antibody or rabbit anti-Daxx antibody. An Alexa 488-conjugated rabbit anti-mouse Ig antibody (green) and a Cy3-conjugated donkey anti-rabbit Ig antibody (red) were used as secondary antibodies for NS5-FLAG and Daxx, respectively. Figure A was an image captured with 60x resulution whilst figure B was a higher resolution of A.

CHAPTER VI
DISCUSSION

As a massive cytokine production was proposed to be an immune-mediated severity in DENV infection rather than to protect immune response, how DENV operates this phenomenon becomes an interested field of research nowadays. Previous studies have already reported the ability of DENV to induce the high production of several cytokines and inflammatory molecules both from natural isolated target DENV cells obtained from human and DENV-infected cell lines/animal model. Some evidence has demonstrated the mechanisms how DENV regulates cytokine production and which DENV proteins manipulate this action. A few DENV-induced cytokines have been identified of which DENV proteins operate the induction. NS5 has been shown to play the most predominant role in cytokine induction, comparing with that of other DENV proteins; thereby NS5 was our interest and we used it for identification of remaining unknown factors about the complicated pathogenesis in DENV infection. RT^2 Profiler PCR Array was used as a tool for large scale screening of DENV-induced cytokines before scaling down to find whether it is due to an NS5 effect in this induction. DENV-infected HEK 293 cells at 24 h p.i. were chosen to be a sample in RT^2 Profiler PCR Array, because it presents healthy productively DENV-infected HEK 293 cells, as described previously. There were 22 genes, which were up-regulated and 7 genes were down-regulated. Only up-regulated cytokine gene was selected for further study in HEK 293 cells expressing NS5, because the aim of this study was to identify the effect of NS5 in the frame of the cytokine storm phenomenon. The top five of highest DENV-induced cytokine genes, including IP-10, RANTES, CXCL-9, IL-8, MIP-1β plus one more extra gene, TNF-α, were chosen for examination of their expression in HEK 293 cells expressing WT-NS5 or MT-NS5. The proposition of generating HEK 293 cells expressing MT-NS5, which cannot translocate to the nucleus, was to clarify the localized compartment for NS5 in cytokine induction. The screening of 6 selected DENV-infected cytokine genes was performed in HEK 293 cells expressing WT-NS5 or MT-NS5 at 48 h p.t by qRT-

PCR, using a specific primer for each gene. The result showed that only three of them showed the differential expression affected by WT-NS5 or MT-NS5, including RANTES, IL-8, and TNF-α. The expression of IL-8 in DENV-infected HEK 293 cells was increased in a time-dependent manner between 24 to 120 h p.i. at the same MOI (22). Furthermore, this profile was also found in blood samples of dengue patients (94). Lastly, the induction of IL-8 in NS5-transfected HEK 293 cells at 48 h p.t. has been reported in several studies, as described previously. For RANTES expression in DENV-infected HEK 293 cells, there is only a study by Medin et al. (11), that reported that RANTES induction could be observed at 48 h p.i. (day 2) and was increased in a time-dependent manner. Although there was no induction at 24 h p.i. and little induction at 48 h p.i of RANTES, Pryor et al. (22) observed the IL-8 induction after 24 h p.i. by using the same DENV-2 strain and cell line. The difference between our result and the result from Medin's group might be due to the variation between DENV strain, as they used DENV-2 strain New Guinea or NGC and a lesser % of infection, i.e. 25-30%, whilst ours is almost 95% infection. Furthermore, the continued rise of RANTES induction has also been found in DENV infection of other cell lines, such as ECV304 lung epithelial cell lines (10). The same explanation could be implied for TNF-α induction as well. Taken together, it suggests that all three NS5-induced cytokine genes might be induced as shows the cytokine expression profile in DENV-infected HEK 293 cells at 48 h p.i., as well.

The differential expression of RANTES, IL-8, and TNF-α in HEK 293 cells expressing WT-NS5 or MT-NS5 could be classified into two groups, consisting of a group of higher expression in HEK 293 cells expressing WT-NS5; this group had only one gene, RANTES, and the group with higher expression in HEK 293 cells expressing MT-NS5 consists of IL-8 and TNF-α. The reason for the possible explanation in case of RANTES induction is that the molecular mechanism for inducing the expression of RANTES might require the nuclear localization of NS5. The details of this are explained later. Moreover, this phenomenon was not due to the difference of the expression level between WT-NS5 and MT-NS5 in HEK 293 cells, because our experiment which was performed to confirm the induction of RANTES by WT-NS5 in TNF-α-treated condition showed the same pattern of RANTES induction in HEK 293 cells expressing the similar level of WT-NS5 and MT-NS5 (45.06% and

40.94% of transfection efficiency), respectively (13). For the IL-8 and TNF-α-inductive profile, there are two possible reasons. Firstly, based on the localization of NS5, it might imply that the induction of both IL-8 and TNF-α is mediated by cytoplasmic NS5. NS5 might activate upstream signaling cascade molecules leading to the activation and nuclear translocation of transcription factor to promote the production of IL-8 and TNF-α. The example of this phenomenon has also been demonstrated in HepG2 cells expressing DENV NS1 which mainly localizes in cytoplasm of the cells. Silva et al. (168) has demonstrated that stable HepG2 cells, expressing NS1 protein increases nuclear translocation of p65 and transcriptional activity of NF-κB, which might be the result of TNF-α and IL-6 induction reported in stable HepG2 cells expressing NS1 protein. In addition, our previous yeast two-hybrid screening showed that NS5 interacted with Fas-associated factor 1 (FAF1), which is a cytoplasmic protein associated with the FAS receptor (169). Besides its role as apoptotic mediator, FAF1 inhibits NF-κB by physically interacting with NF-κB p65 at the cytoplasm and this interaction prevents the translocation of p65 to the nucleus in HEK 293 cells. Moreover, the overexpression of FAF1 decreases the basal level of NF-κB activity in HEK 293 cells. The interaction between cytoplasmic NS5 and the NF-κB inhibitor protein might imply the mechanism how NS5 activates NF-κB activity in the cytoplasm. The secondary explanation for the higher levels of IL-8 and TNF-α in HEK 293 cells expressing MT-NS5 might be the same reason that Pryor et al. and Rawlinson et al. have discussed. They suggested that NS5 enters to the nuclear to suppress the production of IL-8 to enhance DENV RNA replication. In our case, the lower induction of both IL-8 and TNF-α in WT-NS5-transfected cells might be the reason to suppress an antiviral action of these pro-inflammatory cytokines to enhance the replication.

Because of the interesting the role of NS5 in cytokine production and its mysterious role in the nucleus, RANTES was selected for studying the effect of NS5 to its promoter by the luciferase reporter gene system and ChIP assay. The promoter of the RANTES gene was inserted into a luciferase reporter plasmid and co-transfected with the plasmid, expressing WT-NS5 into HEK 293 cells before measuring the luciferase activity. The result showed that NS5 activated RANTES promoter. Then,

the influence of NF-κB in this phenomenon was identified by using the same approach as above, but the NF-κB binding sites on the RANTES gene promoter were mutated. Luciferase activity was reduced in HEK 293 cells expressing WT-NS5 and the RANTES promoter containing the mutation of the NF-κB binding sites, especially in NF-κB 1 binding site (NF-κB 1 mutant). In addition, the influence of NS5 on the DNA-binding activity of NF-κB on to the RANTES promoter was examined in HEK 293 cells expressing WT-NS5 by ChIP assay. HEK 293 cells expressing NS5 showed an increase of NF-κB binding to the RANTES promoter, as compared to the empty plasmid transfection control. These findings correspond to the previous studies, which showed that the DENV-activated RANTES promoter in HEK 293A cells (11) and ECV304 cell line (10). NF-κB activation has been reported in DENV infection in several cell lines such as ECV304 cells (10), HepG2 cells (170), and HEK 293A cells (11). Actually, these results confirm the role of NS5 in NF-κB activation, which has been reported previously by Medin et al. (11) and Wati et al. (100). Although RANTES promoter activation was not found in NS5-transfected HEK 293A cells by Medin et al., it might be because of the difference of time point of luciferase activity measurement, in which their experiments were done at 24 h p.t., whereas in our experiment RANTES expression was measured at 48 h p.t.. Thomas et al. (150) has reported that the regulation of RANTES expression in RSV-infected HEK 293 cells requires the combination of several *cis*-regulatory elements of the RANTES promoter, including NF-κB, C/EPB, CRE, and ISRE for full RANTES activation. ISRE, responsible for the IRF transcription factor family, is a critical element for RSV-induced RANTES expression. In our case, the involvement of other *cis*-regulatory elements in NS5-induced RANTES expression have not been clarified and required further studies, but the mutation of both NF-κB sites on the RANTES promoter (NF-κB 1+2 mutation) in our study could abolish almost luciferase activity affected by WT-NS5. Moreover, Song et al. (137) has reported that only NF-κB is sufficient for RANTES induction in epithelial cells as HEK 293 cells.

For a better understanding about the mechanism how NS5 regulates RANTES production in the nucleus, the proposed interaction between NS5 and the NF-κB inhibitor protein, Daxx, was confirmed by Co-IP and co-localization assay and

suggested a mechanism of NS5 cytokine induction in aspect of virus-host complex interplay. However, the studies of the competitive binding between NS5 and NF-κB to Daxx, or disruption of the interaction between NF-kB and DAXX might need to be done in order to confirm the requirement of this interaction in RANTES induction.

Besides RANTES gene, other NF-κB-regulated genes were induced by NS5 as well. There are 17 genes that were up-regulated in HEK 293 cells, expressing WT-NS5, at 24 h p.t.by using the RT^2 Profiler PCR Array approach (the same experiment as above). The list of the genes sequentially ordered according to induction rate includes c-FOS (AP-1), IL-10, LTA, C4A, TLP-7, IL-8RA, CD40LG, C3, CCR-7, IL-8RB, TNF, IL-1β, IL-8, CXCL-9, IL-23A, CCL-19, and IL-9, respectively (see in appendix). All of these genes were selected by more than 1.5 fold changes compared to those of empty pcDNA3.1/Hygro-transfected HEK 293 cells. From this data, the involvement of NS5 in massive cytokine induction, leading to the cytokine storm phenomenon in DENV infection, is suggested. However, further studies are still needed to clarify this phenomenon.

From all of the results, the proposed mechanism of regulation of RANTES production by DENV NS5 is that in the condition of stimulation such as DENV infection, Daxx protein may localize in the nucleus of the cells and interact with the p65 subunit of NF-κB, which has translocated from cytoplasm to nucleus, to inhibit its acetylation leading to suppressing of NF-κB activity. Once nuclear NS5 is present, NS5 interacts with free nuclear Daxx or competitively bind to Daxx, which generally interacts with p65 and results in the increase of free activated p65, of the DNA-binding ability of NF-κB, and finally to the high level production of RANTES. The proposed model of RANTES regulation by DENV NS5 is shown in the figure 6.1.

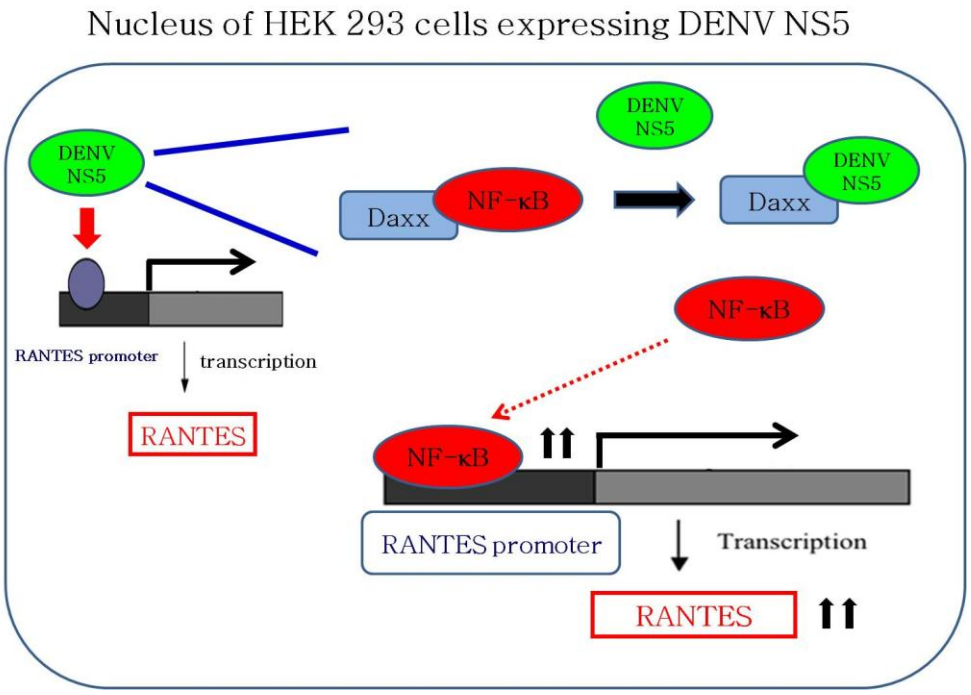

Figure 6.1 The proposed model of RANTES regulation by DENV NS5.

CHAPTER VII
CONCLUSION

Since DENV infection has been reported to be a crucial public health problem worldwide and no effective vaccine is available for protection currently, a better understanding of the pathogenic mechanisms of severity progression is beneficial for future drug design and vaccine developments. The massive cytokine production (the so-called 'cytokine storm') during DENV infection has been proposed to mediate the severity of dengue infection. Several reports demonstrated certain DENV proteins (operating) taking part in this action, including NS1, NS4B, and NS5. NS5 showed to be the most predominant among those proteins in induction of IL-6, IL-8, IP-10, and IFN-γ. In this study, we reported the first evidence that DENV NS5 induces RANTES production in HEK 293 cells. In addition, we further identified that this action of NS5 was manipulated by nuclear NS5. By using a luciferase gene reporter system and ChIP assay, we found that NS5 induces a high level production of RANTES by activating the RANTES promoter though increasing the DNA-binding activity of NF-κB. The increase of NF-κB activity in this phenomenon might be the result of the competitive binding of NS5 with NF-κB or the inhibitor protein, Daxx, thereby liberating activated NF-κB. This suggestion is concluded from the results of interaction and co-localization of nuclear NS5 and Daxx by Co-IP and co-localization assays. However, to prove this proposed mechanism, further experiments are required. Finally, the results of this study provide knowledge of the dengue pathogenesis mechanism, at least in the DENV-induced 'cytokine storm' aspect.

REFERENCES

1. Gubler DJ. Dengue and dengue hemorrhagic fever. Clinical microbiology reviews. 1998;11(3):480-96.
2. Ahmed FU MC, Sharma JD, Hoque SM, Zaman R, Hasan MH. Dengue fever and dengue haemorrhagic fever in chidren the 2000 out break in Chittatong, Bangladesh. . Dengue Bulletin. 2001;25:33–9.
3. Narayanan M, Aravind MA, Thilothammal N, Prema R, Sargunam CS, Ramamurty N. Dengue fever epidemic in Chennai--a study of clinical profile and outcome. Indian pediatrics. 2002;39(11):1027-33.
4. Pancharoen C, Mekmullica J, Thisyakorn U. Primary dengue infection: what are the clinical distinctions from secondary infection? The Southeast Asian journal of tropical medicine and public health. 2001;32(3):476-80.
5. Gurugama P, Garg P, Perera J, Wijewickrama A, Seneviratne SL. Dengue viral infections. Indian journal of dermatology. 2010;55(1):68-78.
6. Ranjit S, Kissoon N, Gandhi D, Dayal A, Rajeshwari N, Kamath SR. Early differentiation between dengue and septic shock by comparison of admission hemodynamic, clinical, and laboratory variables: a pilot study. Pediatric emergency care. 2007;23(6):368-75.
7. Murphy BR, Whitehead SS. Immune response to dengue virus and prospects for a vaccine. Annual review of immunology. 2011;29:587-619.
8. Halstead SB. Neutralization and antibody-dependent enhancement of dengue viruses. Advances in virus research. 2003;60:421-67.
9. Rothman AL. Immunity to dengue virus: a tale of original antigenic sin and tropical cytokine storms. Nature reviews Immunology. 2011;11(8):532-43.
10. Avirutnan P, Malasit P, Seliger B, Bhakdi S, Husmann M. Dengue virus infection of human endothelial cells leads to chemokine production, complement activation, and apoptosis. J Immunol. 1998;161(11):6338-46.

11. Medin CL, Fitzgerald KA, Rothman AL. Dengue virus nonstructural protein NS5 induces interleukin-8 transcription and secretion. Journal of virology. 2005;79(17):11053-61.
12. Kelley JF, Kaufusi PH, Volper EM, Nerurkar VR. Maturation of dengue virus nonstructural protein 4B in monocytes enhances production of dengue hemorrhagic fever-associated chemokines and cytokines. Virology. 2011;418(1):27-39.
13. Khunchai S, Junking M, Suttitheptumrong A, Yasamut U, Sawasdee N, Netsawang J, et al. Interaction of dengue virus nonstructural protein 5 with Daxx modulates RANTES production. Biochemical and biophysical research communications. 2012;423(2):398-403.
14. Egloff MP, Benarroch D, Selisko B, Romette JL, Canard B. An RNA cap (nucleoside-2'-O-)-methyltransferase in the flavivirus RNA polymerase NS5: crystal structure and functional characterization. The EMBO journal. 2002;21(11):2757-68.
15. Koonin EV. The phylogeny of RNA-dependent RNA polymerases of positive-strand RNA viruses. The Journal of general virology. 1991;72 (Pt 9):2197-206.
16. Fatima Z, Idrees M, Bajwa MA, Tahir Z, Ullah O, Zia MQ, et al. Serotype and genotype analysis of dengue virus by sequencing followed by phylogenetic analysis using samples from three mini outbreaks-2007-2009 in Pakistan. BMC microbiology. 2011;11:200.
17. Ray D, Shah A, Tilgner M, Guo Y, Zhao Y, Dong H, et al. West Nile virus 5'-cap structure is formed by sequential guanine N-7 and ribose 2'-O methylations by nonstructural protein 5. Journal of virology. 2006;80(17):8362-70.
18. Issur M, Geiss BJ, Bougie I, Picard-Jean F, Despins S, Mayette J, et al. The flavivirus NS5 protein is a true RNA guanylyltransferase that catalyzes a two-step reaction to form the RNA cap structure. RNA. 2009;15(12):2340-50.
19. Bartholomeusz A, Thompson P. Flaviviridae polymerase and RNA replication. Journal of viral hepatitis. 1999;6(4):261-70.

20. Brooks AJ, Johansson M, John AV, Xu Y, Jans DA, Vasudevan SG. The interdomain region of dengue NS5 protein that binds to the viral helicase NS3 contains independently functional importin beta 1 and importin alpha/beta-recognized nuclear localization signals. The Journal of biological chemistry. 2002;277(39):36399-407.
21. Rawlinson SM, Pryor MJ, Wright PJ, Jans DA. CRM1-mediated nuclear export of dengue virus RNA polymerase NS5 modulates interleukin-8 induction and virus production. The Journal of biological chemistry. 2009;284(23):15589-97.
22. Pryor MJ, Rawlinson SM, Butcher RE, Barton CL, Waterhouse TA, Vasudevan SG, et al. Nuclear localization of dengue virus nonstructural protein 5 through its importin alpha/beta-recognized nuclear localization sequences is integral to viral infection. Traffic. 2007;8(7):795-807.
23. Kapoor M, Zhang L, Ramachandra M, Kusukawa J, Ebner KE, Padmanabhan R. Association between NS3 and NS5 proteins of dengue virus type 2 in the putative RNA replicase is linked to differential phosphorylation of NS5. The Journal of biological chemistry. 1995;270(32):19100-6.
24. Hiscox JA. RNA viruses: hijacking the dynamic nucleolus. Nature reviews Microbiology. 2007;5(2):119-27.
25. Gustin KE. Inhibition of nucleo-cytoplasmic trafficking by RNA viruses: targeting the nuclear pore complex. Virus research. 2003;95(1-2):35-44.
26. Alvisi G, Rawlinson SM, Ghildyal R, Ripalti A, Jans DA. Regulated nucleocytoplasmic trafficking of viral gene products: a therapeutic target? Biochimica et biophysica acta. 2008;1784(1):213-27.
27. Guzman MG, Halstead SB, Artsob H, Buchy P, Farrar J, Gubler DJ, et al. Dengue: a continuing global threat. Nature reviews Microbiology. 2010;8(12 Suppl):S7-16.
28. WHO. Dengue and severe dengue. WHO Media centre,Fact sheet N°117 http://wwwwhoint/mediacentre/factsheets/fs117/en/. 2012.
29. Ross TM. Dengue virus. Clinics in laboratory medicine. 2010;30(1):149-60.

30. Wang E, Ni H, Xu R, Barrett AD, Watowich SJ, Gubler DJ, et al. Evolutionary relationships of endemic/epidemic and sylvatic dengue viruses. Journal of virology. 2000;74(7):3227-34.
31. Beatty ME, Stone A, Fitzsimons DW, Hanna JN, Lam SK, Vong S, et al. Best practices in dengue surveillance: a report from the Asia-Pacific and Americas Dengue Prevention Boards. PLoS neglected tropical diseases. 2010;4(11):e890.
32. Pinheiro FP, Corber SJ. Global situation of dengue and dengue haemorrhagic fever, and its emergence in the Americas. World health statistics quarterly Rapport trimestriel de statistiques sanitaires mondiales. 1997;50(3-4):161-9.
33. Pancharoen C, Rungsarannont A, Thisyakorn U. Hepatic dysfunction in dengue patients with various severity. Journal of the Medical Association of Thailand = Chotmaihet thangphaet. 2002;85 Suppl 1:S298-301.
34. WHO. Dengue haemorrhagic fever : diagnosis, treatment, prevention and control. 2nd ed. Geneva ed: World Health Organization; 1997.
35. WHO. Dengue guidelines for diagnosis, treatment, prevention and control new edition. Geneva ed: World Health Organization; 2009.
36. Edelman R, Wasserman SS, Bodison SA, Putnak RJ, Eckels KH, Tang D, et al. Phase I trial of 16 formulations of a tetravalent live-attenuated dengue vaccine. The American journal of tropical medicine and hygiene. 2003;69(6 Suppl):48-60.
37. Sun W, Cunningham D, Wasserman SS, Perry J, Putnak JR, Eckels KH, et al. Phase 2 clinical trial of three formulations of tetravalent live-attenuated dengue vaccine in flavivirus-naive adults. Human vaccines. 2009;5(1):33-40.
38. Simasathien S, Thomas SJ, Watanaveeradej V, Nisalak A, Barberousse C, Innis BL, et al. Safety and immunogenicity of a tetravalent live-attenuated dengue vaccine in flavivirus naive children. The American journal of tropical medicine and hygiene. 2008;78(3):426-33.
39. Watanaveeradej V, Simasathien S, Nisalak A, Endy TP, Jarman RG, Innis BL, et al. Safety and immunogenicity of a tetravalent live-attenuated dengue

vaccine in flavivirus-naive infants. The American journal of tropical medicine and hygiene. 2011;85(2):341-51.

40. Munoz-Jordan JL, Sanchez-Burgos GG, Laurent-Rolle M, Garcia-Sastre A. Inhibition of interferon signaling by dengue virus. Proceedings of the National Academy of Sciences of the United States of America. 2003;100(24):14333-8.
41. Umareddy I, Pluquet O, Wang QY, Vasudevan SG, Chevet E, Gu F. Dengue virus serotype infection specifies the activation of the unfolded protein response. Virology journal. 2007;4:91.
42. Acosta EG, Castilla V, Damonte EB. Alternative infectious entry pathways for dengue virus serotypes into mammalian cells. Cellular microbiology. 2009;11(10):1533-49.
43. Ma L, Jones CT, Groesch TD, Kuhn RJ, Post CB. Solution structure of dengue virus capsid protein reveals another fold. Proceedings of the National Academy of Sciences of the United States of America. 2004;101(10):3414-9.
44. Limjindaporn T, Netsawang J, Noisakran S, Thiemmeca S, Wongwiwat W, Sudsaward S, et al. Sensitization to Fas-mediated apoptosis by dengue virus capsid protein. Biochemical and biophysical research communications. 2007;362(2):334-9.
45. Cardosa MJ, Wang SM, Sum MS, Tio PH. Antibodies against prM protein distinguish between previous infection with dengue and Japanese encephalitis viruses. BMC microbiology. 2002;2:9.
46. Marks RM, Lu H, Sundaresan R, Toida T, Suzuki A, Imanari T, et al. Probing the interaction of dengue virus envelope protein with heparin: assessment of glycosaminoglycan-derived inhibitors. Journal of medicinal chemistry. 2001;44(13):2178-87.
47. Alcon S, Talarmin A, Debruyne M, Falconar A, Deubel V, Flamand M. Enzyme-linked immunosorbent assay specific to Dengue virus type 1 nonstructural protein NS1 reveals circulation of the antigen in the blood during the acute phase of disease in patients experiencing primary or secondary infections. Journal of clinical microbiology. 2002;40(2):376-81.

48. Avirutnan P, Punyadee N, Noisakran S, Komoltri C, Thiemmeca S, Auethavornanan K, et al. Vascular leakage in severe dengue virus infections: a potential role for the nonstructural viral protein NS1 and complement. The Journal of infectious diseases. 2006;193(8):1078-88.

49. Luo D, Xu T, Hunke C, Gruber G, Vasudevan SG, Lescar J. Crystal structure of the NS3 protease-helicase from dengue virus. Journal of virology. 2008;82(1):173-83.

50. Ackermann M, Padmanabhan R. De novo synthesis of RNA by the dengue virus RNA-dependent RNA polymerase exhibits temperature dependence at the initiation but not elongation phase. The Journal of biological chemistry. 2001;276(43):39926-37.

51. Navarro-Sanchez E, Despres P, Cedillo-Barron L. Innate immune responses to dengue virus. Archives of medical research. 2005;36(5):425-35. Epub 2005/08/16.

52. Wu SJ, Grouard-Vogel G, Sun W, Mascola JR, Brachtel E, Putvatana R, et al. Human skin Langerhans cells are targets of dengue virus infection. Nature medicine. 2000;6(7):816-20.

53. Jessie K, Fong MY, Devi S, Lam SK, Wong KT. Localization of dengue virus in naturally infected human tissues, by immunohistochemistry and in situ hybridization. The Journal of infectious diseases. 2004;189(8):1411-8.

54. Sariol CA, Martinez MI, Rivera F, Rodriguez IV, Pantoja P, Abel K, et al. Decreased dengue replication and an increased anti-viral humoral response with the use of combined Toll-like receptor 3 and 7/8 agonists in macaques. PloS one. 2011;6(4):e19323.

55. Meylan E, Tschopp J, Karin M. Intracellular pattern recognition receptors in the host response. Nature. 2006;442(7098):39-44.

56. Herrero LJ, Zakhary A, Gahan ME, Nelson MA, Herring BL, Hapel AJ, et al. Dengue virus therapeutic intervention strategies based on viral, vector and host factors involved in disease pathogenesis. Pharmacology & therapeutics. 2013;137(2):266-82.

57. Sampath A, Padmanabhan R. Molecular targets for flavivirus drug discovery. Antiviral research. 2009;81(1):6-15.

58. Severa M, Fitzgerald KA. TLR-mediated activation of type I IFN during antiviral immune responses: fighting the battle to win the war. Current topics in microbiology and immunology. 2007;316:167-92.
59. Robertson MJ. Role of chemokines in the biology of natural killer cells. Journal of leukocyte biology. 2002;71(2):173-83.
60. Hilleman MR. Strategies and mechanisms for host and pathogen survival in acute and persistent viral infections. Proceedings of the National Academy of Sciences of the United States of America. 2004;101 Suppl 2:14560-6.
61. Degli-Esposti MA, Smyth MJ. Close encounters of different kinds: dendritic cells and NK cells take centre stage. Nature reviews Immunology. 2005;5(2):112-24.
62. Horvath CM, Stark GR, Kerr IM, Darnell JE, Jr. Interactions between STAT and non-STAT proteins in the interferon-stimulated gene factor 3 transcription complex. Molecular and cellular biology. 1996;16(12):6957-64.
63. Samuel CE. Antiviral actions of interferons. Clinical microbiology reviews. 2001;14(4):778-809, table of contents.
64. Klos A, Wende E, Wareham KJ, Monk PN. International Union of Pharmacology. LXXXVII. Complement peptide C5a, C4a, and C3a receptors. Pharmacological reviews. 2013;65(1):500-43.
65. Lei HY, Yeh TM, Liu HS, Lin YS, Chen SH, Liu CC. Immunopathogenesis of dengue virus infection. Journal of biomedical science. 2001;8(5):377-88.
66. Liu YJ, Kanzler H, Soumelis V, Gilliet M. Dendritic cell lineage, plasticity and cross-regulation. Nature immunology. 2001;2(7):585-9.
67. Churdboonchart V, Bhamarapravati N, Peampramprecha S, Sirinavin S. Antibodies against dengue viral proteins in primary and secondary dengue hemorrhagic fever. The American journal of tropical medicine and hygiene. 1991;44(5):481-93.
68. Valdes K, Alvarez M, Pupo M, Vazquez S, Rodriguez R, Guzman MG. Human Dengue antibodies against structural and nonstructural proteins. Clinical and diagnostic laboratory immunology. 2000;7(5):856-7.

69. Nybakken GE, Oliphant T, Johnson S, Burke S, Diamond MS, Fremont DH. Structural basis of West Nile virus neutralization by a therapeutic antibody. Nature. 2005;437(7059):764-9.

70. Vogt MR, Moesker B, Goudsmit J, Jongeneelen M, Austin SK, Oliphant T, et al. Human monoclonal antibodies against West Nile virus induced by natural infection neutralize at a postattachment step. Journal of virology. 2009;83(13):6494-507.

71. Schlesinger JJ, Brandriss MW, Walsh EE. Protection of mice against dengue 2 virus encephalitis by immunization with the dengue 2 virus non-structural glycoprotein NS1. The Journal of general virology. 1987;68 (Pt 3):853-7.

72. Lai CY, Tsai WY, Lin SR, Kao CL, Hu HP, King CC, et al. Antibodies to envelope glycoprotein of dengue virus during the natural course of infection are predominantly cross-reactive and recognize epitopes containing highly conserved residues at the fusion loop of domain II. Journal of virology. 2008;82(13):6631-43.

73. Dong T, Moran E, Vinh Chau N, Simmons C, Luhn K, Peng Y, et al. High pro-inflammatory cytokine secretion and loss of high avidity cross-reactive cytotoxic T-cells during the course of secondary dengue virus infection. PloS one. 2007;2(12):e1192.

74. Mathew A, Kurane I, Green S, Stephens HA, Vaughn DW, Kalayanarooj S, et al. Predominance of HLA-restricted cytotoxic T-lymphocyte responses to serotype-cross-reactive epitopes on nonstructural proteins following natural secondary dengue virus infection. Journal of virology. 1998;72(5):3999-4004.

75. Kyle JL, Harris E. Global spread and persistence of dengue. Annual review of microbiology. 2008;62:71-92.

76. Rosen L. The pathogenesis of dengue haemorrhagic fever. A critical appraisal of current hypotheses. South African medical journal = Suid-Afrikaanse tydskrif vir geneeskunde. 1986;Suppl:40-2.

77. Clyde K, Kyle JL, Harris E. Recent advances in deciphering viral and host determinants of dengue virus replication and pathogenesis. Journal of virology. 2006;80(23):11418-31.

78. Halstead SB, Rojanasuphot S, Sangkawibha N. Original antigenic sin in dengue. The American journal of tropical medicine and hygiene. 1983;32(1):154-6.
79. Midgley CM, Bajwa-Joseph M, Vasanawathana S, Limpitikul W, Wills B, Flanagan A, et al. An in-depth analysis of original antigenic sin in dengue virus infection. Journal of virology. 2011;85(1):410-21.
80. Mongkolsapaya J, Dejnirattisai W, Xu XN, Vasanawathana S, Tangthawornchaikul N, Chairunsri A, et al. Original antigenic sin and apoptosis in the pathogenesis of dengue hemorrhagic fever. Nature medicine. 2003;9(7):921-7.
81. Basu A, Chaturvedi UC. Vascular endothelium: the battlefield of dengue viruses. FEMS immunology and medical microbiology. 2008;53(3):287-99.
82. Huerre MR, Lan NT, Marianneau P, Hue NB, Khun H, Hung NT, et al. Liver histopathology and biological correlates in five cases of fatal dengue fever in Vietnamese children. Virchows Archiv : an international journal of pathology. 2001;438(2):107-15.
83. Lee YR, Liu MT, Lei HY, Liu CC, Wu JM, Tung YC, et al. MCP-1, a highly expressed chemokine in dengue haemorrhagic fever/dengue shock syndrome patients, may cause permeability change, possibly through reduced tight junctions of vascular endothelium cells. The Journal of general virology. 2006;87(Pt 12):3623-30.
84. Nielsen DG. The relationship of interacting immunological components in dengue pathogenesis. Virology journal. 2009;6:211.
85. Chuang YC, Lei HY, Liu HS, Lin YS, Fu TF, Yeh TM. Macrophage migration inhibitory factor induced by dengue virus infection increases vascular permeability. Cytokine. 2011;54(2):222-31.
86. Matsuda T, Almasan A, Tomita M, Tamaki K, Saito M, Tadano M, et al. Dengue virus-induced apoptosis in hepatic cells is partly mediated by Apo2 ligand/tumour necrosis factor-related apoptosis-inducing ligand. The Journal of general virology. 2005;86(Pt 4):1055-65.
87. Bokisch VA, Top FH, Jr., Russell PK, Dixon FJ, Muller-Eberhard HJ. The potential pathogenic role of complement in dengue hemorrhagic shock syndrome. The New England journal of medicine. 1973;289(19):996-1000.

88. Malasit P. Complement and dengue haemorrhagic fever/shock syndrome. The Southeast Asian journal of tropical medicine and public health. 1987;18(3):316-20.

89. Green S, Rothman A. Immunopathological mechanisms in dengue and dengue hemorrhagic fever. Current opinion in infectious diseases. 2006;19(5):429-36.

90. Ghosh K, Gangodkar S, Jain P, Shetty S, Ramjee S, Poddar P, et al. Imaging the interaction between dengue 2 virus and human blood platelets using atomic force and electron microscopy. Journal of electron microscopy. 2008;57(3):113-8.

91. Lin CF, Wan SW, Cheng HJ, Lei HY, Lin YS. Autoimmune pathogenesis in dengue virus infection. Viral immunology. 2006;19(2):127-32.

92. Huang YH, Chang BI, Lei HY, Liu HS, Liu CC, Wu HL, et al. Antibodies against dengue virus E protein peptide bind to human plasminogen and inhibit plasmin activity. Clinical and experimental immunology. 1997;110(1):35-40.

93. Lin YL, Liu CC, Chuang JI, Lei HY, Yeh TM, Lin YS, et al. Involvement of oxidative stress, NF-IL-6, and RANTES expression in dengue-2-virus-infected human liver cells. Virology. 2000;276(1):114-26.

94. Rathakrishnan A, Wang SM, Hu Y, Khan AM, Ponnampalavanar S, Lum LC, et al. Cytokine expression profile of dengue patients at different phases of illness. PloS one. 2012;7(12):e52215.

95. de-Oliveira-Pinto LM, Marinho CF, Povoa TF, de Azeredo EL, de Souza LA, Barbosa LD, et al. Regulation of inflammatory chemokine receptors on blood T cells associated to the circulating versus liver chemokines in dengue fever. PloS one. 2012;7(7):e38527.

96. Suksanpaisan L, Cabrera-Hernandez A, Smith DR. Infection of human primary hepatocytes with dengue virus serotype 2. Journal of medical virology. 2007;79(3):300-7.

97. Chen J, Ng MM, Chu JJ. Molecular profiling of T-helper immune genes during dengue virus infection. Virology journal. 2008;5:165.

98. Guabiraba R, Marques RE, Besnard AG, Fagundes CT, Souza DG, Ryffel B, et al. Role of the chemokine receptors CCR1, CCR2 and CCR4 in the pathogenesis of experimental dengue infection in mice. PloS one. 2010;5(12):e15680.

99. Chua JJ, Bhuvanakantham R, Chow VT, Ng ML. Recombinant non-structural 1 (NS1) protein of dengue-2 virus interacts with human STAT3beta protein. Virus research. 2005;112(1-2):85-94.

100. Wati S, Rawlinson SM, Ivanov RA, Dorstyn L, Beard MR, Jans DA, et al. Tumour necrosis factor alpha (TNF-alpha) stimulation of cells with established dengue virus type 2 infection induces cell death that is accompanied by a reduced ability of TNF-alpha to activate nuclear factor kappaB and reduced sphingosine kinase-1 activity. The Journal of general virology. 2011;92(Pt 4):807-18.

101. Filipowicz W, Furuichi Y, Sierra JM, Muthukrishnan S, Shatkin AJ, Ochoa S. A protein binding the methylated 5'-terminal sequence, m7GpppN, of eukaryotic messenger RNA. Proceedings of the National Academy of Sciences of the United States of America. 1976;73(5):1559-63.

102. Johansson M, Brooks AJ, Jans DA, Vasudevan SG. A small region of the dengue virus-encoded RNA-dependent RNA polymerase, NS5, confers interaction with both the nuclear transport receptor importin-beta and the viral helicase, NS3. The Journal of general virology. 2001;82(Pt 4):735-45.

103. Forwood JK, Brooks A, Briggs LJ, Xiao CY, Jans DA, Vasudevan SG. The 37-amino-acid interdomain of dengue virus NS5 protein contains a functional NLS and inhibitory CK2 site. Biochemical and biophysical research communications. 1999;257(3):731-7.

104. Reed KE, Gorbalenya AE, Rice CM. The NS5A/NS5 proteins of viruses from three genera of the family flaviviridae are phosphorylated by associated serine/threonine kinases. Journal of virology. 1998;72(7):6199-206.

105. Mackenzie J. Wrapping things up about virus RNA replication. Traffic. 2005;6(11):967-77.

106. Westaway EG, Mackenzie JM, Khromykh AA. Kunjin RNA replication and applications of Kunjin replicons. Advances in virus research. 2003;59:99-140.
107. Kumar A, Buhler S, Selisko B, Davidson A, Mulder K, Canard B, et al. Nuclear localization of dengue virus nonstructural protein 5 does not strictly correlate with efficient viral RNA replication and inhibition of type I interferon signaling. Journal of virology. 2013;87(8):4545-57.
108. Hannemann H, Sung PY, Chiu HC, Yousuf A, Bird J, Lim SP, et al. Serotype-specific Differences in Dengue Virus Non-structural Protein 5 Nuclear Localization. The Journal of biological chemistry. 2013;288(31):22621-35.
109. Tay MY, Fraser JE, Chan WK, Moreland NJ, Rathore AP, Wang C, et al. Nuclear localization of dengue virus (DENV) 1-4 non-structural protein 5; protection against all 4 DENV serotypes by the inhibitor Ivermectin. Antiviral research. 2013;99(3):301-6.
110. Ashour J, Laurent-Rolle M, Shi PY, Garcia-Sastre A. NS5 of dengue virus mediates STAT2 binding and degradation. Journal of virology. 2009;83(11):5408-18.
111. Yap TL, Xu T, Chen YL, Malet H, Egloff MP, Canard B, et al. Crystal structure of the dengue virus RNA-dependent RNA polymerase catalytic domain at 1.85-angstrom resolution. Journal of virology. 2007;81(9):4753-65.
112. Medin CL, Rothman AL. Cell type-specific mechanisms of interleukin-8 induction by dengue virus and differential response to drug treatment. The Journal of infectious diseases. 2006;193(8):1070-7.
113. Schall TJ, Bacon K, Toy KJ, Goeddel DV. Selective attraction of monocytes and T lymphocytes of the memory phenotype by cytokine RANTES. Nature. 1990;347(6294):669-71. Epub 1990/10/18.
114. Nelson PJ, Krensky AM. Chemokines, lymphocytes and viruses: what goes around, comes around. Current opinion in immunology. 1998;10(3):265-70.
115. Schall TJ, Jongstra J, Dyer BJ, Jorgensen J, Clayberger C, Davis MM, et al. A human T cell-specific molecule is a member of a new gene family. J Immunol. 1988;141(3):1018-25.

116. Baggiolini M, Loetscher P. Chemokines in inflammation and immunity. Immunology today. 2000;21(9):418-20.
117. Baggiolini M, Loetscher P, Moser B. Interleukin-8 and the chemokine family. International journal of immunopharmacology. 1995;17(2):103-8.
118. Schall TJ. Biology of the RANTES/SIS cytokine family. Cytokine. 1991;3(3):165-83.
119. Sherry B, Cerami A. Small cytokine superfamily. Current opinion in immunology. 1991;3(1):56-60.
120. Heeger P, Wolf G, Meyers C, Sun MJ, O'Farrell SC, Krensky AM, et al. Isolation and characterization of cDNA from renal tubular epithelium encoding murine Rantes. Kidney international. 1992;41(1):220-5.
121. Kameyoshi Y, Dorschner A, Mallet AI, Christophers E, Schroder JM. Cytokine RANTES released by thrombin-stimulated platelets is a potent attractant for human eosinophils. The Journal of experimental medicine. 1992;176(2):587-92.
122. Springer TA. Traffic signals for lymphocyte recirculation and leukocyte emigration: the multistep paradigm. Cell. 1994;76(2):301-14.
123. Taub DD, Sayers TJ, Carter CR, Ortaldo JR. Alpha and beta chemokines induce NK cell migration and enhance NK-mediated cytolysis. J Immunol. 1995;155(8):3877-88.
124. Adams DH, Lloyd AR. Chemokines: leucocyte recruitment and activation cytokines. Lancet. 1997;349(9050):490-5.
125. Dahinden CA, Geiser T, Brunner T, von Tscharner V, Caput D, Ferrara P, et al. Monocyte chemotactic protein 3 is a most effective basophil- and eosinophil-activating chemokine. The Journal of experimental medicine. 1994;179(2):751-6.
126. Baltus T, Weber KS, Johnson Z, Proudfoot AE, Weber C. Oligomerization of RANTES is required for CCR1-mediated arrest but not CCR5-mediated transmigration of leukocytes on inflamed endothelium. Blood. 2003;102(6):1985-8.
127. Baltus T, von Hundelshausen P, Mause SF, Buhre W, Rossaint R, Weber C. Differential and additive effects of platelet-derived chemokines on

monocyte arrest on inflamed endothelium under flow conditions. Journal of leukocyte biology. 2005;78(2):435-41.

128. Suffee N, Richard B, Hlawaty H, Oudar O, Charnaux N, Sutton A. Angiogenic properties of the chemokine RANTES/CCL5. Biochemical Society transactions. 2011;39(6):1649-53.
129. Bacon KB, Premack BA, Gardner P, Schall TJ. Activation of dual T cell signaling pathways by the chemokine RANTES. Science. 1995;269(5231):1727-30.
130. Taub DD, Turcovski-Corrales SM, Key ML, Longo DL, Murphy WJ. Chemokines and T lymphocyte activation: I. Beta chemokines costimulate human T lymphocyte activation in vitro. J Immunol. 1996;156(6):2095-103.
131. Mantovani A. Tumor-associated macrophages. Current opinion in immunology. 1990;2:689-92.
132. Graves DT, Jiang YL, Williamson MJ, Valente AJ. Identification of monocyte chemotactic activity produced by malignant cells. Science. 1989;245(4925):1490-3.
133. Wilcox JN. Local gene expression in human coronary arteries from transplanted hearts analyzed by in situ hybridization. Circulation. 1990;82(699).
134. Lin R, Heylbroeck C, Genin P, Pitha PM, Hiscott J. Essential role of interferon regulatory factor 3 in direct activation of RANTES chemokine transcription. Molecular and cellular biology. 1999;19(2):959-66.
135. Wathelet MG, Lin CH, Parekh BS, Ronco LV, Howley PM, Maniatis T. Virus infection induces the assembly of coordinately activated transcription factors on the IFN-beta enhancer in vivo. Molecular cell. 1998;1(4):507-18.
136. Nelson PJ, Kim HT, Manning WC, Goralski TJ, Krensky AM. Genomic organization and transcriptional regulation of the RANTES chemokine gene. J Immunol. 1993;151(5):2601-12.
137. Song A, Chen YF, Thamatrakoln K, Storm TA, Krensky AM. RFLAT-1: a new zinc finger transcription factor that activates RANTES gene expression in T lymphocytes. Immunity. 1999;10(1):93-103.

138. Krensky AM, Ahn YT. Mechanisms of disease: regulation of RANTES (CCL5) in renal disease. Nature clinical practice Nephrology. 2007;3(3):164-70.
139. Ortiz BD, Krensky AM, Nelson PJ. Kinetics of transcription factors regulating the RANTES chemokine gene reveal a developmental switch in nuclear events during T-lymphocyte maturation. Molecular and cellular biology. 1996;16(1):202-10.
140. Ahn YT, Huang B, McPherson L, Clayberger C, Krensky AM. Dynamic interplay of transcriptional machinery and chromatin regulates "late" expression of the chemokine RANTES in T lymphocytes. Molecular and cellular biology. 2007;27(1):253-66.
141. Casola A, Henderson A, Liu T, Garofalo RP, Brasier AR. Regulation of RANTES promoter activation in alveolar epithelial cells after cytokine stimulation. American journal of physiology Lung cellular and molecular physiology. 2002;283(6):L1280-90.
142. Moriuchi H, Moriuchi M, Fauci AS. Nuclear factor-kappa B potently up-regulates the promoter activity of RANTES, a chemokine that blocks HIV infection. J Immunol. 1997;158(7):3483-91.
143. Polyanovsky DL, and Stephchenco, A.G. Gene expression regulation: transcription factors. Bioassays. 1990;12:205.
144. Faisst S, Meyer S. Compilation of vertebrate-encoded transcription factors. Nucleic acids research. 1992;20(1):3-26.
145. Tapscott SJ, Davis RL, Thayer MJ, Cheng PF, Weintraub H, Lassar AB. MyoD1: a nuclear phosphoprotein requiring a Myc homology region to convert fibroblasts to myoblasts. Science. 1988;242(4877):405-11.
146. Mercurio F, Karin M. Transcription factors AP-3 and AP-2 interact with the SV40 enhancer in a mutually exclusive manner. The EMBO journal. 1989;8(5):1455-60.
147. Umek RM, Friedman AD, McKnight SL. CCAAT-enhancer binding protein: a component of a differentiation switch. Science. 1991;251(4991):288-92.
148. Akira S, Isshiki H, Sugita T, Tanabe O, Kinoshita S, Nishio Y, et al. A nuclear factor for IL-6 expression (NF-IL6) is a member of a C/EBP family. The EMBO journal. 1990;9(6):1897-906.

149. Genin P, Algarte M, Roof P, Lin R, Hiscott J. Regulation of RANTES chemokine gene expression requires cooperativity between NF-kappa B and IFN-regulatory factor transcription factors. J Immunol. 2000;164(10):5352-61.

150. Thomas LH, Friedland JS, Sharland M, Becker S. Respiratory syncytial virus-induced RANTES production from human bronchial epithelial cells is dependent on nuclear factor-kappa B nuclear binding and is inhibited by adenovirus-mediated expression of inhibitor of kappa B alpha. J Immunol. 1998;161(2):1007-16.

151. Casola A, Garofalo RP, Haeberle H, Elliott TF, Lin R, Jamaluddin M, et al. Multiple cis regulatory elements control RANTES promoter activity in alveolar epithelial cells infected with respiratory syncytial virus. Journal of virology. 2001;75(14):6428-39.

152. Tsai YT, Chen YH, Chang DM, Chen PC, Lai JH. Janus kinase/signal transducer and activator of transcription 3 signaling pathway is crucial in chemokine production from hepatocytes infected by dengue virus. Exp Biol Med (Maywood). 2011;236(10):1156-65.

153. Deng H, Liu R, Ellmeier W, Choe S, Unutmaz D, Burkhart M, et al. Identification of a major co-receptor for primary isolates of HIV-1. Nature. 1996;381(6584):661-6.

154. Dragic T, Litwin V, Allaway GP, Martin SR, Huang Y, Nagashima KA, et al. HIV-1 entry into CD4+ cells is mediated by the chemokine receptor CC-CKR-5. Nature. 1996;381(6584):667-73.

155. Alkhatib G, Combadiere C, Broder CC, Feng Y, Kennedy PE, Murphy PM, et al. CC CKR5: a RANTES, MIP-1alpha, MIP-1beta receptor as a fusion cofactor for macrophage-tropic HIV-1. Science. 1996;272(5270):1955-8.

156. Appanna R, Wang SM, Ponnampalavanar SA, Lum LC, Sekaran SD. Cytokine factors present in dengue patient sera induces alterations of junctional proteins in human endothelial cells. The American journal of tropical medicine and hygiene. 2012;87(5):936-42.

157. Girard S, Vossman E, Misek DE, Podevin P, Hanash S, Brechot C, et al. Hepatitis C virus NS5A-regulated gene expression and signaling revealed

via microarray and comparative promoter analyses. Hepatology. 2004;40(3):708-18.

158. Kato N, Yoshida H, Ono-Nita SK, Kato J, Goto T, Otsuka M, et al. Activation of intracellular signaling by hepatitis B and C viruses: C-viral core is the most potent signal inducer. Hepatology. 2000;32(2):405-12.
159. Su F, Schneider RJ. Hepatitis B virus HBx protein activates transcription factor NF-kappaB by acting on multiple cytoplasmic inhibitors of rel-related proteins. Journal of virology. 1996;70(7):4558-66.
160. Gao S, Song L, Li J, Zhang Z, Peng H, Jiang W, et al. Influenza A virus-encoded NS1 virulence factor protein inhibits innate immune response by targeting IKK. Cellular microbiology. 2012;14(12):1849-66.
161. Kim SY. Hepatitis B virus X protein enhances NFκB activity through cooperating with VBP1. BMB reports. 2007:158-63.
162. Yang X, Khosravi-Far R, Chang HY, Baltimore D. Daxx, a novel Fas-binding protein that activates JNK and apoptosis. Cell. 1997;89(7):1067-76.
163. Park J, Lee JH, La M, Jang MJ, Chae GW, Kim SB, et al. Inhibition of NF-kappaB acetylation and its transcriptional activity by Daxx. Journal of molecular biology. 2007;368(2):388-97.
164. Livak KJ, Schmittgen TD. Analysis of relative gene expression data using real-time quantitative PCR and the 2(-Delta Delta C(T)) Method. Methods. 2001;25(4):402-8.
165. Orlando V. Mapping chromosomal proteins in vivo by formaldehyde-crosslinked-chromatin immunoprecipitation. Trends in biochemical sciences. 2000;25(3):99-104.
166. Agalioti T, Lomvardas S, Parekh B, Yie J, Maniatis T, Thanos D. Ordered recruitment of chromatin modifying and general transcription factors to the IFN-beta promoter. Cell. 2000;103(4):667-78.
167. Soutoglou E, Talianidis I. Coordination of PIC assembly and chromatin remodeling during differentiation-induced gene activation. Science. 2002;295(5561):1901-4.
168. Silva BM, Sousa LP, Gomes-Ruiz AC, Leite FG, Teixeira MM, da Fonseca FG, et al. The dengue virus nonstructural protein 1 (NS1) increases NF-kappaB

transcriptional activity in HepG2 cells. Archives of virology. 2011;156(7):1275-9.

169. Khunchai S. Application of yeast two hybrid system for identification of human proteins interacting with dengue virus nonstructural protein 5 2005.

170. Marianneau P, Cardona A, Edelman L, Deubel V, Despres P. Dengue virus replication in human hepatoma cells activates NF-kappaB which in turn induces apoptotic cell death. Journal of virology. 1997;71(4):3244-9.

APPENDIX

1. Chemicals

Chemicals	Source
Absolute ethanol (C_2H_5OH)	BDH, England, UK
Absolute methanol (CH_3OH)	Lab-Scan, Thailand
Acetic acid glacial (CH_3COOH)	Carlo Erba, Milan, Italy
Acrylamide (C_3H_5NO)	Sigma Chemicals, MO, USA
Agarose	Seakem, Rockland, USA
Ammonium persulfate ((NH_4HCO_3)	USB, OH, USA
Bovine serum albumin	Sigma, St. Louis, USA
Bromophenol blue	Promega, Madison, USA
3, 3-Diaminobenzidine tetrahydrochloride anhydrous (DAB)	Sigma, USA
Diethyl pyrocarbonate (DEPC)	Sigma, St. Louis, USA
EDTA Tetrasodium Dihydrate ($C_{10}H_{12}N_2O_8Na_4.2H_2O$)	USB, OH, USA
Ethidium bromide ($C_{21}H_{20}BrN_3$)	Bio-Rad Laboratorie Hercules, CA, USA
Fetal bovine serum	GIBCO, NY, USA
Formaldehyde 37% w/w	Lab-Scan, Thailand
L-Glutamine	Sigma, St. Louis, USA
Glyceral ($C_3H_8O_3$)	Lab-Scan, Thailand
Glycine ($H_2NCH_2CO_2H$)	USB, USA
Gum tragacanth	Sigma, USA
Hydrochloric acid (HCl)	E. Merck, Darmstadt, Germany
Isopropanol ($CH_3CHOHCH_3$)	BDH, England, UK
ß-Mercaptoethanol ($HSCH_2CH_2OH$)	Fluka, Steinheim, Switzerland

Chemicals	**Source**
Non-essential amino acid	GIBCO, NY, USA
Penicillin ($C_{16}H_{17}N_2O_4SNa$)	Sigma, St. Louis, USA
Protease inhibitor cocktail	Roche, Mannheim, Germany
Potassium chloride (KCl)	E. Merck, Germany
Potassium dihydrogen phosphate (KH_2PO_4)	E. Merck, Germany
Skim milk (Instant non fat milk powder)	Mission, Bangkok, Thailand
Sodium bicarbonate ($NaHCO_3$)	E. Merck, Germany
Sodium chloride (NaCl)	E. Merck, Germany
Sodium dodecyle sulfate or SDS ($C_{12}H_25O_4SNa$)	Sigma, St. Louis, USA
Sodium hydrogen phosphate (Na_2HPO_4)	E. Merck, Germany
Sodium pyruvate	GIBCO, NY, USA
Streptomycin sulfate 750U/mg	Sigma, St. Louis, USA
N,N,N',N'-Tetramethyl ethylenediamine (TEMED)	Bio-Rad Laboratories, USA
Tris (hydroxymethyl aminomethane)	Sigma, St. Louis, USA
Triton X-100	Fluka, Switzerland
Tryptose phosphate broth	Sigma, St. Louis, USA
Tween 20	Sigma, St. Louis, USA
Yeast extract	BD DifcoTm, Franklin Lakes, USA

2. Reagents

2.1 Reagents for molecular cloning and agarose gel electrophoresis

2.1.1 Bacterial media

(1) Low salt Luria-Bertani plate (LB plate)

Per liter:

Tryptone	10	g
Yeast extract	5	g
NaCl	10	g
Agar	15	g

The mixture was shaken until it dissolved and adjusted the final volume of solution to 1 liter with distilled water. Then, this media was sterilized by autoclaving at 121°C for 15 min.

(2) Low salt Luria-Bertani broth (LB broth)

LB broth medium was made the same way as LB plate, leaving out the agar.

(3) Luria-Bertani media with amplicilin

When the Low salt Luria-Bertani broth was cooled down to approximately 50°C, amplicilin was added to medium to a final concentration of 50 μg/ml both LB plate and LB broth.

2.1.2 Agarose gel electrophoresis

(1) 50x Tris-acetate buffer (TAE buffer)

Tris-base	242	g
Glacial acetic acid	57.1	ml
0.5 M EDTA (pH 8.0)	100	ml
Added distilled water to	1000	ml

The solution was mixed and stored at room temperature. It was diluted to 0.5x final concentration (0.5x TAE) for agarose gel preparation and electrophoresis buffer.

(2) 1% (w/v) agarose gel in 0.5x TAE

Per 100 ml		
Agarose powder	1	g
0.5x TAE	100	ml

The slurry was heated in microwave oven until the agarose completely dissolved and then poured the warm agarose solution into gel box.

(3) 3% (w/v) agarose gel in 0.5x TAE

Per 100 ml		
Agarose powder	3	g
0.5x TAE	100	ml

The slurry was heated in microwave oven until the agarose completely dissolved and then poured the warm agarose solution into gel box.

(4) 6× loading dye (0.25% bromophenol blue, 0.25% xylene cyanol FF, 30% glycerol)

Glycerol	3	ml
Xylene cyanol FF	0.025	g
Bromophenol blue	0.025	g

The mixture was mixed and dissolved in distilled water to make the final volume up to 10 ml. Aliquots were kept at –20˚C and diluted to a final concentration of 1x with the sample before use.

2.2 Reagents for mammalian cell culture

(1) Dulbecco's Modified Eagle Medium (DMEM) medium

Per liter:

DMEM powder	1	pack
Sodium bicarbonate (NaHCO3)	3.7	g

One pack of the medium powder was dissolved in distilled water with gentle stirring until complete dissolved. The solution was added with 3.7 g of sodium bicarbonate ($NaHCO_3$) and further stirred. The medium solution was adjusted for the total volume up to 1 liter with distilled water and sterilized by filtration though 0.2-µM cellulose acetate filter membrane under sterile condition and stored at 4˚C.

(2) Minimum Essential Medium (MEM)

MEM powder	1	pack
Sodium bicarbonate ($NaHCO_3$)	2.2	g

One pack of the medium powder was dissolved in distilled water with gentle stirring until complete dissolved. The solution was added with 2.2 g of sodium bicarbonate ($NaHCO_3$) and further stirred. The medium solution was adjusted for the total volume up to 1 liter with distilled water and sterilized by filtration though 0.2-µM cellulose acetate filter membrane under sterile condition and stored at 4˚C.

(3) Leibovitz's L-15 medium

Per liter

L-15 powder	1	pack

One pack of the medium powder was mixed with or without sodium bicarbonate ($NaHCO_3$) and dissolved in distilled water with gentle stirring. The medium solution was adjusted for the total volume up to 1 liter and sterilized by

filtration though 0.2-μM cellulose acetate filter membrane under sterile condition and stored at 4˚C.

(4) 10% FBS DMEM

Per liter:

Heated Fetal Bovine Serum	100	ml
Penicillin G-Streptomycin solution	12	ml
100x Non-essential amino acid	10	ml
100x Sodium pyruvate	10	ml
200 mM L-Glutamine	10	ml

The mixture was added with DMEM up to 1 liter, mixed thoroughly and stored at 4˚C.

(5) Penicillin G-Streptomycin solution (PenG/Strep solution)

Penicillin G	301.81	mg
Streptomycin sulfate	500.00	mg

(6) 200 mM L-Glutamine

L-Glutamine powder	2.923	g
Distilled water	100	ml

The L-Glutamine powder was dissolved in 100 ml of distilled water and sterilized by filtration through 0.2-μM cellulose acetate filter membrane under sterile condition. Aliquots of solution were stored at –20˚C until use.

(7) Fetal Bovine Serum (FBS)

FBS was heat inactivated by heating at 56˚C for 30 min in water bath and stored at 4˚C until use.

(8) 10x Phosphate buffered-saline (PBS), pH 7.4

NaCl	80	g
KCl	2	g

Na2HPO4	14.4	g
KH2PO4	2.4	g

These chemicals were mixed and well dissolved in distilled water with gentle stirring and adjusted pH to 7.4. The solution was made the final volume up to 1 liter prior to sterilization by autoclave at 121˚C for 15 min and stored at room temperature. This buffer was diluted to a final concentration of 1× with distilled water before use.

(9) 2.5 mM EDTA in PBS

EDTA.Na2.2H2O	0.4653	g
PBS (pH 7.4)	500	ml

The chemical was dissolved in PBS (pH 7.4) with stirring and adjusted for the final volume up to 500 ml. The solution was sterilized by autoclave at 121˚C for 15 min and stored at room temperature.

2.3 Reagents for cell lysate preparation for WB and Co-IP assay

(1) 5x Leammli sample buffer

1 M Tris-HCl pH 6.8	12.5	ml
Glyceral	20	ml
SDS	0.5	g
10% Bromophenol blue	0.5	ml
ß-Mercaptoethanol	6.25	ml

The mixture was added with distilled water up to 50 ml and mixed thoroughly.This buffer was aliquot and stored at -20 °C and diluted into 1x of final concentration before use.

(2) 1 M Tris-Cl, pH 7.4

Tris	12.114	g
Distilled water	100	ml

Tris was dissolved in distilled water with stirring and adjusted pH to 7.4 with concentrated hydrochloric acid (conc. HCL). The solution was made the final volume up to 100 ml and sterilized by autoclave at 121˚C for 15 min and stored at room temperature.

(3) 0.5 M EDTA pH 8.0

EDTA.Na4.2H2O	7.31	g
Distilled water	100	ml

EDTA.Na4.2H_2O was dissolved in distilled water and adjusted pH to 8.0. The solution was adjusted the final volume up to 100 ml and sterilized by autoclave at 121˚C for 15 min and stored at room temperature.

(4) 4.0 M NaCl

NaCl	23.376	g
Distilled water	100	ml

NaCl was dissolved in distilled water with stirring and adjusted to a final volume of 100 ml by distilled water. The solution was sterilized by autoclave at 121˚C for 15 min and stored at room temperature.

(5) 10% sodium deoxycholate (DOC)

DOC	5	g
Distilled water	50	ml

Five gram of DOC was dissolved in distilled water and added with distilled water up to final volume up to 50 ml. This solution was stored at room temperature.

(6) RIPA lysis buffer or nondenaturing lysis buffer for Co-IP assay (20 mM Tris-HCl pH 7.4, 5 mM EDTA, 150 mM NaCl, 0.5% DOC, 0.1% SDS, 1% NP-40)

1 M Tris-HCl pH 7.4	1	ml
0.5 mM EDTA	0.5	ml
4 M NaCl	1.875	ml

10% DOC	2.5	ml
10% SDS	5	ml
NP-40	0.5	ml

The mixture was added with sterile distilled water up to 50 ml and mixed thoroughly. This RIPA lysis buffer was stored at 4°C and added with protease inhibitor cocktail into a final concentration of 1x before use.

(7) Protease inhibitor cocktail (25x conc.)

Protease inhibitor cocktail	1	tablet
Sterile distilled water	2	ml

One tablet of protease inhibitor cocktail was dissolved in sterile distilled water, aliquot, stored -20 °C and diluted into 1x of final concentration before use.

(8) Co-IP washing buffer (0.1% Triton X-100, 150 mM NaCl, 20 mM Tris–HCl; pH 7.4, 5 mM EDTA)

1 M Tris-HCl pH 7.4	1	ml
0.5 mM EDTA	0.5	ml
4 M NaCl	1.875	ml
100% Triton X-100	0.05	ml

The mixture was added with sterile distilled water up to 50 ml and mixed thoroughly. This buffer was stored at 4°C.

2.4 Reagents for SDS-PAGE and immunoblot analysis

2.4.1 Reagents for polyacrylamide gel preparation

(1) 30.8% (w/v) Acrylamide-Bisacrylmide

Acrylamide	30.0	g
Bis-acrylamide	0.8	g

These chemicals were dissolved in distilled water with gentle stirring and adjusted the final volume to 100 ml. The reagent was then filtrated through a 125-mm diameter filter paper (Whatman No.1) and stored in the dark at 4˚C.

(2) Resolving gel buffer pH 8.8 (3 M Tris-HCl)

Tris	36.3	g
1 M HCl	48	ml

Tris was dissolved in 1 M HCl and adjusted pH to 8.8. The solution was adjusted the final volume to 100 ml with distilled water.

(3) Stacking gel buffer (0.5 M Tris-HCl, pH 6.8)

Tris	6.0	g
1 M HCl	48	ml

Tris was dissolved in 1 M HCl and adjusted pH to 6.8 with 1 M HCl. The mixture was adjusted the final volume to 100 ml with distilled water.

(4) 10% (w/v) Sodium dodecyl sulfate (10% SDS)

SDS	10	g
Distilled water	100	ml

SDS was dissolved in distilled water to bring the final volume up to 100 ml. The reagent was stored at room temperature.

(5) 10% Resolving gel of SDS-PAGE (for 1 gel)

30.8% (w/v) Acrylamide-bisacrylamide	1.67	ml
3 M Tris-HCL (pH 8.8)	0.630	ml
10% SDS	0.050	ml
10% Ammonium persulfate	0.038	ml
Deionized water	2.63	ml
TEMED	0.0025	ml

(6) 3.85% Stacking gel of SDS-PAGE (for 1 gel)

30.8% (w/v) Acrylamide-bisacrylamide	0.250	ml
0.5 M Tris-HCl (pH 6.8)	0.500	ml
10% SDS	0.020	ml
10% Ammonium persulfate	0.015	ml

Deionized water	1.22	ml
TEMED	0.0015	ml

2.4.2 Buffer for protein electrophoresis and immunoblotting

(1) 10x Running buffer (0.25 M Tris-HCl, 1.92 M Glycine, 1% (w/v) SDS)

Tris	30.3	g
Glycine	144.0	g
SDS	10.0	g

These chemicals were mixed and dissolved in distilled water with gentle stirring and adjusted to the final volume of 1 liter. The buffer was diluted to 1x with distilled water and stored at 4˚C just before use.

(2) Towbin buffer (25 mM Tris, 192 mM Glycine, 20% (v/v) Methanol, 0.1% SDS, pH 8.3)

Tris	3	g
Glycine	14.4	g
SDS	1	g

These chemicals were dissolved in distilled water with gentle stirring and adjusted the volume up to 800 ml. The solution was added with 200 ml of methanol and stored at 4˚C.

(3) 10× Tris buffered saline (TBS, pH 7.6)

Tris	30	g
NaCl	80	g

These chemicals were mixed and well dissolved in distilled water with gentle stirring. The solution was adjusted to pH 7.6 and made the final volume to 1 liter prior to sterilization by autoclave at 121˚C for 15 min. This buffer was stored at room temperature and diluted to a final concentration of 1× with distilled water before use.

(4) 0.1% TBST (0.1% Tween in 25 mM Tris)

10x TBS	100	ml
Tween-20	1	ml

The 10x TBS was diluted with distilled water to a final concentration of 1×. Then, 1 ml of Tween-20 was added into 1xTBS to obtain 0.1% TBST.

(5) 5% skim milk

Non-fat dry milk	5	g
1x PBS or 0.1% TBST	100	ml

Non-fat dry milk was dissolved with 1× PBS or 0.1% TBST by shaking until well dissolved.

2.5 Reagents for immunofluorescence staining

(1) 0.1% formaldehyde in PBS

37 % Formaldehyde	0.135	ml
Distilled water	49.865	ml

Formaldehyde was dissolved in distilled water and mixed homogenously. This solution was stored at room temperature.

(2) 2% Formaldehyde in PBS

37% Formaldehyde	2.7	ml
Distilled water	47.3	ml

Formaldehyde was dissolved in distilled water and mixed homogenously. This solution was stored at room temperature.

(3) 3.7% Formaldehyde in PBS

37% Formaldehyde	5	ml
Distilled water	49.5	ml

Formaldehyde was dissolved in distilled water and mixed homogenously. This solution was stored at room temperature.

(4) 1% BSA in PBS

BSA	0.5	g
PBS	50	ml

BSA was dissolved in PBS and mixed homogenously. This solution was stored at 4°C.

3. Instruments

-Biometra TGradient Thermal Cycler**,** Biometra GmbH, Goettingen, Germany

-GeneAmp® PCR System 9700, Perkin Elmer Cetus, USA

-Vertical gel electrophoretic apparatus model AE-6410E, ATTO corporation, Japan

-SemiPhor semi-dry transphor , Amersham Bioscience, NJ, USA

-G:BOX chemiluminescence imaging system, Syngene, Cambridge, UK

-Confocal laser-scanning microscope, SM 510 Meta, Carl Zeiss, Jena, Germany

-NanoDrop spectrophotometer, Thermo Fisher Scientific Inc, Wilmington, USA

-FACSort™ flow cytometer, Becton–Dickinson, Immunocyometry System, CA, USA

-LightCycler 480 II, Roche, Mannheim, Germany

-Luminometer Lumat LB 9507, Berthold Technology, CA, USA

-Gene Genius Bio Imaging system, Syngene, Cambridge, UK

4. Gene table of RT² Profiler™ PCR Array Human Inflammatory Response & Autoimmunity.

Position	Gene Bank	Symbol	Description	Gene Name
A01	NM_001706	BCL6	B-cell CLL/lymphoma 6	BCL5, BCL6A, LAZ3, ZBTB27, ZNF51
A02	NM_000064	C3	Complement component 3	AHUS5, ARMD9, ASP, CPAMD1
A03	NM_004054	C3AR1	Complement component 3a receptor 1	AZ3B, C3AR, HNFAG09
A04	NM_002986	CCL11	Chemokine (C-C motif) ligand 11	MGC22554, SCYA11
A05	NM_005408	CCL13	Chemokine (C-C motif) ligand 13	CKb10, MCP-4, MGC17134, NCC-1, NCC1, SCYA13, SCYL1
A06	NM_004590	CCL16	Chemokine (C-C motif) ligand 16	CKb12, HCC-4, ILINCK, LCC-1, LEC, LMC, MGC117051, Mtn-1, NCC-4, NCC4, SCYA16, SCYL4
A07	NM_002987	CCL17	Chemokine (C-C motif) ligand 17	A-152E5.3, ABCD-2, MGC138271, MGC138273, SCYA17, TARC
A08	NM_006274	CCL19	Chemokine (C-C motif) ligand 19	CKb11, ELC, MGC34433, MIP-3b, MIP3B, SCYA19

4. Gene table of RT² Profiler™ PCR Array Human Inflammatory Response & Autoimmunity (cont.).

Position	Gene Bank	Symbol	Description	Gene Name
A09	NM_002982	CCL2	Chemokine (C-C motif) ligand 2	GDCF-2, HC11, HSMCR30, MCAF, MCP-1, MCP1, MGC9434, SCYA2, SMC-CF
A10	NM_002989	CCL21	Chemokine (C-C motif) ligand 21	6Ckine, CKb9, ECL, MGC34555, SCYA21, SLC, TCA4
A11	NM_002990	CCL22	Chemokine (C-C motif) ligand 22	ABCD-1, DC, B-CK, MDC, MGC34554, SCYA22, STCP-1
A12	NM_005064	CCL23	Chemokine (C-C motif) ligand 23	CK-BETA-8, CKb8, Ckb-8, Ckb-8-1, MIP-3, MIP3, MPIF-1, SCYA23
B01	NM_002991	CCL24	Chemokine (C-C motif) ligand 24	Ckb-6, MPIF-2, MPIF2, SCYA24
B02	NM_002983	CCL3	Chemokine (C-C motif) ligand 3	G0S19-1, LD78ALPHA, MIP-1-alpha, MIP1A, SCYA3

4. Gene table of RT² Profiler™ PCR Array Human Inflammatory Response & Autoimmunity (cont.).

Position	Gene Bank	Symbol	Description	Gene Name
B03	NM_002984	CCL4	Chemokine (C-C motif) ligand 4	ACT2, AT744.1, G-26, LAG1, MGC104418, MGC126025, MGC126026, MIP-1-beta, MIP1B, MIP1B1, SCYA2, SCYA4
B04	NM_002985	CCL5	Chemokine (C-C motif) ligand 5	D17S136E, MGC17164, RANTES, SCYA5, SISd, TCP228
B05	NM_006273	CCL7	Chemokine (C-C motif) ligand 7	FIC, MARC, MCP-3, MCP3, MGC138463, MGC138465, NC28, SCYA6, SCYA7
B06	NM_005623	CCL8	Chemokine (C-C motif) ligand 8	HC14, MCP-2, MCP2, SCYA10, SCYA8
B07	NM_001295	CCR1	Chemokine (C-C motif) receptor 1	CD191, CKR-1, CKR1, CMKBR1, HM145, MIP1aR, SCYAR1
B08	NM_001123396	CCR2	Chemokine (C-C motif) receptor 2	CC-CKR-2, CCR2A, CCR2B, CD192, CKR2, CKR2A, CKR2B, CMKBR2, FLJ78302, MCP-1-R, MGC103828, MGC111760, MGC168006

4. Gene table of RT² Profiler™ PCR Array Human Inflammatory Response & Autoimmunity (cont.).

Position	Gene Bank	Symbol	Description	Gene Name
B09	NM_001837	CCR3	Chemokine (C-C motif) receptor 3	CC-CKR-3, CD193, CKR3, CMKBR3, MGC102841
B10	NM_005508	CCR4	Chemokine (C-C motif) receptor 4	CC-CKR-4, CD194, CKR4, CMKBR4, ChemR13, HGCN:14099, K5-5, MGC88293
B11	NM_001838	CCR7	Chemokine (C-C motif) receptor 7	BLR2, CD197, CDw197, CMKBR7, EBI1
B12	NM_000591	CD14	CD14 molecule	-
C01	NM_001250	CD40	CD40 molecule, TNF receptor superfamily member 5	Bp50, CDW40, MGC9013, TNFRSF5, p50
C02	NM_000074	CD40LG	CD40 ligand	CD154, CD40L, HIGM1, IGM, IMD3, T-BAM, TNFSF5, TRAP, gp39, hCD40L
C03	NM_005194	CEBPB	CCAAT/enhancer binding protein (C/EBP), beta	C, EBP-beta, CRP2, IL6DBP, LAP, MGC32080, NF-IL6, TCF5
C04	NM_000567	CRP	C-reactive protein, pentraxin-related	MGC149895, MGC88244, PTX1

4. Gene table of RT² Profiler™ PCR Array Human Inflammatory Response & Autoimmunity (cont.).

Position	Gene Bank	Symbol	Description	Gene Name
C05	NM_000757	CSF1	Colony stimulating factor 1 (macrophage)	MCSF, MGC31930
C06	NM_001511	CXCL1	Chemokine (C-X-C motif) ligand 1 (melanoma growth stimulating activity, alpha)	FSP, GRO1, GROa, MGSA, MGSA-a, NAP-3, SCYB1
C07	NM_001565	CXCL10	Chemokine (C-X-C motif) ligand 10	C7, IFI10, INP10, IP-10, SCYB10, crg-2, gIP-10, mob-1
C08	NM_002089	CXCL2	Chemokine (C-X-C motif) ligand 2	CINC-2a, GRO2, GROb, MGSA-b, MIP-2a, MIP2, MIP2A, SCYB2
C09	NM_002090	CXCL3	Chemokine (C-X-C motif) ligand 3	CINC-2b, GRO3, GROg, MIP-2b, MIP2B, SCYB3
C10	NM_002994	CXCL5	Chemokine (C-X-C motif) ligand 5	ENA-78, SCYB5
C11	NM_002993	CXCL6	Chemokine (C-X-C motif) ligand 6 (granulocyte chemotactic protein 2)	CKA-3, GCP-2, GCP2, SCYB6

4. Gene table of RT² Profiler™ PCR Array Human Inflammatory Response & Autoimmunity (cont.).

Position	Gene Bank	Symbol	Description	Gene Name
C12	NM_002416	CXCL9	Chemokine (C-X-C motif) ligand 9	CMK, Humig, MIG, SCYB9, crg-10
D01	NM_000634	CXCR1	Chemokine (C-X-C motif) receptor 1	C-C, C-C-CKR-1, CD128, CD181, CDw128a, CKR-1, CMKAR1, IL8R1, IL8RA, IL8RBA
D02	NM_001557	CXCR2	Chemokine (C-X-C motif) receptor 2	CD182, CDw128b, CMKAR2, IL8R2, IL8RA, IL8RB
D03	NM_003467	CXCR4	Chemokine (C-X-C motif) receptor 4	CD184, D2S201E, FB22, HM89, HSY3RR, LAP3, LCR1, LESTR, NPY3R, NPYR, NPYRL, NPYY3R, WHIM
D04	NM_000639	FASLG	Fas ligand (TNF superfamily, member 6)	APT1LG1, CD178, CD95-L, CD95L, FASL, TNFSF6
D05	NM_005252	FOS	FBJ murine osteosarcoma viral oncogene homolog	AP-1, C-FOS
D06	NM_000619	IFNG	Interferon, gamma	IFG, IFI
D07	NM_000572	IL10	Interleukin 10	CSIF, IL-10, IL10A, MGC126450, MGC126451, TGIF

4. Gene table of RT² Profiler™ PCR Array Human Inflammatory Response & Autoimmunity (cont.).

Position	Gene Bank	Symbol	Description	Gene Name
D08	NM_000628	IL10RB	Interleukin 10 receptor, beta	CDW210B, CRF2-4, CRFB4, D21S58, D21S66, IL-10R2
D09	NM_000585	IL15	Interleukin 15	IL-15, MGC9721
D10	NM_002190	IL17A	Interleukin 17A	CTLA8, IL-17, IL-17A, IL17
D11	NM_001562	IL18	Interleukin 18 (interferon-gamma-inducing factor)	IGIF, IL-18, IL-1g, IL1F4, MGC12320
D12	NM_000575	IL1A	Interleukin 1, alpha	IL-1A, IL1, IL1-ALPHA, IL1F1
E01	NM_000576	IL1B	Interleukin 1, beta	IL-1, IL1-BETA, IL1F2
E02	NM_000877	IL1R1	Interleukin 1 receptor, type I	CD121A, D2S1473, IL-1R-alpha, IL1R, IL1RA, P80
E03	NM_002182	IL1RAP	Interleukin 1 receptor accessory protein	C3orf13, FLJ37788, IL-1RAcP, IL1R3
E04	NM_000577	IL1RN	Interleukin 1 receptor antagonist	DIRA, ICIL-1RA, IL-1RN, IL-1ra, IL-1ra3, IL1F3, IL1RA, IRAP, MGC10430, MVCD4

4. Gene table of RT² Profiler™ PCR Array Human Inflammatory Response & Autoimmunity (cont.).

Position	Gene Bank	Symbol	Description	Gene Name
E05	NM_020525	IL22	Interleukin 22	IL-21, IL-22, IL-D110, IL-TIF, ILTIF, MGC79382, MGC79384, TIFIL-23, TIFa, zcyto18
E06	NM_016584	IL23A	Interleukin 23, alpha subunit p19	IL-23, IL-23A, IL23P19, MGC79388, P19, SGRF
E07	NM_144701	IL23R	Interleukin 23 receptor	-
E08	NM_000879	IL5	Interleukin 5 (colony-stimulating factor, eosinophil)	EDF, IL-5, TRF
E09	NM_000600	IL6	Interleukin 6 (interferon, beta 2)	BSF2, HGF, HSF, IFNB2, IL-6
E10	NM_000565	IL6R	Interleukin 6 receptor	CD126, IL-6R-1, IL-6RA, IL6RA, MGC104991, gp80
E11	NM_000584	IL8	Interleukin 8	CXCL8, GCP-1, GCP1, LECT, LUCT, LYNAP, MDNCF, MONAP, NAF, NAP-1, NAP1
E12	NM_000590	IL9	Interleukin 9	HP40, IL-9, P40

4. Gene table of RT² Profiler™ PCR Array Human Inflammatory Response & Autoimmunity (cont.).

Position	Gene Bank	Symbol	Description	Gene Name
F01	NM_000211	ITGB2	Integrin, beta 2 (complement component 3 receptor 3 and 4 subunit)	CD18, LAD, LCAMB, LFA-1, MAC-1, MF17, MFI7
F02	NM_000893	KNG1	Kininogen 1	BDK, KNG
F03	NM_000595	LTA	Lymphotoxin alpha (TNF superfamily, member 1)	LT, TNFB, TNFSF1
F04	NM_002341	LTB	Lymphotoxin beta (TNF superfamily, member 3)	TNFC, TNFSF3, p33
F05	NM_015364	LY96	Lymphocyte antigen 96	ESOP-1, MD-2, MD2, ly-96
F06	NM_002468	MYD88	Myeloid differentiation primary response gene (88)	MYD88D
F07	NM_003998	NFKB1	Nuclear factor of kappa light polypeptide gene enhancer in B-cells 1	DKFZp686C01211, EBP-1, KBF1, MGC54151, NF-kappa-B, NF-kappaB, NFKB-p105, NFKB-p50, NFkappaB, p105, p50
F08	NM_000625	NOS2	Nitric oxide synthase 2, inducible	HEP-NOS, INOS, NOS, NOS2A

4. Gene table of RT² Profiler™ PCR Array Human Inflammatory Response & Autoimmunity (cont.).

Position	Gene Bank	Symbol	Description	Gene Name
F09	NM_000176	NR3C1	Nuclear receptor subfamily 3, group C, member 1 (glucocorticoid receptor)	GCCR, GCR, GR, GRL
F10	NM_000963	PTGS2	Prostaglandin-endoperoxide synthase 2 (prostaglandin G/H synthase and cyclooxygenase)	COX-2, COX2, GRIPGHS, PGG, HS, PGHS-2, PHS-2, hCox-2
F11	NM_003821	RIPK2	Receptor-interacting serine-threonine kinase 2	CARD3, CARDIAK, CCK, GIG30, RICK, RIP2
F12	NM_000450	SELE	Selectin E	CD62E, ELAM, ELAM1, ESEL, LECAM2
G01	NM_001039661	TIRAP	Toll-interleukin 1 receptor (TIR) domain containing adaptor protein	FLJ42305, Mal, wyatt
G02	NM_003263	TLR1	Toll-like receptor 1	CD281, DKFZp547I0610, DKFZp564I0682, KIAA0012, MGC104956, MGC126311, MGC126312, TIL, TIL. LPRS5, rsc786

4. Gene table of RT² Profiler™ PCR Array Human Inflammatory Response & Autoimmunity (cont.).

Position	Gene Bank	Symbol	Description	Gene Name
G03	NM_003264	TLR2	Toll-like receptor 2	CD282, TIL4
04	NM_003265	TLR3	Toll-like receptor 3	CD283
G05	NM_138554	TLR4	Toll-like receptor 4	ARMD10, CD284, TOLL, hToll
G06	NM_003268	TLR5	Toll-like receptor 5	FLJ10052, MGC126430, MGC126431, SLEB1, TIL3
G07	NM_006068	TLR6	Toll-like receptor 6	CD286
G08	NM_016562	TLR7	Toll-like receptor 7	-
G09	NM_017442	TLR9	Toll-like receptor 9	CD289
G10	NM_000594	TNF	Tumor necrosis factor	DIF, TNF-alpha, TNFA, TNFSF2
G11	NM_003807	TNFSF14	Tumor necrosis factor (ligand) superfamily, member 14	CD258, HVEML, LIGHT, LTg, TR2
G12	NM_019009	TOLLIP	Toll interacting protein	FLJ33531, IL-1RAcPIP
H01	NM_001101	ACTB	Actin, beta	PS1TP5BP1
H02	NM_004048	B2M	Beta-2-microglobulin	-
H03	NM_002046	GAPDH	Glyceraldehyde-3-phosphate dehydrogenase	G3PD, GAPD, MGC88685

4. Gene table of RT² Profiler™ PCR Array Human Inflammatory Response & Autoimmunity (cont.).

Position	Gene Bank	Symbol	Description	Gene Name
H04	NM_000194	HPRT1	Hypoxanthine phosphoribosyltransferase 1	HGPRT, HPRT
H05	NM_001002	RPLP0	Ribosomal protein, large, P0	L10E, LP0, MGC111226, MGC88175, P0, PRLP0, RPP0
H06	SA_00105	HGDC	Human Genomic DNA Contamination	HIGX1A
H07	SA_00104	RTC	Reverse Transcription Control	RTC
H08	SA_00104	RTC	Reverse Transcription Control	RTC
H09	SA_00104	RTC	Reverse Transcription Control	RTC
H10	SA_00103	PPC	Positive PCR Control	PPC
H11	SA_00103	PPC	Positive PCR Control	PPC
H12	SA_00103	PPC	Positive PCR Control	PPC

5. Alignment of amino acid sequences between WT-NS5 construct sequencing result and DENV-2 NS5 strain 16681 reference sequences.

```
Kinney's .                                                  GTGNIGETLGEKWKSRLNALGKSEFQIYK 29
WT-NS5 construct's                                          GTGNIGETLGEKWKSRLNALGKSEFQIYK 29
Block's                                                     GTGNIGETLGEKWKSRLNALGKSEFQIYK 29
Sittisompat's                                               GTGNIGETLGEKWKSRLNALGKSEFQIYK 29
                                                            ****************************

Kinney's          KSGIQEVDRTLAKEGIKRGETDHHAVSRGSAKLRWFVERNMVTPEGKVVDLGCGRGGWSY 89
WT-NS5 construct's KSGIQEVDRTLAKEGIKRGETDHHAVSRGSAKLRWFVERNMVTPEGKVVDLGCGRGGWSY 89
Block's           KSGIQEVDRTLAKEGIKRGETDHHAVSRGSAKLRWFVERNMVTPEGKVVDLGCGRGGWSY 89
Sittisompat's     KSGIQEVDRTLAKEGIKRGETDHHAVSRGSAKLRWFVERNMVTPEGKVVDLGCGRGGWSY 89
                  ************************************************************

Kinney's          YCGGLKNVREVKGLTKGGPGHEEPIPMSTYGWNLVRLQSGVDVFFIPPEKCDTLLCDIGE 149
WT-NS5 construct's YCGGLKNVREVKGLTKGGPGHEEPIPMSTYGWNLVRLQSGVDVFFIPPEKCDTLLCDIGE 149
Block's           YCGGLKNVREVKGLTKGGPGHEEPIPMSTYGWNLVRLQSGVDVFFIPPEKCDTLLCDIGE 149
Sittisompat's     YCGGLKNVREVKGLTKGGPGHEEPIPMSTYGWNLVRLQSGVDVFFIPPEKCDTLLCDIGE 149
                  ************************************************************

Kinney's          SSPNPTVEAGRTLRVLNLVENWLNNNTQFCIKVLNPYMPSVIEKMEALQRKYGGALVRNP 209
WT-NS5 construct's SSPNPTVEAGRTLRVLNLVENWLNNNTQFCIKVLNPYMPSVIEKMETLQRKYGGALVRNP 209
Block's           SSPNPTVEAGRTLRVLNLVENWLNNNTQFCIKVLNPYMPSVIEKMEALQRKYGGALVRNP 209
Sittisompat's     SSPNPTVEAGRTLRVLNLVENWLNNNTQFCIKVLNPYMPSVIEKMETLQRKYGGALVRNP 209
                  ********************************************:***************

Kinney's          LSRNSTHEMYWVSNASGNIVSSVNMISRMLINRFTMRYKKATYEPDVDLGSGTRNIGIES 269
WT-NS5 construct's LSRNSTHEMYWVSNASGNIVSSVNMISRMLINRFTMRYKKATYEPDVDLGSGTRNIGIES 269
Block's           LSRNSTHEMYWVSNASGNIVSSVNMISRMLINRFTMRYKKATYEPDVDLGSGTRNIGIES 269
Sittisompat's     LSRNSTHEMYWVSNASGNIVSSVNMISRMLINRFTMRYKKATYEPDVDLGSGTRNIGIES 269
                  ************************************************************

Kinney's          EIPNLDIIGKRIEKIKQEHETSWHYDQDHPYKTWAYHGSYETKQTGSASSMVNGVVRLLT 329
WT-NS5 construct's EIPNLDIIGKRIEKIKQEHETSWHYDQDHPYKTWAYHGSYETKQTGSASSMVNGVVRLLT 329
Block's           EIPNLDIIGKRIEKIKQEHETSWHYDQDHPYKTWAYHGSYETKQTGSASSMVNGVFRLLT 329
Sittisompat's     EIPNLDIIGKRIEKIKQEHETSWHYDQDHPYKTWAYHGSYETKQTGSASSMVNGVFRLLT 329
                  ************************************************.***********

Kinney's          KPWDVVPMVTQMAMTDTTPFGQQRVFKEKVDTRTQEPKEGTKKLMKITAEWLWKELGKKK 389
WT-NS5 construct's KPWDVVPMVTQMAMTDTTPFGQQRVFKEKVDTRTQEPKEGTKKLMKITAEWLWKELGKKK 389
Block's           KPWDVVPMVTQMAMTDTTPFGQQRVFKEKVDTRTQEPKEGTKKLMKITAEWLWKELGKKK 389
Sittisompat's     KPWDVVPMVTQMAMTDTTPFGQQRVFKEKVDTRTQEPKEGTKKLMKITAEWLWKELGKKK 389
                  ************************************************************

Kinney's          TPRMCTREEFTRKVRSNAALGAIFTDENKWKSAREAVEDSRFWELVDKERNLHLEGKCET 449
WT-NS5 construct's TPRMCTREEFTRKVRSNAALGAIFTDENKWKSAREAVEDSRFWELVDKERNLHLEGKCET 449
Block's           TPRMCTREEFTRKVRSNAALGAIFTDENKWKSAREAVEDSRFWELVDKERNLHLEGKCET 449
Sittisompat's     TPRMCTREEFTRKVRSNAALGAIFTDENKWKSAREAVEDSRFWELVDKERNLHLEGKCET 449
                  ************************************************************
```

5. Alignment of amino acid sequences between WT-NS5 construct sequencing result and DENV-2 NS5 strain 16681 reference sequences (cont.).

```
Kinney's                CVYNMMGKREKKLGEFGKAKGSRAIWYMWLGARFLEFEALGFLNEDHWFSRENSLSGVEG 509
WT-NS5 construct's      CVYNMMGKREKKLGEFGKAKGSRAIWYMWLGARFLEFEALGFLNEDHWFSRENSLSGVEG 509
Block's                 CVYNIMGKREKKLGEFGKAKGSRAIWYMWLGARFLEFEALGFLNEDHWFSRENSLSGVEG 509
Sittisompat's           CVYNIMGKREKKLGEFGKAKGSRAIWYMWLGARFLEFEALGFLNEDHWFSRENSLSGVEG 509
                        ****:************************************************************

Kinney's                EGLHKLGYILRDVSKKEGGAMYADDTAGWDTRITLEDLKNEEMVTNHMEGEHKKLAEAIF 569
WT-NS5 construct's      EGLHKLGYILRDVSKKEGGAMYADDTAGWDTRITLEDLKNEEMVTNHMEGEHKKLAEAIF 569
Block's                 EGLHKLGYILRDVSKKEGGAMYADDTAGWDTRITLEDLKNEAMVTNHMEGEHKKLAEAIF 569
Sittisompat's           EGLHKLGYILRDVSKKEGGAMYADDTAGWDTRITLEDLKNEAMVTNHMEGEHKKLAEAIF 569
                        ****************************************** ******************

Kinney's                KLTYQNKVVRVQRPTPRGTVMDIISRRDQRGSGQVGTYGLNTFTNMEAQLIRQMEGEGVF 629
WT-NS5 construct's      KLTYQNKVVRVQRPTPRGTVMDIISRRDQRGSGQVGTYGLNTFTNMEAQLIRQMEGEGVF 629
Block's                 KLTYQNKVVRVQRPTPRGTVMDIISRRDQRGSGQVGTYGLNTFTNMEAQLIRQMEGEGVF 629
Sittisompat's           KLTYQNKVVRVQRPTPRGTVMDIISRRDQRGSGQVGTYGLNTFTNMEAQLIRQMEGEGVF 629
                        ************************************************************

Kinney's                KSIQHLTITEEIAVQNWLARVGRERLSRMAISGDDCVVKPLDDRFASALTALNDMGKIRK 689
WT-NS5 construct's      KSIQHLTITEEIAVQNWLARVGRERLSRMAISGDDCVVKPLDDRFASALTALNDMGKIRK 689
Block's                 KSIQHLTITEEIAVQNWLARVGRERLSRMAISGDDCVVKPLDDRLPSALTALNDTGKIRK 689
Sittisompat's           KSIQHLTITEEIAVQNWLARVGRERLSRMAISGDDCVVKPLDDRLPSALTALNDTGKIRK 689
                        ******************************************:.******** *****

Kinney's                DIQQWEPSRGWNDWTQVPFCSHHFHELIMKDGRVLVVPCRNQDELIGRARISQGAGWSLR 749
WT-NS5 construct's      DIQQWEPSRGWNDWTQVPFCSHHFHELIMKDGRVLVVPCRNQDELIGRARISQGAGWSLR 749
Block's                 DIQQWEPSRGWNDWTQVPFCSHHFHELIMKDGRVLVVPCRNQDELIGRARISQGAGWSLR 749
Sittisompat's           DIQQWEPSRGWNDWTQVPFCSHHFHELIMKDGRVLVVPCRNQDELIGRARISQGAGWSLR 749
                        ************************************************************

Kinney's                ETACLGKSYAQMWSLMYFHRRDLRLAANAICSAVPSHWVPTSRTTWSIHAKHEWMTTEDM 809
WT-NS5 construct's      ETACLGKSYAQMWSLMYFHRRDLRLAANAICSAVPSHWVPTSRTTWSIHAKHEWMTTEDM 809
Block's                 ETACLGKSYDQMWSLMYFHRRDLRLAANAICSAVPSHWVPTSRTTWSIHAKHEWMTTEDM 809
Sittisompat's           ETACLGKSYDQMWSLMYFHRRDLRLAANAICSAVPSHWVPTSRTTWSIHAKHEWMTTEDM 809
                        ********* ************************************************

Kinney's                LTVWNRVWIQENPWMEDKTPVESWEEIPYLGKREDQWCGSLIGLTSRATWAKNIQAAINQ 869
WT-NS5 construct's      LTVWNRVWIQENPWMEDKTPVESWEEIPYLGKREDQWCGSLIGLTSRATWAKNIQAAINQ 869
Block's                 LTVWNRVWIQENPWMEDKTPVESWEEIPYLGKREDQWCGSLIGLTSRATWAKNIQAAINQ 869
Sittisompat's           LTVWNRVWIQENPWMEDKTPVESWEEIPYLGKREDQWCGSLIGLTSRATWAKNIQAAINQ 869
                        ************************************************************

Kinney's                VRSLIGNEEYTDYMPSMKRFRREEEEAGVLW 900
WT-NS5 construct's      VRSLIGNEEYTDYMPSMKRFRREEEEAGVLW 900
Block's                 VRSLIGNEEYTDYMPSMKRFRREEEEAGVLW 900
Sittisompat's           VRSLIGNEEYTDYMPSMKRFRREEEEAGVLW 900
                        ******************************
```

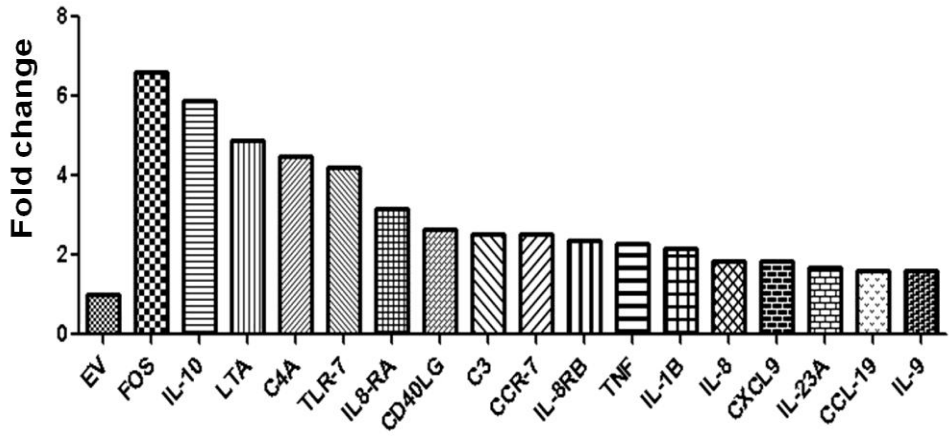

6. RT^2 Profiler™PCR Array results of NF-κB-regulated genes induced by WT-NS5 in HEK 293 cells.

HEK 293 cells were transfected with either empty pcDNA3.1/Hygro or pcDNA3.1/Hygro containing WT-NS5 for 24 h. Then, total RNA was isolated and reverse-transcribed into cDNA. The obtained cDNA of each transfection contition was subjected of RT^2 Profiler™PCR Array screening. After analysis of relative expression (fold change) comparing with empty pcDNA3.1/Hygro-transfected cell control, 38 up-regulated genes with the fold change more than 1.5 were chosen. Seventeen genes of NF-κB-regulated genes were identified and represented in the figure.

BIOGRAPHY

NAME	Miss Sasiprapa Khunchai
DATE OF BIRTH	26 July 1981
PLACE OF BIRTH	Phichit, Thailand
INSTITUTIONS ATTENDED	Naresuan University, 2000-2004 Bachelor of Science (Cardio-thoracic technology) Mahidol University, 2005-2007 Master of Science (Anatomy) Mahidol University, 2008-2013 Doctor of Philosophy (Immunology)
SCHOLARSHIPS	Siriraj Graduate Thesis Scholarship, 2005-2006 Mahidol University, Thailand Strategic Scholarships for Frontier Research Network for the Ph.D. Program Commission on Higher Education, Thailand
HOME ADDRESS	41, Mu 14, Wangsaipoon, Phichit, 16680, Thailand

AWARDS

2010	Ph.D. Student Award, In recognition of her spirit of co-operation and exemplary attitude and manner towards a high quality research in biomedical sciences. The Division of Medical Molecular Biology, Department of Research and

Development, Faculty of Medicine Siriraj Hospital, Mahidol University.

PRESENTATIONS

National presentations

1. **Khunchai S**, Wongwiwat W, Mairiang D, Sriburi R, Sittisombut N, Limjindaporn T. Association of human m-calpain and dengue virus nonstructural protein 5. **Poster presentation**. The 30th Annual Meeting of the Anatomy Association of Thailand, Chiang Mai, Thailand, May 2007.
2. **Khunchai S**, Mairiang D, Wongwiwat W, Sriburi R, Sittisombut N, Malasit P, Yenchitsomanus P, Limjindaporn T. Application of yeast two-hybrid system for identification of human proteins interacting with dengue nonstructural protein 5. **Oral presentation**. Siriraj Graduate Research Conference, Bangkok, Thailand, March 2008.
3. **Khunchai S**, Limjindaporn T, Wongwiwat W, Sawasdee N, Chaowalit P, Songprakhon P, and Yenchitsomanus P. Cytokine production and inflammatory responses induced by dengue virus nonstructural protein 5. **Poster presentation**. Commission on Higher Education Congress III, Chonburi, Thailand, September 2010.

International presentations

1. Limjindaporn T**, Khunchai S**, Mairiang D, Sriburi R, Sittisombut N, Malasit P. Identification of human proteins interacting with dengue virus nonstructural protein5 by using a yeast two-hybrid system. **Poster presentation**. The 3rd Asian Regional Dengue Research Network Meeting, Taiwan, August 2007.
2. **Khunchai S,** Junking M, Limjindaporn T, Yenchitsomanus P. Studies on the role of dengue virus protein NS5 in the cytokine storm. **Poster presentation**. Redox and Inflammation signaling. RedCat Meeting on Redox Catalysis from Chemistry to Biology. Kirchbourg, Luxembourg, January 2012.
3. **Khunchai S**, Junking M, Suttitheptumrong A, Yasamut U, Sawasdee N, Netsawang N, Morchang A, Chaowalit P, Noisakran S, Yenchitsomanus P, Limjindaporn T. A Modulation of RANTES Production by Dengue Virus

Nonstructural Protein 5 and Daxx Interaction. **Poster presentation**. Alternative Strategies against Cancer and Inflammation. Molecular Medicine Conference, Bangkok, Thailand, December 2012.

4. **Khunchai S**, Junking M, Suttitheptumrong A, Kooptiwut S, Haegeman G, Limjindaporn T, Yenchitsomanus P. Dengue virus nonstructural protein 5 enters the nucleus to activate RANTES production via NF-κB. **Poster presentation**. Emerging Cytokine Network Conference. British Columbia, Canada, January 2014.

PUBLICATIONS

1. Limjindaporn T, Mairiang D, **Khunchai S**, Wongwiwat W. A novel yeast two hybrid vector, pEG-NRT for protein-protein interaction. Siriraj Medical Journal 2007;59:175-177.
2. Limjindaporn T, Sawailbud S, Netsawang J, Mairiang D, **Khunchai S**, Wongwiwat W. Cloning of JNK activation domain and Fas-binding domain of human apoptotic Daxx gene by homologous recombination in yeast. Thai Journal of Genetics 1 2008;(1):63-68.
3. **Khunchai S**, Junking M, Suttitheptumrong A, Yasamut U, Sawasdee N, Netsawang N, Netsawang J, Morchang A, Chaowalit P, Noisakran S, Yenchitsomanus P, Limjindaporn T. Interaction of dengue virus nonstructural protein 5 with Daxx modulates RANTES production. Biochemical and Biophysical Research Communications 2012; 423:398-403.
4. Nagila A, Netsawang J, Suttitheptumrong A, Morchang A, **Khunchai S**, Srisawat C, Puttikhunt C, Noisakran S, Yenchitsomanus P, Limjindaporn T. Inhibition of p38MAPK and CD137 signaling reduce dengue virus-induced TNF-α secretion and apoptosis. Virology Journal 2013;10:105.
5. Suttitheptumrong A, **Khunchai S**, Panaampon J, Yasamut U, Morchang A, Puttikhunt C, Noisakran S, Haegeman G, Yenchitsomanus P, Limjindaporn T. Compound A, a dissociated glucocorticoid receptor modulator, reduces dengue virus-induced cytokine secretion and dengue virus production. Biochemical and Biophysical Research Communications 2013; 436(2):283-288.